ISSN 2300-5599

ACTA INNOVATIONS

CENTRUM
BADAŃ I INNOWACJI
PRO - AKADEMIA
RESEARCH AND INNOVATION CENTRE

no. 27

April 2018

Acta Innovations

quarterly

no. 27

Konstantynów Łódzki, Poland, April 2018

ISSN 2300-5599

Original version: online journal

Online open access: www.proakademia.eu/en/acta-innovations

Articles published in this journal are peer-reviewed

Publisher:

Research and Innovation Centre Pro-Akademia
9/11 Innowacyjna Street
95-050 Konstantynów Łódzki
Poland

ACTA INNOVATIONS

no. 27

April 2018

Contents

Joanna Szmyt
Research and Innovation Centre Pro-Akademia
9/11 Innowacyjna Street, 95-050 Konstantynów Łódzki, joanna_szmyt@wp.pl

MODERN REHABILITATION SYSTEMS BASED ON TEXTILES

Abstract
The article presents examples of rehabilitation solutions in which textiles play an important role. They are a fully functional garment, an element of clothing adapted to a given part of the body or a product intended for use in improving health. They are designed with the use of modern production technologies that utilize various raw materials to support the health aspects of the user with their structure and properties.

Key words
Medical compression, electro-stimulation, wholegarment knitted fabrics, spacer knitted fabrics, rehabilitation gloves.

Introduction

Clothing has accompanied people since prehistoric times, providing protection against adverse external conditions [1]. Textiles still play an integral role in human life. In addition to the basic function of protecting the body against cold and heat, excluding the fashion aspect, they complement many areas of human life connected with our functioning in the home environment, at work, during recreation or while doing sports. One important area is the use of textiles in human health. In selected fields, textiles, including knitted fabrics, are used to improve human health due to their structure and body fit as well as the possibility of extensive customization of properties. The following are examples of the use of knitted fabrics in the field of rehabilitation, where knitted fabrics play an integral role in improving the health of the user.

Medical compression

This use is very important from the point of view of many branches of patient's health improvement with the use of textiles with standardized properties of compression on selected parts of the body. Compression products are based on knitting technology. These are mostly products manufactured based on the row knitted fabrics technique on double-bearing cylindrical machines with the use of elastomeric yarn. They are designed as wholegarment products or are used for making garments, in order to adjust the product to a given part of the body as much as possible. As serving to improve health, they are widely analyzed and examined, so that the design of the product and its compression features have strictly defined health functions in terms of the pressure on the patient [2 - 12]. One of the solutions used for improving children's health in terms of sensory feelings are products suited to the child's body in the form of flexible orthoses Hylton® Orthotics (Fig.1). They provide support of the child's body and its balance, as well as its response to deep pressure by improving the control of muscle tone and respiratory mechanics. They help reducing reaction time and in involuntary movements, as well as in auto-stimulation behaviors.

Fig. 1 Compression orthosis of the torso
Source: [13]

These compression orthoses are intended mainly for little patients with childhood cerebral palsy, Down syndrome as well as those diagnosed with muscular atrophy or sensory integration disorders. The second function is to strengthen physical stability and posture control among children with motor function disorders, by means of increased coordination and body awareness, as well as the speed and responsiveness of the child's movements.

Among products with compressible properties, a wide group are pantyhoses with anti-varicose and anti-edema properties. Designed as products with configurable compression, they provide adequate pressure on the body for proper circulation in the lower parts of the body, in pressure classes from 10mmHg to 32mmHg. The most important task of anti-varicose stocking products is to exert a specific pressure on the patient's legs in order to force the venous blood from the lower parts of the legs towards the heart [2-4, 9] (Fig. 2). These products are designed both as seamless and with the use of a flat seam to provide constant configurable compression [14-15] (fig. 3). Products in the form of pantyhoses, stockings or knee-length socks can also provide a preventive effect for people who work in a standing and sitting position, especially those with strictly medical direction for treatment of lower limb varicose veins.

Fig. 2 Anti-varicose stocking
Source: [14]

Fig.3 Seamed compression product
Source: [15]

The group of products of the type fitted to the user's body includes knitted bands, also in seamless form. They are used to stabilize parts of the body such as wrists or other joints (knee, ankle) (Fig. 4). They provide adequate stiffening and compression at the early stages of degenerative disease as well as during chronic, post-traumatic or postoperative irritations in the joint area [5]. They are also used in prevention to save the occurrence of injuries e.g. during practicing competitive sport. These products, in addition to performing the assumed function, thanks to the use of a variety of raw materials, ensure comfort of use. These include additional features such as moisture dissipation, which ensures antibacterial properties, as well as the introduction of the anti-rheumatic function through the addition of a natural ingredient such as amber (enrichment or fiber) or minerals providing a thermal effect by raising the body temperature, which can further contribute to the process of improving health.

Fig. 4 Stabilizer of the wrist and knee
Source: [16]

While discussing the functions of textile products in rehabilitation in terms of immobilization of the patient's body parts, it is necessary to emphasize the role of textiles in the construction of a wide group of products with a stabilizing function in the form of orthoses. These are rehabilitation devices used as orthopedic apparatuses for immobilizing joints, body sections or muscle groups, usually replacing plaster dressing (Fig. 5). Their main task is to ensure a stable position of the joints of the limbs which have been injured e.g. sprains, dislocations or ligament ruptures [6-7]. Regardless of the structure of these products, which can be divided into rigid, semi-rigid (semi-flexible) and soft (elastic), textile materials in the form of woven fabrics, knitted fabrics and tapes play a fundamental role in the composition of orthoses.

Fig. 5 Semi-rigid orthosis
Source: [17]

In combination with rigid composite elements of the orthoses, elastic and soft textile materials placed next to the skin, improve the comfort of use as well as act as an air layer ensuring the removal of moisture from the stiffened part of the body. For this purpose commonly, thanks to their spatial structure and elasticity, spacer knitted fabrics (3D) are used, usually made of polyamide produced both the warp and the weft knitted fabric technology.

Nowadays, thanks to their spatial structure and elasticity, (3D) spacer knitted fabrics are used, usually made of polyamide. Orthoses made entirely of textiles are joined using flat seams with lacing elements or Velcros for comfortable stabilization of the injury. Compression effect of textiles also ensures that the temperature around the given joint is raised and maintained at a constant level.

An important application scope of textiles, including knitted fabrics in rehabilitation, is compression therapy as regards scar treatment. In this area, the use of special devices adapted to the structure and needs of the patient is very important during treatment of post-burn and post-operative marks left after wounds have healed [8-9]. Research works [10-12]present the issues of compression products in terms of the value of individual pressure exerted by the product on various parts of the patient's body, so that the designed compression medical product performs a therapeutic function. The effect of the seam and the tolerance performance of the compression product was analyzed, which was dependent on the stiffness of stretching (compression) fabric for selected parts of the body as a function of the complexity of building the female and male figures.

To improve the effectiveness of patient’s treatment, the force of pressure on the scar must be chosen appropriately – as specified by the doctor. Too much pressure can lead to tissue necrosis as a result of circulatory disturbance, whereas too little pressure will not have the therapeutic effect. A garment individually matched to the wearer using flat seams to minimize the possibility of irritation, has an appropriate value of compression (Fig. 6). These devices can be used on a cured post-burn wound or scar. They should be worn for at least 6 to 24 months regularly and all day round, until there are clear symptoms of healing (the scar flattening, fading away and softening).

Fig. 6 Codopress® garment
Source: [18]

Anti-bedsore protection

One of the issues of rehabilitation is protection of patient health or support for treatment in terms of anti-bedsore protection if the patient is immobilized for too long in a sitting or lying position, leading to pressure on the skin. In such conditions, the patient is exposed to pressures, imprints on skin, which in consequence may lead to the formation of bed-sores [19-20].

One of the effective solutions aimed at preventing the creation of bedsores is a textile product made of technical knitted fabric, namely the MEDiMAT® anti-bedsore bed overlay (Figure 7). It is a 'wholegarment' form of 3D spacer knitted fabric with dimensions of 90cm x 200cm. Thanks to its spatial form and the structure made of a series of densely arranged monofilaments connecting the upper and lower layers of the flat knitted fabric, it gives the product its elasticity and is a very good substitute for foam. The structure of the product is openwork and highly deformable. It creates a layer between the patient's body and the bed that is permeable to air and moisture. Thanks to these features, it helps to protect the patient from pressures and bedsores, as well as improves the health condition when such inconveniences already exist [21].

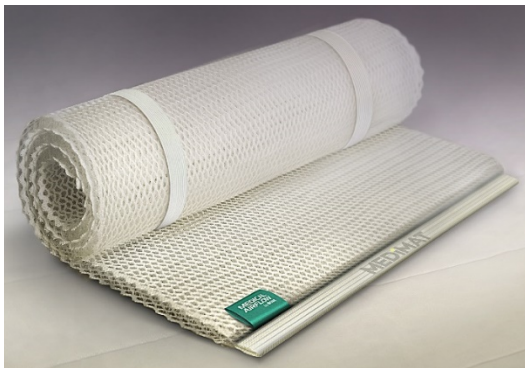

Fig. 7 The MEDiMAT® anti-bedsore overlay
Source: [22]

The mat causes an even distribution of the patient's body pressure, eliminating the risk of point loads. The product has gained a positive reputation among patients and physicians after being tested in hospital conditions at the Clinic of Rehabilitation and Physical Medicine in Łódź and has been registered as a medical device.

Rehabilitation gloves

Interesting solutions aimed at patient health improvement include wholegarment knitted articles for the hand, in the form of gloves. In this type of application, they serve as a carrier for elements of motor nature intended to stimulate the operation of hands and fingers toward making specific moves. Below there are examples of several solutions designed and made for rehabilitation purposes.

One of them is the so-called Cynteract – a rehabilitation system developed for the hand, consisting in wearing gloves and exercising hand fitness in virtual reality. The system consists of a glove, sensors placed at the ends of its fingers and a tether running along each finger to the control system. It is used for treating hand injuries by controlling their movements, in accordance with a programmed set of exercises. With the help of the orientation sensor placed in the glove, the position of the hand in the room is followed. The position of the strings enables the sensors to precisely detect the movements and bending of each finger. This allows to make exercises in accordance with the rehabilitation program presented in the virtual reality on the screen [23].

Fig. 8 Cynteract glove for rehabilitation exercises aimed at improving motor performance of the hand
Source: [24]

For greater patient motivation to regularly use the gloves and thus exercise, they are connected to virtual reality glasses. Under these conditions, in the virtual world, every hand movement is reconstructed to provide both motor and visual feedback. In this game-like environment, exercises become a pleasure.

A solution based on the use of a glove for hand rehabilitation integrated with a computer program is the robotic system shown in Fig.9. This device is based on a flexible glove of a fitted shape connected with cables attached to each of its fingers and directed along the arm to a rucksack. These 'guides' let the hand movement remote control. The system controls each finger independently. The developed electronics let control the position of fingers as part of arranged rehabilitation program. The programmed mode enables the therapist to properly determine the movements of the glove in order to run a given rehabilitation procedure, allowing for individual selection of the exercise regimen to improve the hand performance, well-being and independence of the patient in terms of everyday functioning in their environment [25-26].

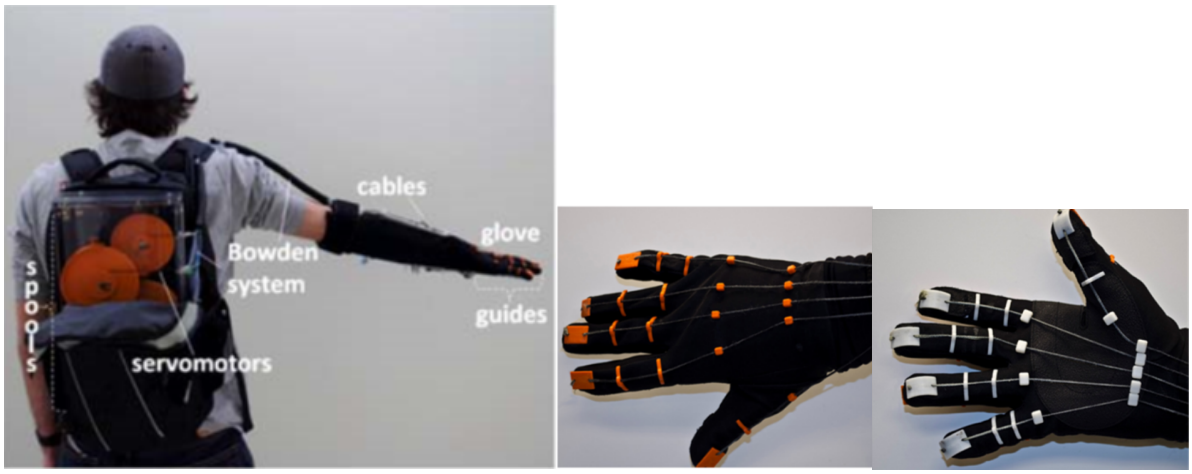

Fig. 9 Prototype of the hand rehabilitation device with a view of the 'guides'
Source: [26]

In the context of using textiles as a carrier for stimulation elements, one of the solutions applied to the hand and forearm is a device that directs hand operation for blind people. The device is designed to help coaches of blind athletes participating in the Paralympic Games to learn appropriate muscle

movements. Until now, trainings consisted in directly moving hands and legs, so that the blind person could remember particular movements and muscle work. Scientists at Imperial College London have developed a device for vibratory feedback, which teaches blind people how to make precise repeatable movements without the presence of a trainer. The 'Ghost' system is able to 'remember' certain movements demonstrated by the trainer. On this basis, an athlete can practice these movements which are monitored on an ongoing basis in terms of accuracy, guided by vibration and sound signals (Fig. 10)

Fig. 10 The 'Ghost' system for stimulation of blind people's hand movements
Source: [27]

It is possible to import recordings of movements from other athletes who will be able to follow the movements and techniques of athletes' muscle work improving their own. The authors emphasize that the system has been designed especially for people with disabilities, but in the future the idea will be oriented towards assistance with rehabilitation of people after strokes and other neurological conditions.

Muscle electro-stimulation

Electro-stimulation of nerves and muscles plays an important role in the field of application of textiles in rehabilitation. Its purpose is to ensure that specific muscles are forced to work in order to improve their condition and function in the field of reeducation of lost muscle function, maintaining or increasing the range of motion in the joints, increasing local blood circulation, or in sports training during regeneration as part of rehabilitation after injuries. This effect is achieved due to a fast change of AC current with different frequency and pulse width in the electrode. The research experimentally determined the conditions of stimulation of muscles of different sizes and their characteristics when using certain FES (Functional Electrical Stimulation) parameters (intensity of stimulation, frequency)[28].

There are many solutions to replace traditional electrodes with those made using conductive textiles based on conductive yarns in the application of fabrics and knitted fabrics [29]. A noteworthy solution for muscle electro-stimulation is based on the silkscreen printing technology in the form of a system of electrodes [30-31].

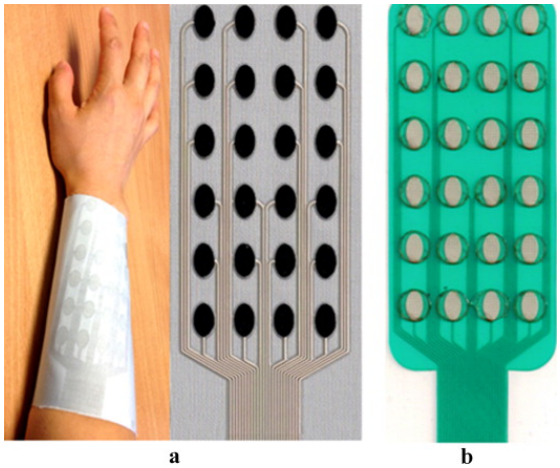

a b
Fig. 11 Flexible printed matrix of electrodes
Source: [32]

It is based on woven fabric and creates a flexible stimulative device. The advantage is that it does not require the use of a hydrogel layer, it has direct contact with dry skin, becoming a convenient element of therapy (Fig.11). Muscle stimulation was performed using programmable patterns to recreate three different hand gestures. Greater hand gesture recreation was achieved than in the case of application of the most popular printed circuit board with a hydrogel layer. It was concluded that the work of the new textile electrode allows therapeutic work comparable to a typical stimulation electrode. The results allowed further work on application of the electrodes in the form of clothing, the so-called e-textiles.

Summary and conclusions

Textiles play an important role in products used in medical rehabilitation, especially in areas such as compression therapy and orthopedics. Programmed pressure in shaped and designed products ensuring a specific and constant unit pressure on a selected body part, contributes to the improvement of motor and sensory functions at children with congenital malformations, improvement of health (varicose veins), health effects of accidents treatment (burn wounds) or injuries (e.g., wrist joint). Knitted fabrics used in orthopedic elements provide an increase in the patient's comfort with lighter joint injuries ensuring an improvement of his or her skin condition (protection against abrasions, ventilation, moisture wicking). These features are also provided for the prevention and treatment of pressure ulcers by using spatial tight knit forms to improve the well-being and health, especially of immobilized patients. In addition to the well-developed textronic solutions used for monitoring the patient's vital parameters, in the rehabilitation the textile-based devices are used for improving the hand and arm movements and functions using different solutions based on the structure of the glove or using muscle stimulation therapies.

References

[1] I. Krucińska. Diagnoza potencjału jednostek badawczo-rozwojowych i procesu komercjalizacji badań, Monograph, Społeczna Wyższa Szkoła Przedsiębiorczości i Zarządzania, Łódź, 2007, pp.6-7

[2] R. Liu, Y.-L. Kwok, Y. Li, T.-T. Lao. Fabric Mechanical-Surface Properties of Compression Hosiery and their Effects on Skin Pressure Magnitudes when Worn. FIBRES & TEXTILES in Eastern Europe 2010, Vol. 18, No. 2 (79) pp. 91-97.

[3] A. Ilska, K. Kowalski, M. Kłonowska, T. M. Kowalski. Influence of Stress and Relaxation Characteristics of Knitted Fabrics on the Unit Pressure of Compression Garments Supporting External Treatment, FIBRES & TEXTILES in Eastern Europe 2014, 22, 4(106), pp.87-92.

[4] A. Belbasisa, F. K. Fussa, J. Sidhua. Muscle activity analysis with a smart compression garment, 7th Asia-Pacific Congress on Sports Technology, Procedia Engineering 112 (2015), pp. 163 -168.

[5] M. Senthilkumar, L. A. Kumar, N. Anbuman. Design and Development of a Pressure Sensing Device for Analysing the Pressure Comfort of Elastic Garments. FIBRES & TEXTILES in Eastern Europe, 2012, 20, 1(90), 64-69.

[6] W. Trümper, C. Sachse, O. Diestel, C. Cherif. Innovative flat-knitted spacer fabrics for orthoses, Technical Textiles, Aug. 2011, Vol. 54, Issue 4, p.171

[7] D. Ališauskienė, D. Mikučionienė. Influence of the Rigid Element Area on the Compression Properties of Knitted Orthopaedic Supports. FIBRES & TEXTILES in Eastern Europe 2012; 20, 6A(95): 103-107.

[8] L. Macintyre, M. Baird. Pressure garments for use in the treatment of hypertrophic scars—a review of the problems associated with their use, Burns 32 (2006),pp.10–15

[9] L. Wang, M. Felder, J. Y. Cai. Study of Properties of Medical Compression Fabrics, Journal of Fiber Bioengineering & Informatics 4:1 (2011),pp.15–22

[10] E. Maklewska, A. Nawrocki, J. Ledwoń, K. Kowalski. Modelling and Designing of Knitted Products Used in Compressive Therapy. FIBRES & TEXTILES in Eastern Europe January / December 2006, Vol. 14, No. 5 (59)

[11] A. Ilska, K. Kowalski, M. Kłonowska, T. M. Kowalski, W. Sujka. Issues Regarding the Design of Textile Compression Products for Small Body Circumferences FIBRES & TEXTILES in Eastern Europe 2016; 24, 6(120): 116-120

[12] K. Kowalski, K. Karbowski, M. Kłonowska, A. Ilska, W. Sujka, M. Tyczyńska, B. Włodarczyk, T. M. Kowalski. Influence of a Compression Garment on Average and Local Changes in Unit Pressure. FIBRES & TEXTILES in Eastern Europe 2017; 25, 6(126): 68-74.

[13] www.stanley.poznan.pl

[14] www.pani-teresa.com.pl

[15] www.secondskin.com.au

[16] www.mj-corporation.pl

[17] www.reh4mat.com

[18] www.tricomed.pl

[19] R. M. Allman, C. A. Laprade, L. L. Noel and others. Pressure Sores Among Hospitalized Patients, Ann Intern Med.1986 Sep; 105(3), 37-42.

[20] L. Guttmann. The problem of treatment of pressure sores in spinal paraplegics, British Journal of Plastic Surgery, Vol. 8, 1955–1956, pp. 196-213.

[21] S. F. Tong, J. Yip, K. L. Yick. The possibility of using weft knitted spacer fabric as the wound dressing for pressure ulcer, International Journal of Advances in Science Engineering and Technology, Vol.4, Iss-4, Spl. Issue-1 Nov.2016, pp.13-19.

[22] www.bowi.pl

[23] www.cynteract.de

[24] www.emag.medicalexpo.com

[25] M. A. Delph, S. A. Fischer, P. W. Gauthier, C. H. Matrinez Luna, E. A. Clancy, and G. S. Fischer. Development of a Cable Driven Flexible Robotic Rehabilitation Glove, Biomedical Engineering Society Annual Meeting - BMES, Atlanta, GA, October 2012

[26] M. A. Delph, S. A. Fischer, P. W. Gauthier,C. H. Martinez Luna, E. A. Clancy, G. S. Fischer. A Soft Robotic Exomusculature Glove with Integrated sEMG Sensing for Hand Rehabilitation, 13th International Conference on Rehabilitation Robotics (ICORR), Seattle, WA, June 2013

[27] www.medgadget.com

[28] M. Vromansa, P. D. Faghria. Functional electrical stimulation-induced muscular fatigue: Effect of fiber composition and stimulation frequency on rate of fatigue development. Journal of Electromyography and Kinesiology 38 (2018) 67–72.

[29] A. Curteza, V. Cretu, L. Macovei, M. Poboroniuc. The manufacturing of textile products with incorporated electrodes. AUTEX Research Journal, Vol. 16, No 1, March 2016, pp.13-18.

[30] J. Zieba, M.Frydrysiak, M. Tokarska. Research of Textile Electrodes for Electrotheraphy, FIBRES & TEXTILES in Eastern Europe, 2011, Vol.19, No.5 (88), pp. 70-74.

[31] M. Kutlu, C. T. Freeman, E. Hallewell, A.-M. Hughes, D. S. Laila. Upper-limb stroke rehabilitation using electrode-array based functional electrical stimulation with sensing and control innovations, Medical Engineering and Physics, 38 (2016), pp.336-379.

[32] K. Yang, C. Freeman, R. Torah, S. Beeby, J. Tudor. Screen printed fabric electrode array for wearable functional electrical stimulation, Sensors and Actuators A: Physical, Volume 213, 1 July 2014, pp. 108-115.

Anna Rył, Piotr Owczarz
Lodz University of Technology, Faculty of Process and Environmental Engineering,
Department of Chemical Engineering
213 Wolczanska str., 90-924 Lodz, Poland, anna.ryl@edu.p.lodz.pl, piotr.owczarz@p.lodz.pl

INFLUENCE OF FISH COLLAGEN ON VISCOELASTIC PROPERTIES AND SOL-GEL PHASE TRANSITION OF CHITOSAN SOLUTIONS

Abstract
The thermosensitive hydrogels are widely used in tissue engineering due to their non-invasive application. Special interest of researchers, due to the specific characteristics of both materials, is aimed at composites of natural origin obtained from chitosan hydrogels combined with collagen. The mechanical properties of the thermosensitive chitosan-fish collagen hydrogels and the sol-gel phase transition parameters were determined by the rotational rheometry measurement techniques. Based on comparison of the obtained storage modulus G' curves, it was found that the addition of collagen negatively affects the mechanical properties of composite scaffolds. The addition of this protein substance decreases their elasticity. Only the smallest concentration (0.25g collagen/1 g chitosan) of collagen improves the mechanical properties of composite hydrogels, from 56 kPa to 61 kPa. Conducted non-isothermal studies allowed to conclude that the addition of collagen causes an increasing temperature of sol-gel phase transition. However, the observed changes are not a monotone function of the biopolymer concentration.

Key words
Injectable scaffold, sol-gel phase transition, chitosan, fish collagen

Introduction

Hydrogels are three-dimensional, hydrophilic porous polymeric structures, capable of binding water and many biological fluids [1]. These systems are insoluble due to non-covalent interactions between the polymer chains (physical crosslinking) or secondary polymerization caused by the addition of cross-linking substances (formation of covalent interactions) [2,3]. These structures, known as scaffolds, are used in tissue engineering as temporary matrices for local delivery of cells, growth factors and drugs [4]. Hydrogels have attracted noticeable interest, e.g. in bone tissue engineering, for their structural similarity to cartilage, which is a highly hydrated tissue composed of chondrocytes deposited in type II collagen and glycosaminoglycans (GAG) [5]. Hydrogels may show thermosensitivity through the ability to undergo a sol-gel phase transition. Those systems are characterized by a relatively low viscosity and predominance of viscous properties in the sol phase and a significantly higher viscosity and the domination of elastic properties in the gel phase. The main difference between this two phases is the observed flow phenomenon characteristic for viscous liquid and no flow for the viscoelastic fluid [6]. Recently, thermosensitive hydrogels are an object of interest for many researchers with high potential due to the lower invasiveness compared to implant scaffolds [7,8]. Furthermore, due to the fluid form, the use of injectable scaffold allows to fill complex defects [8]. Another advantage is the ability to control important properties such as porosity, size, geometry and the degree of connection pores. This leads to the possibility of imitating the topological and microstructural properties of the extracellular matrix [9].

In recent years, there has been a growing interest in using polymers of natural origin for the production of scaffolds (also hydrogels) used in tissue engineering. Among the most commonly used groups the polysaccharides (chitosan) and the protein substances (collagen) should be mentioned [2,9,10]. Their most important properties are biocompatibility and biodegradability in a physiological environment [9,11]. Due to the properties of both biopolymers, chitosan-collagen composites are often used for the manufacture of implantable scaffolds [12–16]. Furthermore, collagen is the source of particularly desirable amino acids in tissue engineering such as arginine and lysine [17].

For chitosan - collagen colloidal solutions, measurements of rheological properties presented in the literature are usually limited to rotational tests with the determination of flow and viscosity curves [18,19]. In the literature, there are not many studies on the thermosensitivity of chitosan-collagen systems. Few oscillatory studies indicate viscoelastic properties of systems. At low temperatures a predominance of viscous properties

over elastic ones is observed, at high temperatures the elastic properties dominate over viscous ones [20]. Nevertheless, these studies are often conducted within a narrow measurement range of angular frequency.

The study of thermosensitivity (changes in viscoelastic properties under the influence of heating) of colloidal chitosan-collagen solutions is discussed in detail in the paper [21]. In these studies, the authors concluded unequivocally negative effect of the addition of collagen on the mechanical properties of composite hydrogels obtained. It was also found that the addition of collagen drastically increases the phase transition temperature. However, the observed change is not a monotone function of the biopolymer concentration. It is worth noticing that in the studies cited, the authors used collagen of bovine origin.

Available studies indicate that fish-derived collagen is characterized by better bioavailability than bovine-derived. This is due to the fact that the fish collagen molecules are smaller than bovine [22]. Its advantages are also a lower degree of crosslinking and higher solubility [23]. The last significant advantage of fish-derived collagen is an easier purification process, which leads to smaller damage to protein chains [24].

The aim of this study was to investigate the influence of the addition of fish-derived collagen on viscoelastic properties and condition of sol-gel phase transition of colloidal chitosan solutions.

Materials and methods

For the present study, chitosan (DD=81.8%, MW= 680 kDa) from crab shells (Sigma Aldrich Product no. 50494) and fish-derived Type 1 collagen (Kolagen NCN – Collagen Premium Fish) were used. Furthermore, as a solvent the 0.1M hydrochloric acid (Fluka Product no. 84415) was used. The disodium β-glycerophosphate (Sigma Aldrich Product no. 50020) was added as a substance neutralizing chitosan solutions to physiological pH and maintaining the biopolymer chain in solution in a hydrophilic form [25–27].

Thermosensitive chitosan hydrogels were prepared based on the commonly used method [26]. 0.4 g of chitosan was dissolved in 16ml 0.1M hydrochloric acid. After thorough mixing, the colloidal solution was left at room temperature for 24h to completely dissolve the biopolymer. The fish-derived collagen– due to its solubility – was added in an acidic environment, by dissolving appropriately 0.1g, 0.2g, 0.4g – Table 1 (sample no. 2-4). After this, a suspension of disodium β-glycerophosphate was prepared by dissolving 2g of the substance in 2ml of distilled water. Both solutions were cooled to 4 °C. Next drop by drop the glycerophosphate suspension was added to the colloidal solution of chitosan with the addition of collagen. Sample no. 1, without the addition of collagen, was a reference solution.

Table 1. Composition of tested samples.

Sample	**Chitosan [g]**	**Hydrochloric acid [ml]**	**β-NaGP [g]**	**Collagen [g]**	**Collagen/Chitosan weight ratio [g collagen/1 g chitosan]**
Sample no.1	0.4	16.0	2.0	0.0	0.00
Sample no.2				0.1	0.25
Sample no.3				0.2	0.50
Sample no.4				0.4	1.00

Source: Author's

Test samples were measured using rotational rheometry techniques. Rheological properties were investigated in the cone-plate measuring system (50 mm diameter, 1° slope angle, 48 µm truncation) of Anton Paar Physica MCR 301 rheometer. The sol-gel phase transition temperature and change of mechanical properties (change in the value of the storage modulus G') during heating were determined in non-isothermal measurements in the range of 5° C - 60° C, with constant deformation (ω=5 s^{-1}, γ=1%). The viscoelastic properties and thermosensitivity were determined in the frequency sweep test (ω = 0.005 s^{-1} - 500 s^{-1}) also called the

mechanical spectra. The studies were conducted for all samples at the temperatures of 5 °C, 25 °C, 30 °C, 35 °C, 40 °C.

Results and discussion

The results of non-isothermal measurements at constant deformation of all tested samples are shown in Fig. 1. The obtained experimental curves allow to determine the sol-gel phase transition temperature. According to the theory proposed by Chambron and Winter, the point at which the tangent of the phase shift angle tanδ reaches the value of unity determines the gelation point [28]. The temperatures of the phase change determined by this method are presented in Table 2. The obtained results indicate that the addition of collagen to the colloidal chitosan solution increases the gelation temperature in comparison to the sample without this protein. However, this increase in gelation temperature is not a monotonous function of collagen concentration. This confirms previous studies of thermosensitive hydrogels with the addition of bovine collagen [21]. Low protein concentration causes a temperature increase from 26.5 ° C to 37.4 ° C and 38.4 ° C respectively for samples 2 and 3. This may be due to the presence of large particles of biopolymer, which in the case of low concentration constitute a spatial blockage and make it difficult to bring the polysaccharide chains closer together. Moreover, the constant concentration of the glycerophosphate salt may be partially absorbed as a protein chain protecting substance [29,30]. The addition of the highest collagen concentration (sample 4) causes a decrease the gelation temperature. However, the obtained value is higher than gelation temperature of control sample. In the case of this sample, the decrease of gelation temperature, as compared to samples 2 and 3 (with lower concentration of protein), may be due to the fact that the collagen molecules are also crosslinked. Thus, the internal structure and interactions between chitosan and collagen chains are changed. As a result, there is a different crosslinking of the three-dimensional polymer matrix because of the same concentration of both polymers.

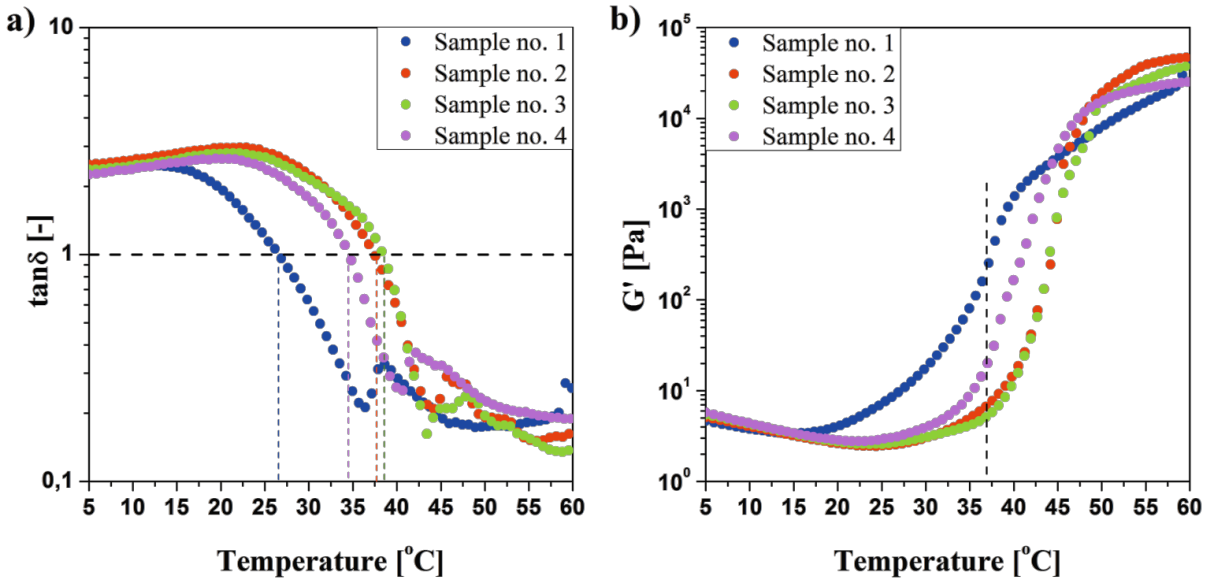

Fig. 1. Results of non-isothermal measurements with constant mechanical deformation, a) tanδ as a function of temperature, b) storage modulus G' as function of temperature.
Source: Author's

Analysis of changes in the value of the storage modulus G' at the gelation point indicates that the solutions containing the collagen additive show less mechanical strength than the pure chitosan solution – Fig. 1b. The analysis of changes in the value of the storage modulus at 37 °C (reference temperature) was also carried out – Table 2. The reference temperature is in the region of rapid [31] gelation for all tested solutions. Nevertheless, for samples no. 2 and no. 3 the reference temperature is lower than the determined gelation temperature. It means that for both samples viscous properties dominate over elastic ones. Comparing samples no. 1 and 4, there is a significant reduction in mechanical strength for a sample containing collagen. It also results from another phase of formation of the final structure. The results of non-isothermal measurements indicate that for temperatures above 45 °C all solutions containing collagen reach higher values of the storage modulus G'. Thus demonstrating better mechanical strength. However, for the design of thermosensitive hydrogels formed in vivo, which can be used in tissue engineering, such high temperatures are not included in the analysis.

Table 2. The temperatures of sol-gel phase transition of tested samples and storage modulus G' values in critical points i.e. the sol-gel phase transition point and at reference temperature 37°C

	The sol-gel phase transition (tanδ=1)		**T=37°C**	
Sample	**Temperature [°C]**	**G' [Pa]**	**tanδ [-]**	**G' [Pa]**
Sample no. 1	26.5	9.1	0.2	226.0
Sample no. 2	37.4	7.5	1.1	6.9 (*)
Sample no. 3	38.4	7.0	1.3	5.2 (*)
Sample no. 4	34.5	7.9	0.5	19.7

(*) Gelation temperature is higher than reference temperature (37 °C). *Source: Author's*

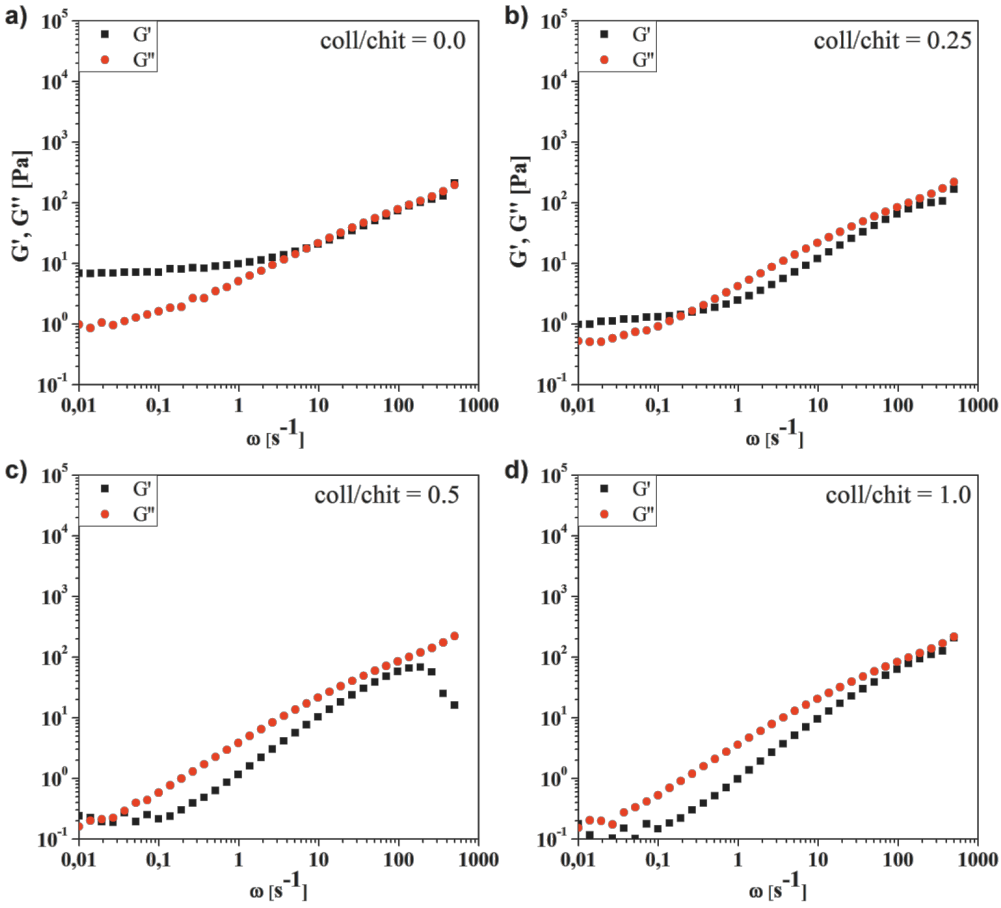

Fig. 2. Experimental curves of storage G' (■) and loss G" (●) moduli in a wide range of angular frequency ω, a) sample no. 1, b) sample no. 2, c) sample no. 3, d) sample no. 4 at temperature 5 °C.
Source: Author's

The results of the mechanical spectra obtained for the solutions tested at 5 ° C are shown in Fig. 2. The graphs show that the addition of collagen to the colloidal chitosan solution causes a change in the dominant character of the medium in the studied range of angular frequency ω. In the case of sample No. 1 (without the addition of collagen) - Fig. 2a, a significant predominance of elastic properties over viscous ones (G' > G") for low values of angular frequency is observed. For higher values ω, viscous properties dominate over elastic ones but not so significantly. The addition of collagen causes increased domination of viscous properties over elastic ones in a whole range of angular frequencies ω - Fig. 2b-d. The dominance of elastic properties over viscous is observed only for the smallest collagen concentration tested below ω=0.2 s^{-1}. It was also observed that the addition of collagen causes not only a change in the dominant properties of the solutions, but also affects the mechanical strength of the samples tested. It was determined on the basis of the decrease in the value of the storage modulus G'. The lowering of storage modulus G' value of sample no.2 for low angular frequency, from 20 Pa to 2 Pa was noticed. A further increase in the concentration of the collagen additive (sample no. 3 and 4) causes a

decrease of the storage modulus G ' value to about 1 Pa. For high values of angular frequency ω, the values of modules for individual samples are similar. This means that the samples store comparable amounts of energy in each deformation cycle. The obtained results of angular frequency sweep test are fully consistent with data presented in the literature for chitosan solutions with addition of bovine collagen.

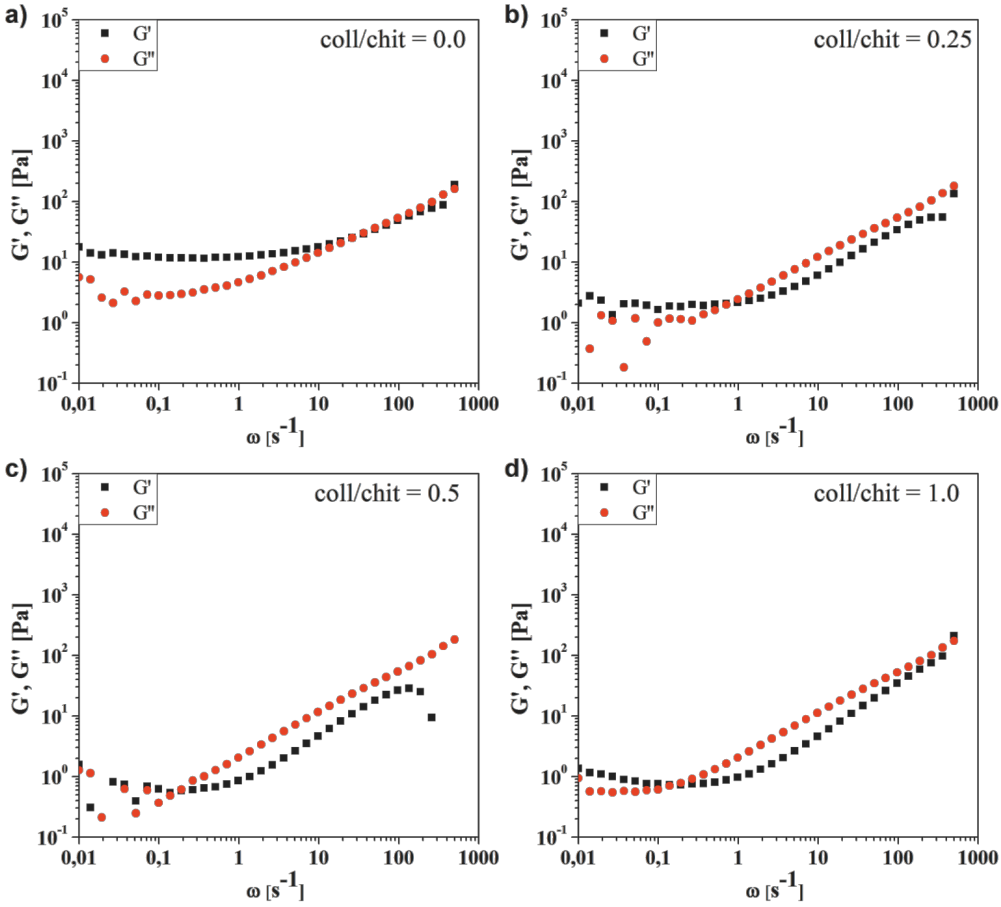

Fig. 3 Experimental curves of storage G' (■) and loss G" (●) moduli in a wide range of angular frequency ω, a) sample no. 1, b) sample no. 2, c) sample no. 3, d) sample no. 4 at temperature 25 °C.
Source: Author's

Interpretation of the results of measurements carried out for a higher temperature (Fig. 3) indicates that the dependences presented above are maintained. More precisely, the addition of collagen causes a stronger domination of viscous properties over elastic ones in a wider range of angular frequency and reduction the mechanical strength. However, for all experimental curves, a shift toward a stronger domination of the highly elastic region on the theoretical curve [21,32] is observed. For all samples, the dominance area of elastic properties over viscous ones is stronger noted. These shifts result from a change in the temperature at which the measurement is carried out and is characteristic for thermosensitive polymers and biopolymers systems. The obtained mechanical spectra indicate shortening the characteristic relaxation times. This parameter was determined as the inverse of the angular frequency ω, for which the intersection of the storage G' and loss G" curves was observed. Moreover, for samples no. 2 and 3, structure instabilities for low values of angular frequency, defined as discontinuities of the obtained experimental data were observed.

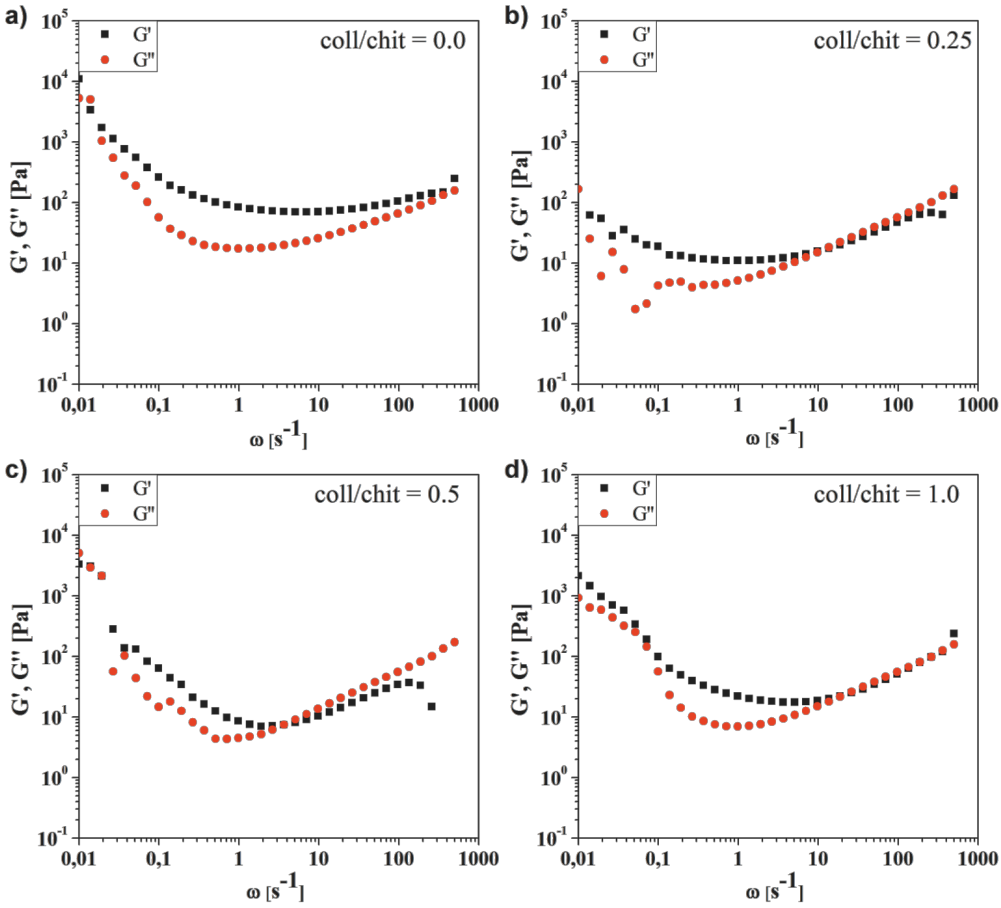

Fig. 4. Experimental curves of storage G' (■) and loss G" (●) moduli in a wide range of angular frequency ω, a) sample no. 1, b) sample no. 2, c) sample no. 3, d) sample no. 4 at temperature 30 °C.
Source: Author's

Further heating of the tested samples leads to the largest changes in the course of the experimental curves – Fig. 4. At 30 ° C, only the control sample (without the addition of collagen) in the whole range of the angular frequency shows the dominance of elastic properties over viscous ones (G' > G"). The addition of collagen leads to a change in the dominant properties of the tested solutions depending on the applied deformation. It is worth noting that the most similar shape, compared to sample no. 1, has a sample with the highest concentration of collagen – Fig. 4d. Although the shape of the experimental curves is similar, especially for low angular frequency ω, the storage G' and loss G" modules of sample no. 4 reach lower values by a decade compared to sample no. 1. In the case of samples no. 2 and no. 3 for low values of the angular frequency, the discontinuity of the obtained experimental data, which may indicate structural disorders, is again observed. It was also found that as the temperature of the measurement increases, the characteristic relaxation times for each solution are shortened. Their determination was possible only for samples containing a collagen additive. For those systems the unambiguous intersection of the experimental curves of the storage G' and loss G" modulus was observed.

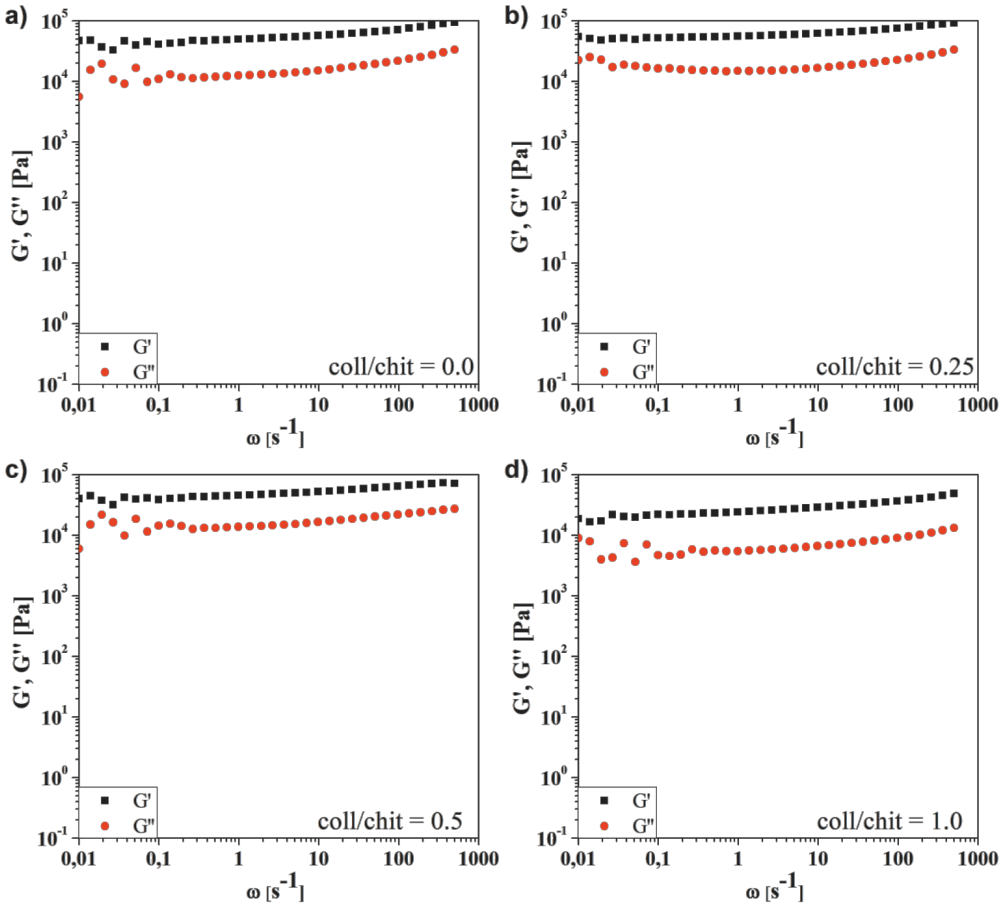

Fig. 5. Experimental curves of storage G' (■) and loss G" (●) moduli in a wide range of angular frequency ω, a) sample no. 1, b) sample no. 2, c) sample no. 3, d) sample no. 4 at temperature 40 °C.
Source: Author's

The mechanical spectra obtained at 40 ° C are shown in Fig. 5. For all samples tested, the independence of both experimental curves from the applied deformation, characteristic for gel phase, is observed. This demonstrates the formation of infinite, three-dimensional structure. Based on the values of storage modulus G', which represents the stored energy as well as strength or mechanical rigidity, the mean value was calculate – see Fig. 6. It has been found that the addition of collagen in the lowest concentration (0.25g collagen/1 g chitosan) leads to improvement mechanical strength. However, increasing the concentration causes a decrease in mechanical strength – Fig. 6. The negative effect of collagen addition on mechanical properties of chitosan hydrogels is consistent with the results of studies with bovine-derived collagen [21]. The obtained mechanical spectra at 35 °C were almost no different from the curves shown in Fig. 5. Samples at 35 °C were characterized by lower mechanical strength, both modules have reached lower values.

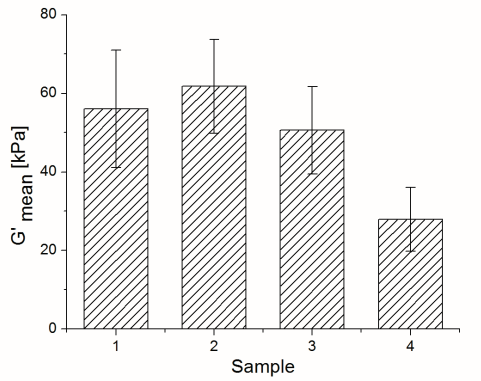

Fig. 6. The mean value of the storage modulus G ' with error bars for the full range of deformation at temperature 40 ° C.
Source: Author's

Conclusions

The conducted studies indicate a significant effect of fish collagen addition on the viscoelastic properties of colloidal chitosan solutions. Different viscoelastic properties cause different sol-gel phase transition temperatures. Regardless of the collagen concentration, an increase in gelation temperature was always observed. Moreover, it was shown that the dependence of sol-gel phase transition temperature is not a monotonous function of collagen concentration. Furthermore, the conducted research indicates that the presence of fish collagen negatively affects the mechanical strength of the obtained scaffolds, the lower values of the storage modulus G' was observed. Only the smallest concentration (0.25g collagen/1 g chitosan) of the collagen additive has improved the mechanical properties. The obtained results of viscoelastic properties as well as temperatures of sol-gel phase transition are consistent with the studies presented in literature for thermosensitive hydrogels chitosan-collagen of bovine origin.

Acknowledgements

This work was supported by the National Science Center of Poland – Grant NCN UMO – 2014/15/B/ST8/02512

References

[1] N.A. Peppas, P. Bures, W. Leobandung, H. Ichikawa, Hydrogels in pharmaceutical formulations, Eur. J. Pharm. Biopharm. 50 (2000) 27–46. doi:10.1016/S0939-6411(00)00090-4.

[2] S.K.L. Levengood, M. Zhang, Chitosan-based scaffolds for bone tissue engineering, J. Mater. Chem. B. 2 (2014) 3161–3184. doi:10.1039/C4TB00027G.

[3] W.E. Hennink, C.F. van Nostrum, Novel crosslinking methods to design hydrogels, Adv. Drug Deliv. Rev. 54 (2002) 13–36.

[4] D. Howard, L.D. Buttery, K.M. Shakesheff, S.J. Roberts, Tissue engineering: strategies, stem cells and scaffolds, J. Anat. 213 (2008) 66–72. doi:10.1111/j.1469-7580.2008.00878.x.

[5] J.L. Drury, D.J. Mooney, Hydrogels for tissue engineering: scaffold design variables and applications, Biomaterials. 24 (2003) 4337–4351. doi:10.1016/S0142-9612(03)00340-5.

[6] B. Jeong, S.W. Kim, Y.H. Bae, Thermosensitive sol–gel reversible hydrogels, Adv. Drug Deliv. Rev. 64 (2012) 154–162. doi:10.1016/j.addr.2012.09.012.

[7] M. Liu, X. Zeng, C. Ma, H. Yi, Z. Ali, X. Mou, S. Li, Y. Deng, N. He, Injectable hydrogels for cartilage and bone tissue engineering, Bone Res. 5 (2017) 17014. doi:10.1038/boneres.2017.14.

[8] A. Solouk, H. Mirzadeh, S. Amanpour, Injectable scaffold as minimally invasive technique for cartilage tissue engineering: in vitro and in vivo preliminary study, Prog. Biomater. 3 (2014) 143–151. doi:10.1007/s40204-014-0031-x.

[9] T. Garg, O. Singh, S. Arora, R. Murthy, Scaffold: a novel carrier for cell and drug delivery, Crit. Rev. Ther. Drug Carrier Syst. 29 (2012) 1–63.

[10] F.J. O'Brien, Biomaterials & scaffolds for tissue engineering, Mater. Today. 14 (2011) 88–95. doi:10.1016/S1369-7021(11)70058-X.

[11] T. Freier, H.S. Koh, K. Kazazian, M.S. Shoichet, Controlling cell adhesion and degradation of chitosan films by N-acetylation, Biomaterials. 26 (2005) 5872–5878. doi:10.1016/j.biomaterials.2005.02.033.

[12] Z. Chen, X. Mo, C. He, H. Wang, Intermolecular interactions in electrospun collagen–chitosan complex nanofibers, Carbohydr. Polym. 72 (2008) 410–418. doi:10.1016/j.carbpol.2007.09.018.

[13] K. Zhang, Y. Qian, H. Wang, L. Fan, C. Huang, A. Yin, X. Mo, Genipin-crosslinked silk fibroin/hydroxybutyl chitosan nanofibrous scaffolds for tissue-engineering application, J. Biomed. Mater. Res. A. 95A (2010) 870–881. doi:10.1002/jbm.a.32895.

[14] F. Yan, W. Yue, Y. Zhang, G. Mao, K. Gao, Z. Zuo, Y. Zhang, H. Lu, Chitosan-collagen porous scaffold and bone marrow mesenchymal stem cell transplantation for ischemic stroke, Neural Regen. Res. 10 (2015) 1421–1426. doi:10.4103/1673-5374.163466.

[15] L. Peng, X. R. Cheng, J. W. Wang, D. X. Xu, G. Wang, Preparation and Evaluation of Porous Chitosan/Collagen Scaffolds for Periodontal Tissue Engineering, J. Bioact. Compat. Polym. 21 (2006) 207–220. doi:10.1177/0883911506065100.

[16] Lie, C. Gao, Z. Mao, J. Shen, X. Hu, C. Han, Thermal dehydration treatment and glutaraldehyde cross-linking to increase the biostability of collagen–chitosan porous scaffolds used as dermal equivalent, J. Biomater. Sci. Polym. Ed. 14 (2003) 861–874. doi:10.1163/156856203768366576.

[17] C. Tangsadthakun, S. Kanokpanont, N. Sanchavanakit, T. Banaprasert, S. Damrongsakkul, Properties of collagen/chitosan scaffolds for skin tissue engineering, J. Met. Mater. Miner. 16 (2006). http://ojs.materialsconnex.com/index.php/jmmm/article/view/250 (accessed December 30, 2017).

[18] D. Wawro, W. Stęplewski, K. Brzoza-Malczewska, W. Święszkowski, Collagen-Modified Chitosan Fibres Intended for Scaffolds, Fibres Text. East. Eur. Nr 6B (96) (2012). http://yadda.icm.edu.pl/yadda/element/bwmeta1.element.baztech-a6957882-f6a1-42d5-84e4-91cc971380e9 (accessed December 30, 2017).

[19] J. Elango, J. Zhang, B. Bao, K. Palaniyandi, S. Wang, W. Wenhui, J.S. Robinson, Rheological, biocompatibility and osteogenesis assessment of fish collagen scaffold for bone tissue engineering, Int. J. Biol. Macromol. 91 (2016) 51–59. doi:10.1016/j.ijbiomac.2016.05.067.

[20] C.D.F. Moreira, S.M. Carvalho, H.S. Mansur, M.M. Pereira, Thermogelling chitosan–collagen–bioactive glass nanoparticle hybrids as potential injectable systems for tissue engineering, Mater. Sci. Eng. C. 58 (2016) 1207–1216. doi:10.1016/j.msec.2015.09.075.

[21] P. Owczarz, A. Rył, Z. Modrzejewska, M. Dziubiński, The influence of the addition of collagen on the rheological properties of chitosan chloride solutions, Prog. Chem. Appl. Chitin Its Deriv. 22 (2017) 176–189. doi:10.15259/PCACD.22.18.

[22] R. Sripriya, R. Kumar, A Novel Enzymatic Method for Preparation and Characterization of Collagen Film from Swim Bladder of Fish Rohu (Labeo rohita), Food Nutr. Sci. 06 (2015) 1468. doi:10.4236/fns.2015.615151.

[23] S. Yamada, K. Yamamoto, T. Ikeda, K. Yanagiguchi, Y. Hayashi, Potency of Fish Collagen as a Scaffold for Regenerative Medicine, BioMed Res. Int. (2014). doi:10.1155/2014/302932.

[24] M.M. Schmidt, R.C.P. Dornelles, R. Mello, E.H. Kubota, M. Mazutti, A. Kempka, I. Demiate, Collagen extraction process, Int. Food Res. J. 23 (2016) 913–922.

[25] P. Owczarz, P. Ziółkowski, Z. Modrzejewska, S. Kuberski, M. Dziubiński, Rheo-Kinetic Study of Sol-Gel Phase Transition of Chitosan Colloidal Systems, Polymers. 10 (2018) 47. doi:10.3390/polym10010047.

[26] A. Chenite, M. Buschmann, D. Wang, C. Chaput, N. Kandani, Rheological characterisation of thermogelling chitosan/glycerol-phosphate solutions, Carbohydr. Polym. 46 (2001) 39–47. doi:10.1016/S0144-8617(00)00281-2.

[27] S. Supper, N. Anton, N. Seidel, M. Riemenschnitter, C. Schoch, T. Vandamme, Rheological Study of Chitosan/Polyol-phosphate Systems: Influence of the Polyol Part on the Thermo-Induced Gelation Mechanism, Langmuir. 29 (2013) 10229–10237. doi:10.1021/la401993q.

[28] F. Chambon, H.H. Winter, Linear Viscoelasticity at the Gel Point of a Crosslinking PDMS with Imbalanced Stoichiometry, J. Rheol. 31 (1987) 683–697. doi:10.1122/1.549955.

[29] V. Vagenende, M.G.S. Yap, B.L. Trout, Mechanisms of Protein Stabilization and Prevention of Protein Aggregation by Glycerol, Biochemistry (Mosc.). 48 (2009) 11084–11096. doi:10.1021/bi900649t.

[30] V. Kumar, R. Chari, V.K. Sharma, D.S. Kalonia, Modulation of the thermodynamic stability of proteins by polyols: Significance of polyol hydrophobicity and impact on the chemical potential of water, Int. J. Pharm. 413 (2011) 19–28. doi:10.1016/j.ijpharm.2011.04.011.

[31] J. Cho, M.-C. Heuzey, A. Bégin, P.J. Carreau, Physical gelation of chitosan in the presence of beta-glycerophosphate: the effect of temperature, Biomacromolecules. 6 (2005) 3267–3275. doi:10.1021/bm050313s.

[32] S. Kasapis, J. Mitchell, R. Abeysekera, W. MacNaughtan, Rubber-to-glass transitions in high sugar/biopolymer mixtures, Trends Food Sci. Technol. 15 (2004) 298–304. doi:10.1016/j.tifs.2003.09.021.

Monika Janas, Alicja Zawadzka
Faculty of Process and Environmental Engineering, Lodz University of Technology,
90-924 Lodz, Wolczanska 213
monika.janas@edu.p.lodz.pl

ASSESSMENT OF ENVIRONMENTAL IMPACT OF AGRICULTURAL BIOGAS PLANTS

Abstract
Operation of biogas plants, anaerobic fermentation processes, collection and purification of biogas and its subsequent combustion may be a source of environmental hazard. The construction and operation of biogas plants is inextricably connected with the generation and emission of solid, liquid and gaseous pollutants into the environment. The aim of the work is to analyze environmental hazards resulting from the construction and operation of biogas plants. As part of the work, a comprehensive analysis of their impact on individual components of the environment was made. The effect of biogas plants on atmospheric air, soil and water environment and acoustic climate was analyzed and the potential range of these impacts was presented.

Key words
agricultural biogas plant, biomass, biogas, environmental impact

Introduction

Deepening climate changes and increasing environmental pollution contribute to undertaking actions to reduce emissions from some industrial processes. Power industry is a sector that particularly burdens the environment, especially since it is based mainly on conventional (nonrenewable) resources, i.e. hard coal, crude oil and natural gas. An alternative to burning fossil fuels is the production of energy from renewable sources such as wind, water, sun, geothermal resources and biomass. This last source is the most prospective for Poland. Biomass can be obtained from three main organic wastes: from agri-food industry, from municipal waste and from animal waste (agricultural sector). In Poland, 377,000 tons of waste is produced annually in the fruit and vegetable processing sector and 661,000 tons is generated by meat processing industry. Both types of waste are good raw materials for biogas plants. On the other hand, Polish agriculture produces 80,700,000 tons of manure and about 35 million m^3 of liquid manure per year. Of this about 30% can be used for biogas production [1]. Depending on the nature and composition of biomass, it can be used for the production of solid fuels, liquid and gas biofuels. A wide range of technologies of biomass processing for energy, biomass availability and diversification are an opportunity for farms that can become important suppliers of energy resources and consumers of energy from these sources [2-4].

One of the processes that use biomass for energy purposes, which can be applied in agricultural farms, is methane, anaerobic fermentation carried out in agricultural biogas plants. According to the type of biomass feedstock, biogas derived from anaerobic fermentation typically contains 52–85% methane (CH_4), 14–50% carbon dioxide (CO_2) and trace amounts of hydrogen sulfide (H_2S), ammonia (NH_3), siloxanes, hydrogen (H_2), nitrogen (N_2), oxygen (O_2) and other gas pollutants. The composition of biogas is variable and depends mainly on the raw material used and technological process being implemented [5].

Biogas production is still very controversial in Poland. On the one hand, biogas plants as new objects in the modern countryside are important for acquiring green energy. On the other hand, the construction and operation of such facilities is connected with the generation and emission of pollutants into the environment [3-5].

The aim of the work is the analysis of threats to the environment and agricultural landscape in the aspect of emerging new installations such as biogas plants. The impact of biogas plants on particular components of the environment including atmospheric air, soil and water as well as acoustic climate was analyzed.

Characteristics of biogas and agricultural biogas plants

Directive 2009/28/EC defines biogas as 'gaseous fuel produced from biomass and/or a biodegradable part of waste that can be purified to the quality of natural gas, for use as biofuel, or wood gas' [8]. According to national legislation, biogas is 'the gas obtained from biomass, in particular from installations for treating animal or vegetable waste, sewage treatment plants and landfills', and agricultural biogas is defined as 'the gas obtained in the process of methane anaerobic fermentation of agricultural raw materials, agricultural by-products, liquid or solid animal manure, by-products, wastes or residues from the processing of products of agricultural origin or forest biomass, or plant biomass collected from the areas other than those recorded as agricultural or forestry, excluding biogas obtained from raw materials originating from sewage treatment plants and landfills' [9]. In its chemical composition, this gas contains mainly methane, which accounts for 52-85% of the composition of the mixture. Its composition depends strictly on the type of material being fermented and its dry matter content. Typical contents of individual components in biogas are presented in Table 1, while Table 2 gives the amount of biogas yield from various substrates [5-7].

Table 1. Biogas composition

Component	Content %	Average content %
Methane CH_4	52 – 85	65
Carbon dioxide CO_2	14 – 48	34.8
Hydrogen sulfide H_2S	0.08 – 5.5	0.2
Hydrogen H_2	0 – 5	Trace amounts
Carbon monoxide CO	0 – 2.1	Trace amounts
Nitrogen N_2	0.6 – 7.5	Trace amounts
Oxygen O_2	0 – 1	Trace amounts
Ammonia NH_3	<1	Trace amounts
Siloxane	0-0.02	Trace amounts
VOC	<0.6	Trace amounts

Source: Authors' report based on [3]

Table 2. Amount of biogas and methane acquired from agricultural waste

Substrate	Amount of biogas		CH_4 content [% vol.]
	[m^3/t substrate]	[m^3/t organic *dry matter]*	
Corn silage	170-200	450-700	50-55
Cattle slurry	20-30	200-500	60
Pig slurry	20-35	300-700	60-70
Cattle manure	40-50	210-300	60
Pig manure	55-65	270-450	60
Chicken manure	70-90	250-450	60

Source: [5]

The properties of biogas produced in the process of biochemical transformations in the absence of oxygen make it important in the economic sense [3]. Biogas is a medium-energy fuel that can be used in industry, in households and in agriculture as a heat and electric energy carrier, or be used as fuel for vehicles [4-6]. The percentage of methane in biogas determines the calorific value, i.e. energy properties. The greater its share, the greater the calorific value of biogas. Biogas containing about 65% of methane usually has a calorific value of 23MJ/m^3, which after purification reaches up to 35MJ /m^3 [6].

Agricultural biogas is produced in a set of devices which together constitute a biogas plant. In the biogas plant a strictly defined technological process (methane fermentation of biomass) is carried out and, as a result, biogas is produced. The construction and operation of such an installation is a major resource and logistical challenge. The construction of each such facility is individual and depends on various factors, mainly on the type of batch material. Due to the type of substrates used, biogas plants are classified into several types. One of them are agricultural biogas plants in which agricultural products or wastes from the agri-food industry are processed [2-

4]. The basic parameters affecting the energy balance of such a biogas plant include the type of material fermented and its dry matter content, quantitative proportions of ingredients (in the case of so-called co-fermentation, i.e. fermentation of at least two raw materials from different sources), temperature and its fluctuations over time, hydraulic retention time, amount and frequency of feed supply, fermentation chamber load, frequency and accuracy of mixing [3, 6].

An agricultural biogas plant, due to its specificity, is an installation that makes it possible to rationally solve the problem of managing various organic wastes, generating electricity and heat as well as digestates which are an excellent fertilizer, and contributing to the reduction of emissions of harmful substances, mainly methane emissions from the agricultural sector [7].

The object of study

The analysis of the environmental impact of a biogas plant is based on a functioning agricultural biogas plant. As a result of the combustion of biogas from anaerobic fermentation of organic substrates (maize silages), electricity and heat are generated in the cogeneration unit. The installation consists of a biomass feeding system and a tank of liquid substrates, two digesters operating in a flow-retention system, a storage tank for fermented substrates, a cogeneration unit, an emergency flare, and accompanying infrastructure, which consists of vehicle weighing scales, maneuvering areas and internal roads, transformer station and office facilities. The total area of the agricultural biogas plant is about 1.3 ha (13,000 m^2), of which the fermentation block covers an area of about 2000 m^2, internal roads, maneuvering areas and other paved areas about 1000 m^2, a separation block about 200 m^2, a social block about 20 m^2, and silage silos about 3600 m^2. In the biogas plant, approximately 4,340 MWh of electricity, about 15,662 GJ of thermal energy and about 12,000 ton/year of natural fertilizers are produced per year.

Silage for the production of biogas accumulated in storage silos is fed via a storage tank to digesters where the process of methane (anaerobic) fermentation consisting of four phases takes place. The fermentation liquid transported to a storage tank specifically designed for its collection is then pumped and used as a natural fertilizer in agriculture. The produced biogas is first subjected to a biological desulfurization process. This process is carried out by bacteria called Sulfobacter oxidans, which in the presence of oxygen convert hydrogen sulfide to pure sulfur and water. Only after the removal of hydrogen sulfide, biogas is directed to the cogeneration module – a gas engine in which the chemical energy of biogas is converted into electricity and heat. Part of the electricity is resold to a power plant, while heat energy is used in technological processes (to maintain the necessary temperature in digesters or to dry filter cake). If the cogeneration system does not work, biogas is burnt in a gas flare. Such cases usually last short and are sporadic. The biogas power plant is equipped with devices and subassemblies ensuring safe operation (including biogas detection system, separate level and pressure protection systems) and remote monitoring (control and monitoring automation systems).

Analysis of environmental impact of a biogas plant

The construction and operation of an agricultural biogas plant, like any other industrial plant, carry some risks. Each such investment causes the generation and emission of solid, liquid and gaseous pollutants to the environment.

Emissions of pollutants to the atmosphere

The greatest concerns are related to the emissions of atmospheric pollutants such as nitrogen dioxide, sulfur dioxide, carbon monoxide, particulate matter, aromatic hydrocarbons and non-standard odorous substances (hydrogen sulfide). During the operation of a biogas plant, the source of small stack emission to the atmosphere is biogas combustion in the TCG 2016 V16 gas engine coupled with an electric generator (CHP), or in emergency situations in a flare, i.e. an emergency flare to burn excess biogas.

Emissions of nitrogen dioxide, carbon monoxide and formaldehyde were calculated based on engine emission standards defined by the manufacturer, and sulfur dioxide emissions were calculated using values presented in the study entitled “Guidelines for provincial emission inventories for current assessments and air protection programs” [10]. The results of emissions from energy biogas combustion in a cogeneration unit are summarized in Table 3. This emission does not exceed the emission standards for biomass combustion installations [11].

Table 3. Calculated emission of pollutants from the CHP unit

Pollutant type	Emission	Emission standard for biomass combustion installations
	[mg/m^3]	[mg/m^3]
Sulfur dioxide SO_2	8	200
Nitrogen dioxide NO_2	350	500
Carbon monoxide CO	210	300
Formaldehyde CH_2O	45	60

Source: Authors'

During the operation of an agricultural biogas plant, the source of fugitive emissions is the process of maize ensiling and storage in silos as well as storage and application of fermentation liquid in the fields. Maize silage is produced and stored in two silos. In order to ensure anaerobic conditions, the silos are filled in the shortest possible time, and then they are tightly covered with plastic sheets and loaded to keep the sheeting in place. The range of emissions of compounds being the products of lactic fermentation (lactic acid, acetic acid, ethyl alcohol, carbon dioxide, hydrogen and others) is limited to the nearest vicinity of the silos. The fermentation liquid is stored in sealed tanks, which practically minimizes emissions to the air. The retention time in digesters enables complete degradation of the organic part of the substrate and elimination of odor substances such as volatile fatty acids and hydrogen sulfide due to biochemical transformation. As a result, the fermentation liquid contains only traces of volatile organic acids causing the emission of odors such as: acetic acid, butyric acid, lactic acid or propionic acid. These emissions occur cyclically, without causing a nuisance in the areas adjacent to the plant.

In the biogas plant there is minimal fugitive emission (including carbon monoxide, oxide and nitrogen dioxide, aldehydes, lead and polyaromatics (benzo[a]pyrene)), which is associated with the combustion of fuels in diesel engines (bulldozers) and means of transport moving around it. It has a negligible effect on the cleanliness of air in the biogas plant area.

Impact on the soil and water environment

The main waste produced in the analyzed agricultural biogas plant as a result of anaerobic fermentation of substrates of organic origin (maize silage) is fermentation liquid. The amount of fermentation liquid produced in a biogas plant per year is shown in Table 4.

Table 4. Amount of produced fermentation liquid vs. the quantity of loaded substrates

Substrates	Mass	Organic dry matter	Organic dry matter prior to the process	Organic dry matter decomposi-tion	Organic dry matter after the process	Mass
	[ton/year]	[%]	[ton/year]	[%]	[ton/year]	[ton/year]
Maize silage	10 000	96	3 360	60	1344	7984
Water	4 000	0	0	0	0	40 000
Total:	**14 000**		**3 360**			**11 984**

Source: Authors'

The 14,000 ton/year of substrates processed in the biogas plant per year results in the decomposition of 2016 ton/year of dry organic matter and production of about 12,000 ton/year of fermentation liquid (about 7.2% d.m.) per year. The fermentation mixture is recovered by means of the R10 recovery process – Spreading on the ground for fertilization or soil improvement – under the conditions specified, i.e. in the Regulation on the R10 recovery process of the Minister of the Environment of 20 January 2015 [12].

The biogas plant also produces small amounts of waste from technical and social facilities, waste from maintenance and repairs of used machines, packaging waste as well as cleaning waste. Due to the proper management of solid waste – selective collection and temporary collection of waste, and then transfer for

recovery or disposal to appropriate companies with proper permits for waste management required by law, they do not pose a threat to the environment.

In the analyzed agricultural biogas plant no process wastewater is generated. In the process consisting in the production of biogas, due to cooling of the biogas in a shell-and-tube exchanger only a condensate of water is formed with traces of impurities dissolved in it, i.e. ammonia and hydrogen sulfide. The resulting condensate is collected in a check tank and then recycled to the biogas plant. Therefore, only wastewater from social facilities is generated in the plant. It is discharged into tight septic tanks which, in turn, are successively emptied with the use of specialized vacuum trucks transporting wastewater to a sewage treatment plant.

In addition, as a result of rinsing internal roads and maneuvering area in the biogas plant on the surface of paved areas rainwater is contaminated due to settling of air (particulate matter) and vehicle pollutants. Concentrations of oil derivatives and total suspended solids on the plant site are definitely lower than the maximum permissible concentration values of these substances in sewage introduced into water and soil established in the Regulation of the Minister of Environment of 18 November 2014 on conditions to be met when introducing sewage into water or soil, and on substances particularly harmful to the aquatic environment, i.e. <100 mg/l of total suspended solids and <15 mg/l of petroleum hydrocarbons [13]. Rainwater is also formed within the silage silos. Leachates from the silos are discharged into the nearby wells and then used in the anaerobic fermentation process. In order to reduce formation of the leachates the silos are tightly covered with plastic sheets.

Impact on the acoustic climate

In the biogas plant, noise is generated by a functioning cogeneration unit and pumping system as well as vehicle traffic on the plant site. Due to the location of devices inside the building and low traffic, the permissible noise levels are not exceeded in the nearest areas in terms of acoustic climate, both at day and night time, as defined in the Regulation of the Minister of Environment [14].

Summary and conclusions

The construction and operation of every industrial plant, including an agricultural biogas plant, poses a threat to the natural environment. To indicate the impact of biogas plants on the environment, a comparison was made in the form of the Leopold matrix which in three steps evaluates the impact of the analyzed agricultural biogas plant on individual elements of the environment – Table 5.

In the matrix, a potential environmental impact was assessed. Digits specify the subjective impact of biogas plants on the environment (small – 1 to 2, moderate – 3 to 5 and large – 6 to 10).

Table 5. Leopold matrix for potential environmental impacts of biogas plants

Environmental impact / Elements of the environment	Regime modification	Surface transformation	Urbanization and structures on the surface	Changes in vehicle traffic	Pollutant movement	Use of chemicals	Extraordinary hazards and accidents
Soil	2 ○		3 ●	4 ●	4 ●	1 ○	2 ○
Water	1 ○	1 ○		4 ●	3 ●	1 ○	2 ○
Atmosphere	4 ●		4 ●	5 ●			2 ○
Land use	3 ●	1 ○				1 ○	
Qualities of the landscape	2 ○						
Infrastructure		1 ○	3 ●	2 ○			

Impact level: ○ - weak ● - medium ● - strong

Source: Authors'

The most important impacts of agricultural biogas plants on the natural environment, which according to Leopold's matrix have medium intensity, include atmospheric air – covering energy emissions of gases generated as a result of biogas combustion in CHP units and noise propagation, and water and soil environment – in terms of potential soil and groundwater contamination with fermentation liquid, leachates from maize silage silos and rainwater. However, due to the full tightness of all installations, the use of protective devices and correct and environmentally safe methods of handling substrates, fermentation mixture, fermentation liquid, generated sewage and solid waste, the analyzed agricultural biogas plant does not have a significant negative impact on the environment, and the occurring impacts are small and do not go beyond the plant boundaries.

The biogas production technology has a high development potential in Poland due to significant resources of raw materials, the demand for energy in a distributed system and the need to meet obligations concerning production of energy from renewable sources [2]. It also provides opportunities for rural development, new jobs, stable market for agricultural products and economic development. The undeniable advantages include, among others, creation of a local source of 'clean' electricity and heat, and reduction of pollutant emissions through the use of renewable fuel for the production of energy (substitution of fossil fuels), and thus the implementation of low-carbon economy programs. Combustion of biogas is associated with a hundredfold lower emission of sulfur dioxide and three times lower emissions of nitrogen oxides as compared to emissions from coal combustion. In addition, the stable and efficient organic fertilizer produced in biogas plants in the form of fermentation liquid ensures recycling of nutrients in the soil and reduces the demand for fertilizers [3-6].

Many economic, social and environmental benefits that result from biogas production mean that biogas plants have a chance for dynamic development in Poland.

Acknowledgements
This research did not receive any specific grant from funding agencies in the public, commercial, or not-for-profit sectors.

References

[1] Environmental Protection 2016, Central Statistical Office, Warsaw

[2] M. Collotta, G. Tomasoni, The environmental sustainability of biogas production with small sized plant, Energy Procedia. 128 (2017) 38-45.

[3] B. Igliński, R. Buczkowski, M. Cichosz, Biogas production in Poland – current state, potential and perspectives. Renew Sust Energ Rev. 50 (2015) 686-695.

[4] A. Oniszk-Popławska, M. Matyka, E.D. Ryńska, Evaluation of a long-term potential for the development of agricultural biogas plants: A case study for the Lubelskie Province, Poland. Renew Sust Energ Rev. 36 (2014) 329-349.

[5] M. Fugol, J. Szlachta, Zasadność kiszonki z kukurydzy i gnojowicy świńskiej do produkcji biogazu. Inżynieria Rol. 1 (2010) 169-174.

[6] M. Muradin, Z. Foltynowicz, Potential for producing biogas from agricultural waste in rural plants in Poland. Sustainability. 6(8) (2014) 5065-5074.

[7] M. Kimming, C. Sundberg, A. Nordberg, A. Baky, S. Bernesson, et al., Biomass from agriculture in small-scale combined heat and power plants – A comparative life cycle assessment, Biomass and Bioenergy. 35 (2011) 1572-1581.

[8] European Parliament Directive 2009/28/EC of the European Parliament and of the Council of 23 April 2009 Off J Eur Union, 140 (2009).

[9] Ustawa z dnia 20 lutego 2015r. o odnawialnych źródłach energii (Dz.U. 2015 poz. 478).

[10] Wskazówki dla wojewódzkich inwentaryzacji emisji na potrzeby ocen bieżących i programów ochrony powietrza, Ministerstwo Środowiska, Główny Inspektorat Ochrony Środowiska, Warszawa 2003.

[11] Rozporządzenie Ministra Środowiska z dnia 4 listopada 2014 r. w sprawie standardów emisyjnych dla niektórych rodzajów instalacji, źródeł spalania paliw oraz urządzeń spalania lub współspalania odpadów (Dz.U. 2014 poz. 1546).

[12] Rozporządzenie Ministra Środowiska z dnia 20 stycznia 2015 r. w sprawie procesu odzysku R10 (Dz.U. 2015 poz. 132).

[13] Rozporządzenie Ministra Środowiska z dnia 18 listopada 2014 r. w sprawie warunków, jakie należy spełnić przy wprowadzaniu ścieków do wód lub do ziemi, oraz w sprawie substancji szczególnie szkodliwych dla środowiska wodnego (Dz.U. 2014 poz.1800).

[14] Rozporządzenie Ministra Środowiska z dnia 1 października 2012 r. zmieniające rozporządzenie w sprawie dopuszczalnych poziomów hałasu (Dz.U. 2012 poz.1109).

Anna M. Pozdniakova
Research Centre of Industrial Problems of Development of NAS of Ukraine
Inzhenernyy prov., 1a, 61166 Kharkiv, Ukraine, mira37cle@gmail.com

SMART CITY STRATEGIES "LONDON-STOCKHOLM-VIENNA-KYIV": IN SEARCH OF COMMON GROUND AND BEST PRACTICES

Abstract
The article aims to analyse the strategies of the selected progressive smart cities (London-Stockholm-Vienna) based on the methodology described below along with the strategy of the emerging smart city (Kyiv). The idea is to see which components of Smart Sustainable city Framework are covered by the "actual" strategies and how they are presented, which projects are currently underway and prioritised and how the evolvement process goes in different cities. We wanted to find common elements and approaches among the selected cities along with the best practices which can be taken into account by the cities when developing their own Smart City Strategy based on the experience already available.

Key words
Smart Sustainable city, strategy, ICT, sustainability, digitalization, "Triple bottom line".

Introduction

Urbanization and its consequences combined with the fast ICTs development led to establishment of a new trend in urban studies during late 90th, a so called "Smart Sustainable cities" concept. Typing this term in search engine today will generate more than 15 million hits [1]. According to Navigant Research, the global market for smart city solutions and services is expected to grow from US$40.1 billion in 2017 to US$97.9 billion in 2026 [2]. The initially limited concept that focused only on technology aspect was successfully overcome by the following waves of smart cities that focus on actually making cities smart instead of just forming a market for tech solutions (i.e. Smart City 3.0 concept). However, nowadays, the concept still remains vague and uncertain, allowing basically any city in the world to claim its "smartness" and "sustainability". For example, according to IHS Technology by 2025 we will have at least 88 smart cities worldwide, that are working on the integration of information, communications and technology (ICT) solutions across three or more different functional areas of a city (mobile and transport, energy and sustainability, physical infrastructure, governance, safety and security). While according to a new report from Navigant Research, there are more than 250 smart city projects from 178 cities around the world with the majority focus on government and energy initiatives [2].

In 2017, a number of cities that rely on a comprehensive smart city plan instead of simply implementing a few separate innovative projects without an overall smart plan increased tremendously [3]. For the years different academics (Cohen B, Giffinger R., Lombardi P., Schaffers H., Murray A., Minevich M. and Abdoullaev A etc.), institutions (EU, UN-Habitat, IESE, OECD) and businesses (Arup, IBM, Siemens, Ericsson) managed to produce many theoretical concepts on components and definition of the term.

However, the current article aims to review the question from the practical point of view, thus analysing 4 selected smart cities with formally accepted strategies and comparing them to understand what sustainability and smartness mean in a city context and what best practices can be applied by the emerging smart cities preparing their strategies and development plans. In order to address this aim, the paper sets the following research objectives:

- Based on our subjective criteria to select 3 cities that aim to become smart and sustainable and possess formally accepted strategies for development;
- To review their strategies, websites, positions in international rankings and development process;
- To create a comparison table and summarizing chart for the selected cities;
- To draw a conclusion on key pointers that allow to create a comprehensive and successful smart city strategy.

To achieve the aims we have used the methods of theoretical, logical and systematic analysis of literature (strategies, agendas, plans) along with the methods of comparative analysis.

Research Framework

The definition suggested by the ITU (International Telecommunication Union) for a Smart sustainable city is considered to be one of the most comprehensive till date. It states, that "A Smart sustainable city is an innovative city that uses ICTs and other means to improve quality of life, efficiency of urban operation and services, and competitiveness, while ensuring that it meets the needs of present and future generations with respect to economic, social and environmental aspects". They have identified 6 factors that are crucial for smart sustainable cities building and development: smart living, smart people, smart environment and sustainability, smart governance, smart mobility and smart economy.

Below you may find components distinguished by different schools (Table 1).

Table 1. Smart City components

Author/Concept	Components
Barrionuevo, 2012, the basis for IESE Cities in motion index	▪ Economic (GDP, sector strength, international transactions, foreign investment); ▪ Human (talent, innovation, creativity, education); ▪ Social (traditions, habits, religions, families); ▪ Environmental (energy policies, waste and water management, landscape); ▪ Institutional (civic engagement, administrative authority, elections).
Kourtit and Nijkamp 2012	▪ Economy and innovation: creative economic and entrepreneurial capital; ▪ Mobility: infrastructural, logistic, connectivity and communication capital; ▪ Society: social and cultural capital; ▪ Ecology: environmental and ambiance capital.
Giffinger R. et al. (2007)	▪ Smart Economy (Competitiveness); ▪ Smart People (Social and Human capital); ▪ Smart Governance (Participation); ▪ Smart Mobility (Transport and ICT); ▪ Smart Living (Quality of life); ▪ Smart Environment (Natural resources).
Nam and Pardo, 2012	▪ Technology Factors (Physical infrastructure, Smart technologies, Mobile technologies, Virtual technologies, Digital networks); ▪ Institutional Factors (Governance, Policy, Regulations); ▪ Human Factors (Human infrastructure, Social capital).
ITU (International telecommunication Union)	▪ Economic: The ability to generate income and employment for the livelihood of the inhabitants; ▪ Social: The ability to ensure well-being (safety, health, education etc.) of the citizens can be equally delivered despite differences in class, race or gender; ▪ Environmental: The ability to protect future quality and reproducibility of natural resources; ▪ Governance: The ability to maintain social conditions of stability, democracy, participation, and justice.
Arcadis sustainable city index	▪ People; ▪ Planet; ▪ Profit dimensions.
Networked Society Index Ericsson	▪ Triple Bottom Line: - Social (Health, education, social inclusion), - Economy (Productivity and competitiveness), - Environment (Resources, pollution, climate change). ▪ ICT (affordability, usage, infrastructure).

Author/Concept	Components
Smart City Wheel (Boyd Cohen)	▪ Smart People (Embrace creativity, inclusive society, 21 century education); ▪ Smart Economy (Entrepreneurship, productivity, local and global interconnectedness); ▪ Smart Environment (Green buildings, green energy, green urban planning); ▪ Smart Governance (Enabling supply and demand side policy, transparency & open data, ICT and e-gov); ▪ Smart Living (Culturally vibrant and happy, safe, healthy life); ▪ Smart Mobility (Mixed-modal access, clean and non-motorized options, integrated ICTs).

Source: Author's based on [4, 5, 6, 7, 8, 9, 10, 11]

As seen from the table above, most researchers cover in their analysis 4 dimensions: Smart People, Smart Economy, Smart Environment (that represent a so called "Triple bottom line") and Smart Governance that is included into each of the mentioned above dimensions but also represents the ability to ensure social stability, justice and participation. To this we add ICTs component as a helping tool to build a Smart City Framework. Author's generalization is presented below:

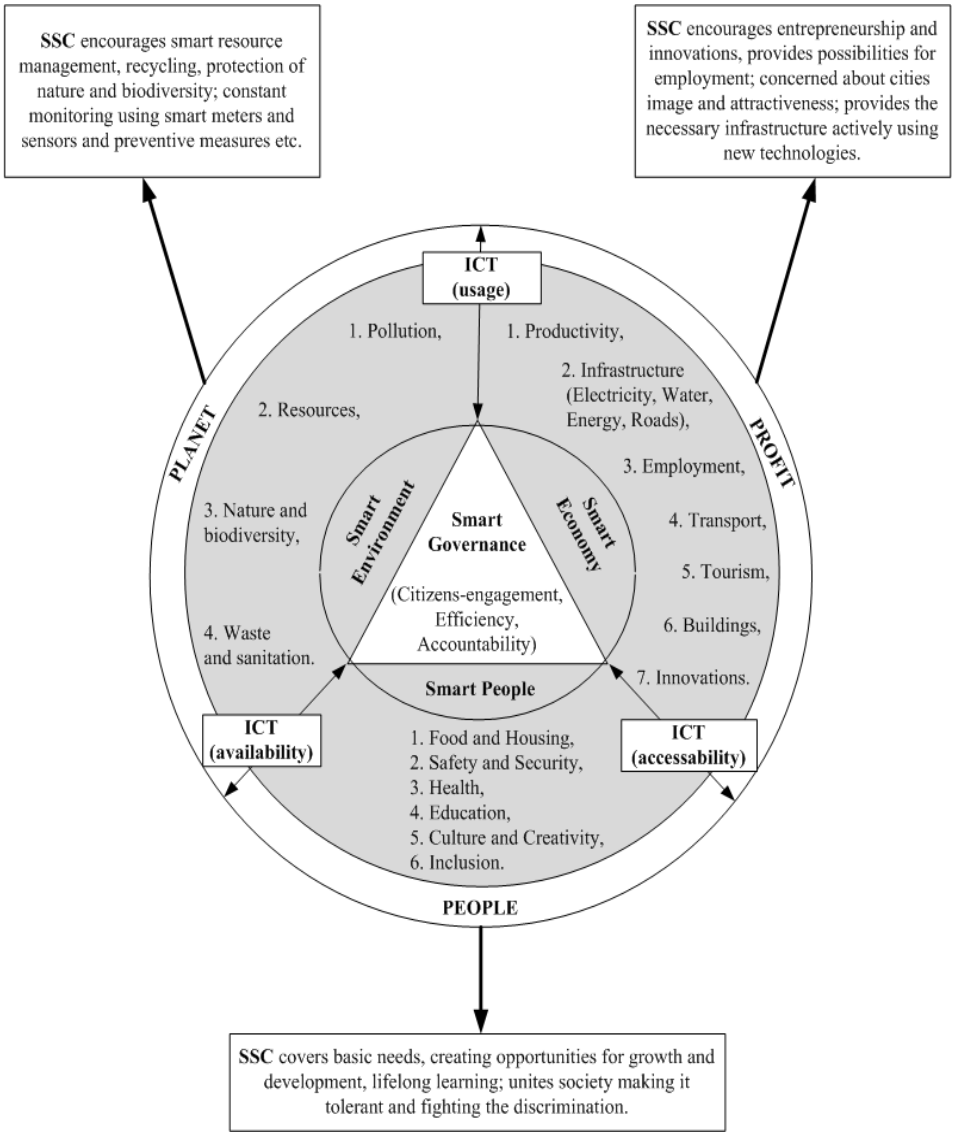

Fig. 1. Smart Sustainable city Framework
Source: Author's

In our research we would like to review which components are presented in the strategies of the selected Smart Cities.

Selection of Cities

Our aim is to compare three selected European cities strategies along with Kyiv Smart city that just started its way of "smartization".We have used the following selection process:

1) Checked the top lists of the indexes that measure smartness and sustainability (Arcadis sustainable city index, Cities in motion index, Networked society index, Global Power City Index) (see Table 2);
2) Checked conformation to the general idea of smart city concept (definition, components);
3) Filtered the cities according to strategic approach to become smart (formally accepted);
4) Checked availability of the up-to-date information (See Fig. 2).

Table 2. European cities positions in different rankings measuring smartness and sustainability

Ranking	Arcadis sustainable city index	Cities in motion index	Networked society index	Global Power City Index
1	Zurich	London	Stockholm	London
2	Stockholm	Paris	London	Paris
3	Vienna	Berlin	Paris	Amsterdam
4	London	Amsterdam	Copenhagen	Berlin
5	Frankfurt	Zurich	Helsinki	Frankfurt

*We have included only European cities in rankings, removing other continents.
Source: [8, 10, 11, 12]

Based on our methodology, we have selected 3 cities: Stockholm, London and Vienna along with Kyiv as mentioned above, since this city is actively developing its Strategy and concept and we are in a search of some best practices that might be applied here.

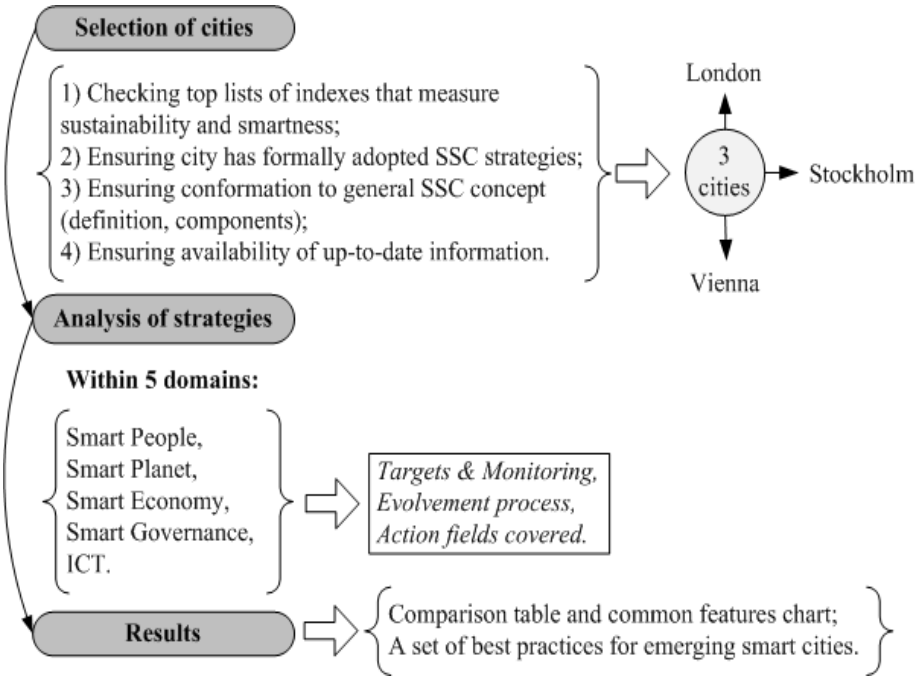

Fig. 2. Methodology of research
Source: Author's

Sector comparison according to Cities in Motions Index 2017 for the selected cities provides some basic overview of the strong and weak sides of each city (Fig. 3.).

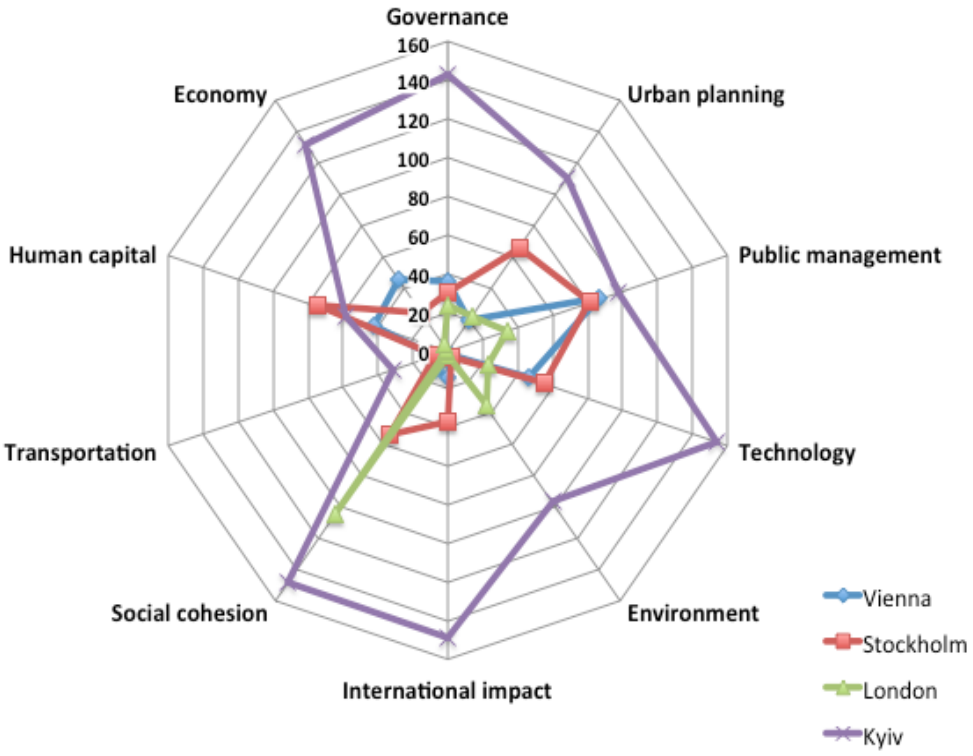

Fig. 3. Cities in Motion index comparison for the selected cities
Source: Author's based on [8]

Overall, Kyiv has the worst positions in most categories. For Vienna - Public management and Technology form the negative pick, for Stockholm - Public Management and Human Capital, for London - Social cohesion.

Smart City London Strategy

In December 2013 the Mayor's Smart London Plan was published, it outlines how data and technology can be used to improve Londoners' lives. The plan includes measurements of success and targets with the desired deadlines. The same year Smart London Board was established, it includes academics and entrepreneurs as a helping hand to authorities. In 2016 an updated version of plan was issued, outlining the progress in different areas.

According to Smart London Plan, Smart London is where the linkages between different city systems are better understood, where digital technology is used to better integrate these different systems, and London as a whole works more efficiently as a result - for the benefit of its inhabitants and visitors [13].

Smart City Vienna Strategy

The initiative "Smart City Wien" was announced by the Mayor of Vienna in march 2011 and after cooperation between civil society, research institutions, private sector and city administration the strategy was accepted in June 2014. The strategy states that its key goal for 2050 is to offer optimum quality of life, combined with the highest possible resource preservation, for all citizens, which can be achieved through the comprehensive innovations [14].

The evolvement of Smart City includes the following stages thus covering intermediate objectives:

1) Short-term planning (2012 – 2015) − Implementation of first measures/demo-sites;
2) Medium-term planning (Roadmap for 2020 and beyond) − Development of „Low Carbon" Scenarios and package of measures;
3) Long term thinking (Vision 2050) − Includes CO2 Reduction, Energy-Efficiency and Production of renewable Energy.

Smart City Stockholm Strategy

A strategy for Stockholm as a smart and connected city has been formally adopted by the City Council of Stockholm on April 3, 2017. However, the actual development began much earlier. The city is a member of GrowSmarter EU project, which brings together cities and industry to develop and spread 12 smart city solutions in energy, infrastructure and transport sectors. City's Vision for 2040 states that by the year 2040, Stockholm should become the smartest city in the world. According to the strategy, a smart city is a city that utilizes digitalization and new technology to simplify and improve the life for its residents, its visitors and businesses [15].

Smart City Kyiv Strategy

The strategy was developed in 2015 and accepted in 2017, it supposes close cooperation between private, public sectors and end-users. Kyiv smart city is a modern city management model based on advanced knowledge and introduction of modern information and communication technologies aiming to create a comfortable urban environment along with a stable, successful and prosperous future of citizens [16].

According to strategy transformation into a smart city requires 3 levels of changes:

1) Technological changes (city is a system of systems: accumulation, storage and analysis of data; open data; creation of an open integrated architecture and operating platform of the city);
2) Changes in governance (integration and optimization of city governance: establishment of the department of innovations and information technologies, office of the mayor of "Smart city", situational centre (centralized management 24/7), e-services);
3) Society changes (participatory platform: society-university-business; social media as a cooperation tool; crowdsourcing, innovative cluster, hackathons, hubs, networks, citizens as smart users).

ICT and technology sector

London is one of the leaders in technologies and digitization, around 78% of adults own a smartphone and 90% of population have access to the internet. Free WI-FI is provided for over 80 public buildings and libraries. There are 40,000 digital businesses and 200,000 employees in London's technology sector.

High-speed affordable digital connectivity is a priority for the city. The Connectivity Advisory Group has been established and Connectivity Summits are being held constantly to ensure everyone in London has access to affordable high-speed connectivity. A connectivity map was created in 2014 to assist in decision-making process. Along with the Mayor's Digital Connectivity Rating Scheme (2015), which allows to rate the quality of digital connectivity in buildings and provides the corresponding status (a platinum, gold, silver or bronze) along with the possible improvements. Afterwards the rating is listed on a searchable property directory. Recently created London DataStore plays an important role in overcoming city challenges, it allows keeping citizens up-to-date and helps to create applications based on the raw data available [13].

Stockholm is believed to be one of the most connected cities in the world with the largest open fibre network Stokab. Starting from 1994 the City has strategically invested in the development of an open, fibre network for everyone. Stokab aimed to build a competition-neutral infrastructure to satisfy future communication needs, boost economic activity, diversity and freedom of choice, as well as minimising disruption to the city's streets [17]. So today the city enjoys 100% broadband coverage and ranks #1 in Networked society index 2016 [11]. Open Stockholm portal (2011) provides around 100 open data sources.

Vienna has its own information system wien.at Public WLAN with access points (~400) thrown around the city. Approximately 54,000 people are employed in 5,700 information technology businesses in Vienna [18]. Currently the City is working on The Digital Agenda Vienna, actively involving citizens (Stage I: Online Discussions).

Around 90% of people have access to internet in Kyiv. However, public Wi-Fi is available only in 7 outdoors public places and on 29 underground stations. The city has started to build its smart infrastructure only 2 years ago. The strategy has been accepted only this year [16]. Unfortunately, till now the quality of the online services provided by administrative authorities left much to be desired. The situation started to change only recently, in 2015 Digital Capital strategy (2015-1018) has been accepted by the city, it includes steps to create new informational-communication systems and subsystems along with new platforms, support existing

systems and to establish effective systems of information protection. Below we have composed a comparative table for some ICTs variables (Table 3).

Table 3. Some ICTs components comparison

	Broadband download speed (mbps)	Mobile download speed (mbps)	Cost of broadband ($/month)
Stockholm	26,18	21,48	44
London	24,21	24,7	18
Vienna	23,76	18	25
Kyiv	23,2	8,46	8

Source: [19, 20]

Smart people

The aim of the Smart City London states "To put Londoners at the core, with access to open data, leveraging London's research, technology, and creative talent, brought together through networks, to enable London to adapt and grow and City Hall to better serve Londoners needs, offering a "smarter" experience for all [13]." Authorities stress the importance of human capital for future development. Basically they want to build smart city for smart people and by smart people, encouraging active citizen engagement in policy development. Mayor's Digital Talent Programme (includes various courses) was launched to tackle skills gap and encourage digital inclusion and growth in tech sectors. According to Smart London Plan, city hopes employment in tech sector will increase to 200,000 by 2020 [21]. City works on Digital Health.London, a collaborative programme delivered by MedCity, and London's three Academic Health Science Networks, it is supported by the Mayor's office. The idea is to create a platform where digital health solutions are traded and favourable conditions are created for industry [22]. Another well-known successful project, Queen Elizabeth Olympic Park - a progressive park filled with innovative tech solutions that embeds five world class sporting venues, new low CO2 emission homes, a new international quarter for business, a world class cultural and education quarter and a new media and digital hub. It actively uses Internet of Things concept, weather stations and solar sensors are already at place while more are to follow [13].

In Stockholm Social sustainability section of the Strategy the following aims are stated [23]:

- Digital inclusion, where digitalization and new technologies are deployed to bridge social divides;
- Helping city dwellers to communicate, work, study, experience, and have an active life, based on each person's unique circumstances;
- Increasing perceived safety, both in private and in public spaces, and creating vibrant and safe neighbourhoods.

There is a number of tools which aim to help elderly to stay in home and make their life easier using digital solutions (Stockholm Digital Care). Digitalization of schools made a priority through digital lift programme which includes providing Wi-Fi in all school buildings, the establishment of a new educational platform, the procurement of new infrastructure that will respond to the needs of the schools, an administrative support to manage the schools'. Another component is self-assessment tool for teachers to raise their digital maturity. In 2016 a tool that detects reading difficulties was launched, this technology scans eye movements during reading and using AI (artificial intelligence) identifies pupils who are at risk for reading and writing difficulties [23].

Vienna Smart City Strategy targets for Smart People component covers 3 areas: education, social inclusion and healthcare [14]. Education area focuses on lifelong learning and increase of the number of young people who continue to their higher level education. Vienna Business Agency has organized a number of events: annual Research Festivals since 2008 to raise technology awareness among citizen, especially youth; the vocational orientation workshop Future Jobs etc. Big attention is paid to increasing the role of nature and energy efficiency in our lives starting from the childhood ("Hanging Gardens" project) [24]. Social inclusion component covers active women inclusion into planning, decision-making and implementation processes; affordable and

high-quality housing for all; active participation at work, fair remuneration that covers basic needs; good neighbourly and safe life conditions for all. For example, WAALTeR project (2016-2019) aims to allow elderly to stay in their surroundings as long as they want having active living with the help of technological solutions (mobile emergency systems, indoor tumble detection sensors, tumble prevention systems and telemedicine), similarly to Stockholm Digital Care Programme [24]**.** Healthcare dimension aims to promote health literacy among citizens and provide medical care at the highest level for all citizens. The city encourages "Outpatient over inpatient" motto (letting people stay in their own home for as long as possible while offering top-notch nursing quality). Vienna also actively develops eHealth (the electronic health record, mobile monitoring equipment, measures for data protection and data security) and mobile Health systems (simple explanation of illness, transmitting data from sensors to doctor, booking appointments etc.) [24].

Kyiv Smart City strategy states that "Citizens is a key driver for city development". The strategy sets the following targets:

- Enhancing possibilities of citizens to manage the city and impact the decisions;
- Opening access to databases, that can be used to address the needs of citizens;
- Involving citizens, businesses, IT specialists and experts to form city development agenda using online platform and social media channels;
- Establishing direct communication between citizens and authorities through city portal and social networks;
- Development of new partnership models to realize smart city projects;
- Establishment of independent expert council to monitor project selection and concept implementation;
- Establishment of projects pull along with the platform to look for alternative financing sources;
- Establishment of clear, effective estimation system for decisions and activities of municipal authorities (including establishment of online service to conduct these estimates);
- Encouragement and development of new educational forms and qualifications to stimulate innovations and sustainable development of Kyiv;
- Support and encouragement of new innovation formats for cooperation: hackathons, innovation and educational weekends, experimental labs etc. [16].

Some implemented solutions include: Participatory budget, E-petitions, E-portal to keep citizens up-to-date. City organizes free coding courses for kids. Also city aims to improve accessibility for people with disabilities (Open World UA - a project for blind people), improvement of educational services and health services (e-health system development). To decrease the danger of Ukrainian roads, "Smart roads" project will be implemented. The application will allow to track dangerous places where accidents took place and include voting for the locations that need to be upgraded first thing by local authorities [16].

Smart Environment

London is focused on encouraging new smarter heating, electricity, waste and water networks that use resources efficiently and do more with less investments. City's performance data is an important component here. Right now main areas of data measurement include: The London Energy and Greenhouse Gas Inventory (energy consumption by homes, workplace, transport); The London Atmospheric Emissions Inventory (air pollution); Assessing London's indirect carbon emissions [25]. By 2020 London aims to have the best air quality of any major world city, which will require significant (c. 50%) reduction in emissions from London's transport sector. Mayor aims London to become a zero carbon city by 2050 [13]. Clean and efficient transport is encouraged through different measures. One of the recent decision (October 2017) includes a T-Charge (£10) which targets older more polluting vehicles (diesel and petrol vehicles registered before 2006) [25]. Among smart solutions are Smart LampPosts for electric car charging, green entrepreneurs competition, new agile logistics (zero emissions), re-usage of underground energy (Bunhill Energy Centre), numerous ideas for waste facilities in London (principle "Rubbish in - Resources out"). Much attention is paid to greening, green roofs and walls project has already 700 green roofs in central London, covering the area of over 175,000m2 (green spaces map allows to see the progress). London fights food wastage and encourages food surplus usage to feed the needy, livestock or for composting and energy production. Since 2013 FoodSave prevented over 150 tonnes a year of food waste [25]. Right now two action plans have been developed and discussed publicly: Draft Solar Action Plan and Environment Strategy. So we should expect their acceptance shortly.

Environmental component is paid a great attention to in Stockholm Smart City Framework. City sets the following targets [23]:

- To use digitalization and new technologies to make it easier for residents and businesses to be environmentally friendly;
- To reduce energy consumption and carbon footprint;
- To provide sustainable solutions for modern transport;
- To use digitalization and new technologies to stimulate biological diversity and conservation;
- To produce goods and services in a resource efficient way with minimal environmental impact.

Some smart solutions include: BigBelly (waste bins use solar power and pack the trash automatically when needed, notifying when they need emptying), Smart lighting (Sensor-controlled LED lighting for pedestrian and bicycle paths, self-controlled LED street lights with preset lighting schedules and remote-controlled lights). City actively develops the idea of eco-districts (Hammarby closed eco-cycle model, the Stockholm Royal Seaport etc.). And works with retrofitting of older buildings to make them more energy efficient [15]. Stockholm has also set target to become fossil-fuel free already by 2040. All public transport should become fossil-fuel free by 2025 (solutions include congestion charge, investments in clean transport etc.). For this Green IT concept was introduced, which is about using ICT to reduce environmental impact. This can be applied for energy-efficient buildings (monitoring and optimization), transportation (intelligent transport solutions (ITS)), digital meetings and mobile workings. The vision of 2040 includes targets to generate 10% of the city's energy by human powered vehicles and creation of 4 688 public roof gardens and offline zones [26].

Vienna sets objectives in several areas to ensure environmental sustainability (see Table 3).

Table 3. Environmental targets of Vienna Smart City

Sector	Description
Energy	• Increase of energy efficiency and decrease of final energy consumption per capita by 40% by 2050 (compared to 2005). • The per-capita primary energy input drop from 3,000 to 2,000 watt. • In 2030, over 20%, and in 2050, 50% of Vienna's gross energy consumption will originate from renewable sources.
Mobility	• Strengthening of CO2-free modes (walking and cycling), maintenance of high share of public transport and decrease of motorised individual traffic (MIT) in the city to 20% by 2025, to 15% by 2030, and to less than 15% by 2050. • By 2050, all motorised individual traffic within the municipal boundaries is to make so without conventional propulsion technologies. • By 2030, commercial traffic is to be largely CO2-free. • Reduction of energy consumption by passenger traffic across municipal boundaries by 10% in 2030.
Buildings	• Cost-optimised zero-energy building standards for all new structures, additions and refurbishments from 2018/2020. • Activities entail the reduction of energy consumption of existing buildings by 1% per capita and per year.
Environment	• By 2030, the share of green spaces must be kept at over 50%. • In 2020, the savings achieved by municipal waste management have already attained approx. 270,000 tonnes of CO2 equivalents as a result of further planned measures and improvements.

Source: [14]

In autumn 2017 parliament has moved into temporary buildings on Heldenplatz, the sustainable and demountable modular system which is highly re-usable for other purposes. The city encourages greening of facades which helps with dust filtration and air improvement. And Vienne is proud of its first zero-energy

balance hotel (The Boutiquehotel Stadthalle) which is supplied with solar panels, photovoltaic panels, LED and energy-saving lamps [24]. Energy efficiency is also targeted via smart usage of energy from metro brakes, waste heat, e-taxis, CO2 neutral delivery etc. The city believes in active involvement of citizens in particular, through community-funded solar power plants.

Kyiv works towards establishment of comfortable, safe, healthy and smart urban environment according to its Strategy. In this dimension we may found ecological targets though they are quite vaguely separated:

- Increasing standards of life, accepting European standards of urban sustainable development, decreasing CO2 emissions;
- Ensuring effective usage of resources and cost cutting technologies [16].

The city also works on promotion of smart metering for energy consumption monitoring and adjustment.

Smart Economy

London promotes circular economy and leads an EU-funded network "Sharing cities". The City Hall aims to create and support a smart, connected businesses through numerous programs and networks (The Smart London Districts, The Smart London Infrastructure Network etc.). Moreover, the city supports a development and increase of the "innovation active" businesses (at least by 10% up to 2020). Private sector is involved in solving city challenges (Smart London Innovation Challenge programme, Tech.London) [13]. London takes measurements to protect its businesses infrastructure from cybercrime attacks. The city has leading positions in FinTech innovations, for example, a digital money index published by Imperial College London together with the municipality. Private and education sectors aiming to provide the needed skills and talents organized a Digital Business Academy - a free online learning platform. Smart London plan sets three priorities in working with business: Breaking boundaries, Scaling up innovations and Ensuring connectivity [13].

Stockholm demonstrates high economic growth along with a high employment rate. Financial component of Stockholm Smart city strategy includes:

- Attractive, innovative and growing city, with the perspective of making an investment or establishing a business;
- A central node in a global network of successful cities;
- One of the best start-up scenes in the world;
- Develops and grows through entrepreneurship and intrapreneurship in digitalization and new technologies;
- Attracts talent and visitors, international and national;
- Cost efficiently manages its public operations by making full use of digitalization and new technologies;
- Has a wide range of businesses, with a favourable environment for an inclusive labour market [23].

Examples of smart solutions include traffic control, main bus lines (buses with many passengers) are prioritized at traffic lights. Buses that are behind the schedule are given preference. By 2040, the city aims to ensure max 3 min waiting time for public transport and 100% of Stockholm public transport to be driverless [26]. Automatic job centres will help to match available work with the needed competencies of human workers and autonomous jobots.

Vienna aims by 2050 to remain one of the ten European regions with the highest purchasing power based on per-capita GDP and strengthen its position as the preferred company headquarters city in Central/South-eastern Europe. Vienna believes in active entrepreneurship development and aims for 10,000 persons annually set up an enterprise in Vienna. City understands the importance of technology-intensive production and aims to increase its share of technology-intensive products in the export volume to 80% by 2050 [14]. Sharing economy principles also getting spread actively, for example, Library of things (Leila) project or EcoBuy Vienna which sets environmentally friendly procurement principles: minimal packaging, phosphate and formaldehyde-free products, no PVC, no chlorine bleach, no aggressive detergents, no tropical wood etc. [24].

Kyiv smart city strategy aims to establish innovative environment. Which includes support of innovative businesses and start-ups and removing barriers for them, development of new forms of cooperation between citizens, business and authorities. The city has launched "Property" system (2016) which allows to get information about the property and other objects of the city territory (vehicles, roads, parking, buildings etc.).

Kyiv was the first one to introduce electronic procurement system Prozorro to prevent corruption, ensure equal opportunities for all players and transparency of the processes [27].

Smart Governance

This dimension covers rather similar smart solutions across cities that involve citizens and encourage bottom-up approach in city development.

London among others uses crowdfund London platform that allows to gather money for the most important projects voted by citizens. Tech Londoners brings together innovators to solve city's challenges using digital tools. While Speed volunteering helps to mobilize the needed resources in a most optimized way. Citizens engagement is actively increased through hackathons (e.g. Climathon) [13].

In Stockholm, "Make a suggestion" app (2013) allows to notify authorities about any issues and deficiencies citizens experience [15].

Vienna is one of the first European cities to launch an Open Government Portal. "Sag's Wien" application allows citizens to communicate their concerns to the city administration in 30 seconds. While wiengestalten.at similarly to Speed Volunteering in London aims to provide information about volunteering in Vienna in a convenient form. Completed volunteering projects can also be accessed, with links to the people and/or organisations responsible [24].

All three cities contribute greatly to ensuring data openness and availability through Open data portals.

"1551" service in Kyiv works similarly to "Make a suggestion" app and offers citizens possibility to suggest improvements and mention complaints. Citizens have an option to influence urban development through Participatory budget. Which allows every citizen to participate in the distribution of the local budget through the creation of projects to improve the city and/or vote on them [27]. Open budget contributes to transparency and provides a real-time opportunity for all stakeholders to monitor the revenues and expenditures of the city budget, including the spending of public funds.

Conclusions

Based on our analysis each of the four analysed strategies has its own peculiarities that we have tried to summarize below:

Smart London city

It does not differentiate clearly Smart City Components as per outlined initially framework but all the dimensions are covered through the aims Smart London Plan sets. The version of 2013 included measurements and deadlines for some goals. In 2016 the plan was revised and status update provided for each goal. Activity areas are rather wide and cover all the dimensions of life, all the information is published on the City of London website. Innovations and tech solutions are put at the core of the Strategy.

Smart Stockholm city

Strategy sets goals within four sustainability components, however, the goals are rather vague without any measurement parameters. This was compensated in the 2040 Vision which sets numeric targets. The Strategy was adopted only recently even though smart solutions and projects have been there since late 90th. Digital Demo Stockholm arena as a product of public-private cooperation has been created to run innovative and smart projects. The City has built its competence on large-scale full cycle projects (Hagastaden, Stockholm Royal Seaport, Slussen etc.). Living Labs is one of the popular tools in Stockholm and the city itself presents "a Living Lab" being a part of GrowSmarter EU thus willing to cooperate and go international. The city heavily focuses on environmental component. Stockholm has also specified their standards for implementation and development of smart solutions to ensure their effectiveness and flexibility.

Smart Vienna city

Vienna has one of the most detailed strategies in terms of components and targets with time-lines, covering all the Framework dimensions. The Strategy has identified short-term and long-term goals (2030, 2050

milestones). Projects are presented on the website and updated continuously. The city actively involves different stakeholders into cooperation. Aspern city (2013) serves as a testbed for numerous technological solutions and Smart city implementation of the large scale, aimed to be completed by 2018.
One of the general drawbacks is lack of monitoring and status updates on targets set.

Smart Kyiv city
The strategy was accepted just recently (2017) prior to preparing the needed infrastructure and users themselves. It mostly focuses on smart governance dimension and structural changes. The strategy does not include any set time-frames, which makes it vague and difficult for progress monitoring. Besides, environmental component is poorly presented in the strategy. Obviously, the city just makes its first steps on the way of smartization. However, the projects and their status are continually updated on website and any volunteers are encouraged for co-creation.

Below you may find a summarization table for the reviewed cities (Table 4).

Table 4. Comparison of the selected Smart cities

	Vienna	**Stockholm**	**London**	**Kyiv**
Mercer Quality of living ranking 2017	1	20	40	174
City in motion index 2017	15	25	2	119
Population	1 867 582	963 920	8 787 892	2 925 760
Separate web-site	Yes	No. Part of the city website.	No. Part of the city website.	Yes
Adopted strategy (year)	Vision 2050 (2014)	Strategy for Stockholm as a smart and connected city (2017)	Smart London Plan (2013), updated version in 2016	Kyiv smart city 2020 (2017)
Components	1) Resource preservation; 2) Quality of life; 3) Innovations.	1) Ecological; 2) Financial; 3) Social; 4) Democratic sustainability.	1) Engaging citizens; 2) Enabling good growth; 3) Working with business.	1) Comfortable and safe urban environment; 2) Smart and open city governance; 3) Innovative environment; 4) Central role of citizens.
Principles	1) Openness; 2) Cooperation; 3) Efficiency.	1) Collaboration; 2) Common IT-solutions (allowing multiple suppliers to develop and operate them); 3) Open and shared data; 4) Security and privacy.	1) Technology and Innovations; 2) Collaboration and engagement; 3) Efficiency and resource management; 4) Open data and transparency.	1) Citizens-orientation; 2) Widespread informatization; 3) Openness and cooperation; 4) Forward-looking way.
Core focus	Energy efficiency and resource preservation.	Green IT.	Innovations and citizens engagement.	Governance and digitalization.

Source: Authors based on [13-16, 27, 28]

All four cities have some similar approaches to Smart city development within outlined domains, summarized in a scheme below:

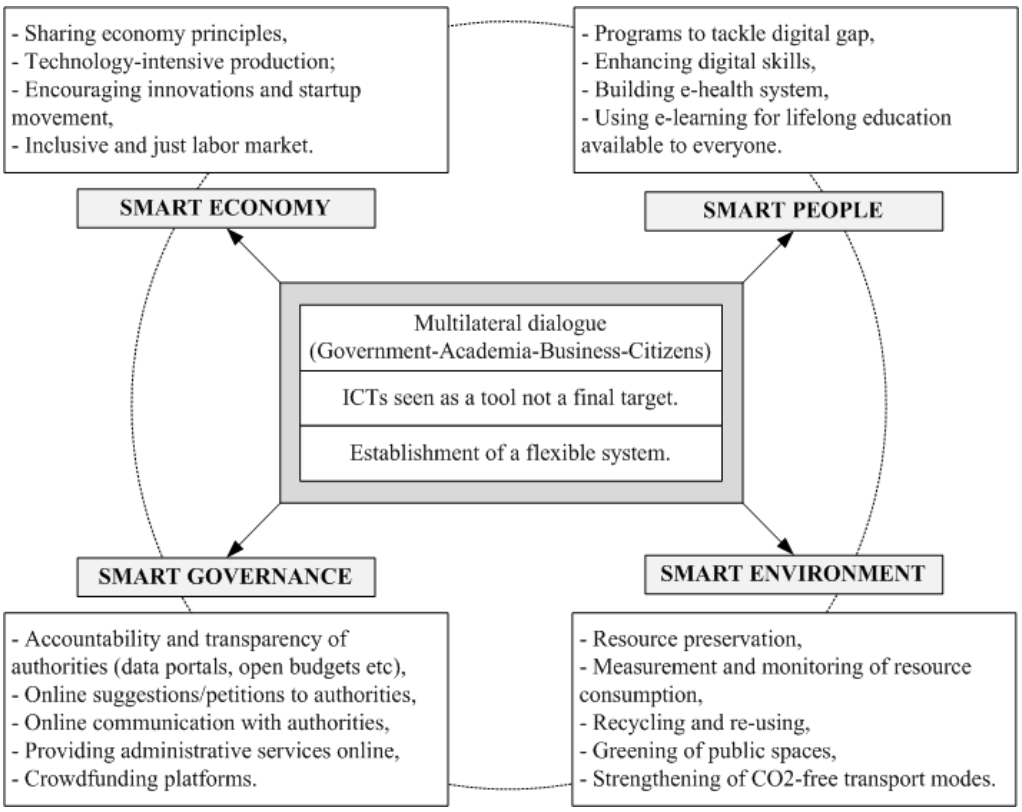

Fig. 4. Common approaches in the reviewed Smart Sustainable Cities
Source: Author's

And based on the studied strategies we have prepared a list of best practices that should help to create a successful smart city strategy for emerging smart cities:

- The strategy should be a product of cooperation between different stakeholders (academics, business, municipality, civil society), outlining both interests and responsibilities of each group;
- Encouragement of co-creation from different stakeholders;
- The strategy may cover a wide spectrum of solutions but they should form one holistic system;
- The strategy should include targets and tools to monitor their achievement;
- Free access to up-to-date information with progress reviews is important;
- Living Labs is a good tool for the initial results testing and spreading them for a wider market later;
- Constant openness for public feedback is a must;
- Even though strategy is a product of a common development, coordinating body should be established for the purposes of accountability, transparency and monitoring.

References

[1] What being 'smart' means for cities (2017). Racounter [ONLINE] Available at: https://www.raconteur.net/technology/what-being-smart-means-for-cities [Last Accessed 24 January 2018].

[2] Smart Cities. Navigant Research [ONLINE] Available at: https://www.navigantresearch.com/research/smart-cities [Last Accessed 24 January 2017].

[3] K.Pyzyk (2018). 6 trends that will define smart cities in 2018. Smart Cities Dive. [ONLINE] Available at: https://www.smartcitiesdive.com/news/6-trends-that-will-define-smart-cities-in-2018/513889/ [Last Accessed 24 January 2017].

[4] K.Kourtit, P. Nijkamp (2013). THE 'NEW URBAN WORLD' – THE CHALLENGE OF CITIES IN DECLINE. Romanian Journal of Regional Science, [ONLINE] Available at: http://www.rrsa.ro/rjrs/V7SP2.Kourtit.pdf. [Last Accessed 24 January 2017].

[5] B. Cohen (2011). The Top 10 Smart Cities On The Planet. [ONLINE] Available at: http://www.fastcoexist.com/1679127/the-top-10-smart-cities-on-the-planet. [Last Accessed 24 January 2017].

[6] R. Giffinger, et al. Smart Cities Ranking of European Medium-sized Cities. Centre of Regional Science, Vienna UT, Oct. 2007. 28 p. [ONLINE] Available at: http://www.smartcities.eu/download/smart_cities_final_report.pdf. [Last Accessed 24 January 2017].

[7] T. Nam, T. A. Pardo (2011). Conceptualizing Smart Sustainable City with Dimensions of Technology, People, and Institutions. [ONLINE] Available at: http://www.ctg.albany.edu/publications/journals/dgo_2011_smartcity/dgo_2011_smartcity.pdf. [Last Accessed 24 January 2017].

[8] IESE (2016). Cities in Motion Index. [ONLINE] Available at: http://www.iese.edu/en/facultyresearch/research-centers/cgs/citiesmotionstrategies/?_ga=1.250510531.491872120.1449127639. [Last Accessed 24 January 2017].

[9] ITU-T Focus Group on Smart Sustainable Cities (2014). Smart sustainable cities: An analysis of definitions. [ONLINE] Available at: http://www.itu.int/en/ITU-T/focusgroups/ssc/Pages/default.aspx. [Last Accessed 24 January 2017].

[10] Arcadis (2016). Sustainable cities index 2016. [ONLINE] Available at: https://www.arcadis.com/media/0/6/6/%7B06687980-3179-47AD-89FDF6AFA76EBB73%7DSustainable%20Cities%20Index%202016%20Global%20Web.pdf. [Last Accessed 24 January 2017].

[11] Ericson (2016). Networked City Index 2016. [ONLINE] Available at: https://www.ericsson.com/res/docs/2016/2016-networked-society-city-index.pdf. [Last Accessed 24 January 2017].

[12] Global Power City Index (2017). [ONLINE] Available at: http://mori-m-foundation.or.jp/pdf/GPCI2017_en.pdf [Last Accessed 24 January 2017].

[13] Smart London Plan (2013). [ONLINE] Available at: https://www.london.gov.uk/sites/default/files/smart_london_plan.pdf
*Updated Smart London Plan https://www.london.gov.uk/sites/default/files/gla_smartlondon_report_web_4.pdf. [Last Accessed 24 January 2017].

[14] Wien Smart City (2014). [ONLINE] Available at: https://smartcity.wien.gv.at/site/files/2016/12/SC_LF_Kern_ENG_2016_WEB_Einzel.pdf [Last Accessed 24 January 2017].

[15] Stockholm Smart city [ONLINE] Available at: http://international.stockholm.se/city-development/the-smart-city/. [Last Accessed 24 January 2017].

[16] KYIV SMART CITY Strategy (2017) [ONLINE] Available at: http://kyivsmartcity.com/Kyiv-Smart-City-Concept.pdf. [Last Accessed 24 January 2017].

[17] Stokab [ONLINE] Available at: https://www.stokab.se/In-english/ [Last Accessed 24 January 2017].

[18] City of Wien official web-site (ICT strategy). [ONLINE] Available at: https://www.wien.gv.at/ikt/ [Last Accessed 24 January 2017].

[19] European digital city index (2016). [ONLINE] Available at: https://digitalcityindex.eu/city/32

[20] BandwidthPlace [ONLINE] Available at: http://www.bandwidthplace.com

[21] Digital Talent Programme. Available at: https://www.london.gov.uk/what-we-do/business-and-economy/skills-and-training/digital-talent-london [Last Accessed 24 January 2017].

[22] Digital Health.London. Available at: https://digitalhealth.london/ [Last Accessed 24 January 2017].

[23] Smart and Connected City Stockholm (2017). Available at: http://international.stockholm.se/globalassets/ovriga-bilder-och-filer/smart-city/brochure-smart-and-connected.pdf [Last Accessed 24 January 2017].

[24] Vienna Smart City projects. Available at: https://smartcity.wien.gv.at/site/en/projects/ [Last Accessed 24 January 2017].

[25] London City web-site [ONLINE] Available at: https://www.london.gov.uk/what-we-do/environment [Last Accessed 24 January 2017].

[26] Welcome to the smartest city in the world (2016) [ONLINE] Available at: http://international.stockholm.se/globalassets/ovriga-bilder-och-filer/smart-city/welcome-to-the-smartest-city-in-the-world-english-designfiction-sthlm-stad.pdf. [Last Accessed 24 January 2017].

[27] Kyiv Smart City Projects [ONLINE] Available at: https://www.kyivsmartcity.com/projects/ [Last Accessed 24 January 2017].

[28] Mercer Quality of living ranking (2017). [ONLINE] Available at: https://mobilityexchange.mercer.com/Insights/quality-of-living-rankings [Last Accessed 24 January 2017].

Anna Adamska, Zdzisław Pakowski
Faculty of Process and Environmental Engineering, Lodz University of Technology
90-924 Łódź, Wólczańska 213, anna.adamska@edu.p.lodz.pl, zdzislaw.pakowski@p.lodz.pl

PRESSURE MEASUREMENT AS A TOOL TO IDENTIFY MOISTURE TRANSPORT MECHANISMS IN CONVECTIVE DRYING OF NON-SHRINKING MATERIAL

Abstract
The drying process is one of the most important stages in the production of building materials. The choice of the drying method affects the chemical and physical properties of the final product. The aim of this research is to measure and analyze the dynamic changes of internal pressure in non-shrinking, porous material during convective drying. In this work the problem will be discussed with special attention to the behavior of rewetted plaster. A commercial gypsum of company PIOTROWICE II (Alpol brand), typically used in construction and decorative plastering was applied. Gypsum was mixed with water in recommended proportion of 0.6 water/gypsum and drying experiments were performed at 50°C. The changes in sample overall mass as well as pressure and material temperature on the midpoint of sample axis were monitored. On the basis of the obtained experimental data of axial pressure, it is possible to perform a more detailed analysis of mass and heat transfer mechanisms than based on the drying kinetics alone. The pressure trends in the sample allow one to determine the moment of transition from the first to the second drying period, without the need to determine the kinetics of drying. The element of novelty consists of using a direct internal pressure measurement to provide information on the variation of the actual drying rate and mass transfer mechanisms.

Key words
Gypsum, convective drying, internal pressure, mass transfer.

Introduction

The convection drying process belongs to one of the oldest and most frequently used unit operations in various branches of industry. The drying rate is one of the most important parameter for this process. Setting the process parameters in such a way as to obtain the highest drying rate, on one hand accelerates drying and is justified from the economic point of view, on the other hand, is a factor often deteriorating the quality of the final product. Therefore, in industrial practice it is very important to find an optimum drying rate regarding both energy consumption and the quality of the product obtained. One of the ways to achieve this goal may be the use of new, combined method for controlling the conditions of the drying process in response to the behavior of the dried material.

Analysis of microstructural changes and interaction between water and solid, especially during mass and heat exchange processes, is a key issue, especially for the design of final strength properties of construction products. The use of uncontrolled conditions may lead to the appearance of shrinkage, deformation and cracks, that was described and subjected to modeling in many works e.g. [1-2].

One of the advantages of plaster is its high porosity. This property can facilitate transport of many compounds (moisture, low molecule weight vapors, CO_2 etc.) found in indoor or outdoor environments [3]. However, convective drying of freshly cured gypsum is an important stage in their production process. Optimization of this drying process is required to enhance processing efficiency, in terms of energy consumption and production time, without reduction in the product quality. Most presented works on calculations and simulations of heat and mass transport in gypsum boards focused on its application regarding fire resistance and only accounting for water vapor transport. There is a need to find a key parameter to understand the transport of heat and mass phenomena in porous media, which has an effect on structural defects and final mechanical properties [4].

The literature on the subject presents numerous models that allow predicting the moisture content in time and space in building materials. However, it is necessary to perform experiments in which thermal properties will be determined e.g.: thermal conductivity and transport factors for mass transfer such as diffusivity [5,6] or permeability [7,8].

Previously published papers indicate that minimizing negative effects during convection drying can be achieved by performing the process in non-stationary conditions, i.e. slowing down the process when there is a danger of material destruction and accelerating when there is no such danger. This technique, referred in the literature as "intermittent drying", in most cases consists of a controlled supply of thermal energy that changes at regular or irregular intervals. Most often, the control of introduced changes takes place by means of controllers, e.g. MPC (Model Predictive Control), based on the examined drying kinetics and current readings of the solid temperature or humidity of the drying agent. The relationship between the residence time of the dried material and the humidity of the material and other measured parameters is determined in most cases, by previously developed drying models, sometimes based on neural networks.

The analysis of the pressure evolution within the dried material has already been undertaken in several works. So far, most of the work on convection drying has only considered the existence of capillary pressure. These are mainly considerations based on theoretical dependencies, because the measurement of this pressure is complicated. One of the first reports from experimental research comes from 1996 where the authors suggested a complex procedure for investigating shrinkage stresses in the process of drying colloidal capillary-porous bodies like peat and presented distribution of capillary and internal pressure as a function of moisture content [9]. Attempts to measure and analyze this pressure were made in the work of E. Holt, where the evolution of internal capillary pressure for autogeneous shrinkage of concrete was investigated [10]. However, the pressure generated during mass transport, especially in the case of multiphase flow, is also influenced by the properties of the material itself, hence the difficulty in finding a universal method of measuring this parameter, which gives a lot of meaningful information about the drying process and the ability to control the shrinkage and cracks on the surface of the dried material [11].

This work focuses on the analysis of mass transport phenomena in the drying process, based on the pressure trend in the porous material that does not show any drying shrinkage. The obtained results can be used to control the drying agent parameters directly in response to the changing stresses generated in the structure of the dried material. Thanks to the use of telemetric pressure measurements, it could be used without any problem on an industrial scale.

Materials and methods

In experimental part a commercial gypsum of company PIOTROWICE II (Alpol brand), typically used in construction and decorative plastering was applied. The skeletal density of prepared samples was 2570 kg/m^3 and the porosity 0.65.

The preparation of samples for drying experiments included three basic steps described below:

- in the first stage, after mixing gypsum with distilled water in the amount recommended by the producer (2.4 dm^3 per 4 kg of gypsum), cylinders with a diameter of 28 mm and a height of 54 mm were cast in which thermocouples and a syringe needle with attached pressure transducer were used to monitor the temperature and internal pressure on the periphery and on the axis. The axial thermocouple of 0.5 mm external diameter was passed through the syringe needle of internal diameter of 0.9 mm (cf. Fig.1) and inserted axially so that the end of the needle was 27 mm above the cylinder base. This allowed for simultaneous measurement of pressure and temperature in the same point. The prepared samples were left to dry for 24 hours at room temperature,
- in the next step the samples were soaked in distilled water for min. 24h to get the material fully saturated,
- the last stage included insulating both bases of the cylinder with hydrocyanide glue so as to ensure one-dimensional mass and heat transport. Each sample before being placed in the drying tunnel was measured and weighed. The appearance of the sample before placing in the tunnel is shown in Fig.1.

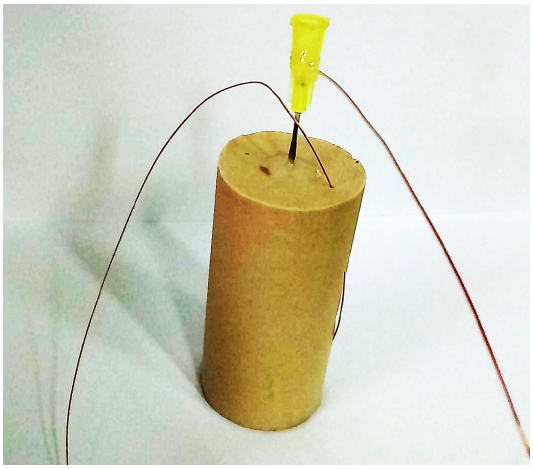

Fig. 1. Cylindrical sample of gypsum with thermocouples and syringe needle for pressure measuring
Source: Authors'

To determine the kinetics and temperature curves for the material, a drying tunnel was used as shown in Fig. 2. It is divided into two sections that allow air to circulate. The fixed flow of the drying medium is provided by an axial fan. In the tunnel there is a number of control and measurement devices enabling observation and recording of key process parameters. These devices include an electronic balance by means of which the loss of mass was measured, PT100 sensors to control the temperature in different points in the tunnel as well as air humidity sensor inside the tunnel and atmospheric pressure sensor outside. All readouts were recorded at pre-set time intervals.

The gypsum cylinders before insertion into the tunnel, were placed on a weighing dish with additional sensors allowing for temperature read out on the sample wall and axis as well as pressure read out in the sample axis at one minute intervals. The relative accuracy of pressure read out was ±0.2% and the absolute accuracy of temperature read out ±0.5°C . Absolute accuracy of the weight measurement was 0.001 g.

The dynamic changes of pressure inside the sample were recorded using a MadgeTech pressure sensor that was modified for the experiment and connected directly to the syringe needle inserted in the sample. Both thermocouples and the needle were placed in the samples during plaster casting, so there was no need to drill the sample after its preparation that would deteriorate the contact between the needle and the material. For measuring the current atmospheric pressure a second, identical pressure sensor was used, which was mounted in the laboratory.

The measurements were made at a temperature of 50°C at a drying agent speed of 1 m/s. The recording of parameters was carried out until the equilibrium moisture content was reached (about 7h). To determine the mean moisture content change of the material after drying and dry mass, the samples were placed in an oven and dried to constant weight at 105°C. The measurements were performed in duplicate for each sample in most cases. The following definitions were used to calculate variables in Fig. 3 and 4.

$$X = \frac{m_{w.b.} - m_{d.b.}}{m_{d.b.}} \tag{1}$$

$$w_D = \frac{m_{d.b.}}{A}\frac{\Delta X}{\Delta t} \tag{2}$$

where:

X – moisture content [$kg_{H2O}/kg_{d.b.}$];
$m_{w.b.}$ – mass of wet sample [kg];
$m_{d.b.}$ – mass of dry sample [kg];
$w_{D.}$ – drying rate [kg_{H2O}/m^2s];
A. – surface of evaporation [kg_{H2O}/m^2s];
t – time [s].

a)  b) 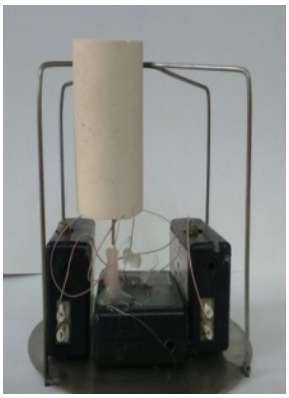

Fig. 2. View of the drying tunnel (a) and sample on weighing dish with temperature and pressure sensor (b)
Source: Authors'

To analyze the phenomena occurring during removal of moisture from the material, the difference between the atmospheric pressure and the one measured on the sample axis was used, according to the formula (3):

$$p_n = p_{in} - p_{atm} \tag{3}$$

where:

p_n – nominal pressure [Pa];
p_{atm} – atmospheric pressure [Pa];
p_{in} – internal pressure (absolute) [Pa].

Results

Fig. 3 presents a set of curves of internal pressure evolution, drying kinetics and temperature for selected measurement series (one of ten performed). It can be clearly seen in graph in Fig. 3 that in the first 20 minutes of drying, the pressure decreases, which is related to the slow process of material heating and removal of moisture mainly due to evaporation of water from the surface of the material. The maximum evaporation rate observed at the beginning of the process generates a large pressure gradient and development of underpressure in the dried material.

After 20 minutes, the pressure on the sample axis gradually increases above the atmospheric pressure, the water evaporates from the core of the rigid skeleton of plaster. After about 1 hour, the pressure reaches a maximum value of approx. 950 Pa. This pressure is maintained for about 1.5 hours and then increases again to about 1150 Pa. The link between pressure change trend in the dried material and the temperature curve is clearly visible here. After analyzing the temperature curve, it can be observed that the pressure begins to increase again after 2 hours from the start of drying, i.e. at the transition from the first to the second drying period, when the material reaches a temperature higher than the wet-bulb temperature. Then the pressure increases with the temperature and after reaching the gas temperature the pressure drops. It should be noted here that the samples were put into the drying tunnel immediately after the removal from the distilled water (after blotting the excess of liquid), therefore the initial temperature of the material is about 10°C.

In the 4th hour of the process the pressure stabilizes at the level higher that atmospheric pressure. It can be explained by the fact that while soaking the gypsum samples, a migration of microcrystals is observed and during drying these crystals are transported with the stream of moisture from core to the surface and clog pores of the material. This phenomenon is also connected to porosity changes during drying [12].

In the first period of drying in the gypsum pores there is only liquid physically bound with the skeleton. In the second drying period moisture transport resistance is much larger, the water is removed in the form of vapor, therefore the efficiency of the process decreases. In the first drying period the Darcy stream is dominant and in the second period the diffusion transport prevails. The nature of the pressure changes in the sample also indicates the presence of evaporation front, observed as a steep reduction of pressure after 3.5 hours.

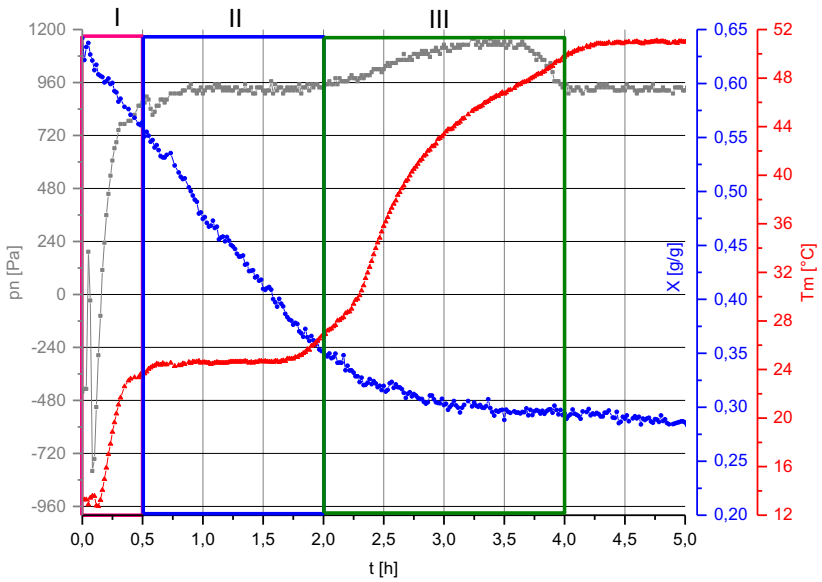

Fig. 3. The pressure (■), temperature (▲) and mean moisture content (●) data points for experimental series #7
Source: Authors'

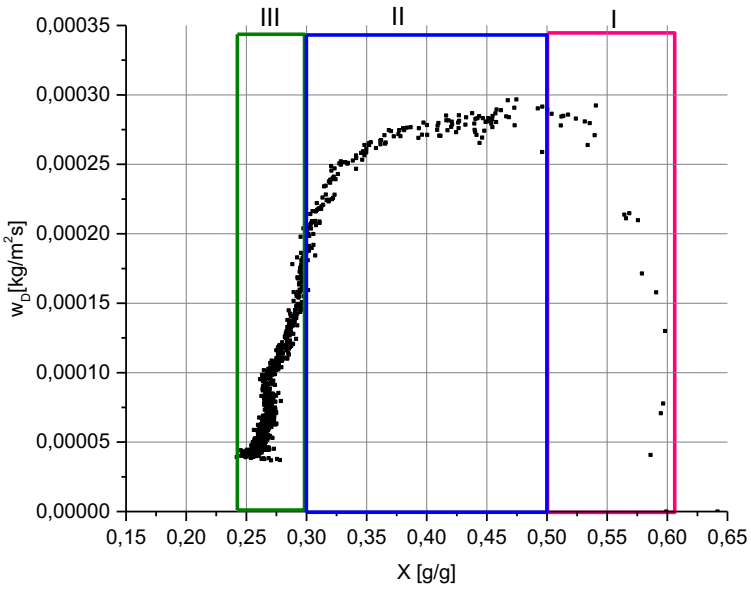

Fig. 4. The drying rate data points for experimental series #7
Source: Authors'

In Fig. 3 and 4 the areas of characteristic change in the pressure course are marked, for each measured parameter. The calculated drying rate for series #7 is presented in Fig. 4. When the evaporation stream in the second characteristic area is maximal the internal pressure stays at the same level. However, when the drying rate in the last stage of process decreases, the internal pressure rises again. This observation contradicts the claim that the water transport is more important for stress generation than that the heat transport during drying [13].

On the basis of the drying kinetics alone only the moment of transition from the first to the second drying period can be determined, similarly as for the temperature curve. The pressure course inside the material additionally shows quite intense phenomena related to tensile and compressive stresses, which appear mainly

during the heating of the material in the first drying period and additional phenomena present in the second drying period associated with the relaxation of the material.

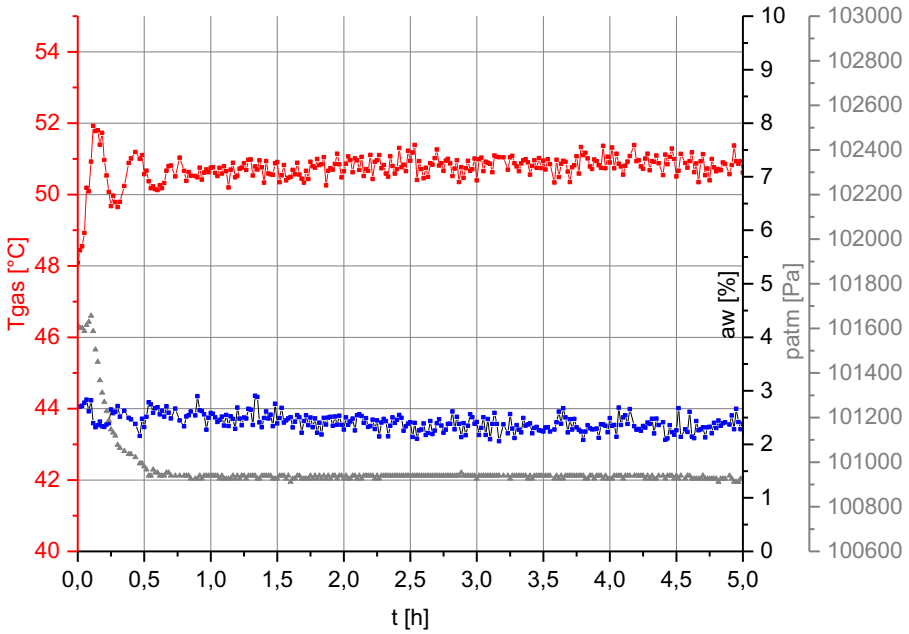

Fig. 5. Parameters of drying air: pressure (■),temperature (▲) and humidity (●) for experimental series #7
Source: Authors'

Fig. 5 presents the dynamic changes in temperature, air humidity and atmospheric pressure for drying agent. The significant fluctuations can be observed for the reference (atmospheric) pressure, what should be included in the calculation of internal pressure and also modeling calculations. In most of the works connected with drying modeling this value is constant. So far the evolution of internal pressure was only predicted by some advanced models [14-16]. They concentrated on the analysis of drying-related stresses in materials of relatively small shrinkage: kaolin, unglazed ceramics and wood, which is directly related to process control in order to avoid product defects. Moreover the theoretically predicted pressure values are usually much higher than the ones observed in this work. No experimental work, including [9,10], so far has presented the evolution of internal pressure in such detail as the present work.

Based on the presented results, it can be concluded that the internal pressure is more sensitive to changes occurring in the material than the temperature or mass change and can be used to control the drying process.

Conclusions

The analysis of pressure changes inside the drying non-shrinking material, enables more precise observation of phenomena of moisture transport and changes in the nature of stresses generated in the dried material (initially compression and then stretching of the material). In addition, it clearly shows where the transition from the first to the second drying period takes place.

The obtained results will enable us to build a mathematical model to describe the convection drying process taking into account the pressure gradient. Due to that, it will be possible to follow the drying stresses generated in the material on a regular basis and control the process parameters so as to obtain the desired product without defects.

Thanks to the use of telemetric pressure measurements, the method can be easily applied in an industrial scale to control the drying process. It is an ideal solution that can also be used for materials that exhibit shrinkage such as ceramic products and also to predict when the drying shrinkage ends. However, the analysis of pressure changes in shrinking materials is more intricate and is outside the scope of this work.

References

[1] C.M. Tam, V.W.Y. Tam, K.M. Ng, Assessing drying shrinkage and water permeability of reactive powder concrete produced in Hong Kong, Construction and Building Materials, 26 (2012) , 79-89.

[2] S.D. Beyea, B.J. Balcom, T.W. Bremner, P.J. Prado, A.R. Cross, R.L. Armstrong, P.E. Grattan-Bellew, The influence of shrinkage-cracking on the drying behaviour of White Portland cement using single-point imagining (SPI), Solid State Nuclear Magnetic Resonance, 13, (1998) , 93-100.

[3] M. Kalender, Determination of effective diffusivities and convective coefficients of CO_2 in gypsum plasters by dynamic single pellet experiments, Building and Environment, 105, (2016) , 164-171.

[4] T. Defraeye, G. Houvenaghel, J. Carmeliet, D. Derome, Numerical analysis of convective drying of gypsum boards, International Journal of Heat and Mass Transfer, 55, (2012) , 2590–2600.

[5] O.C.G. Adan, Determination of moisture diffusivities in gypsum renders, HERON-ENGLISH EDITION, 40, (1995), 201-216.

[6] L. Bennamoun, L. Kahlerras, F. Michel, L. Courard, T. Salmon, L. Fraikin, Determination of moisture diffusivity during drying of mortar cement: experimental and modeling study, International Journal of Energy Engineering, 3, (2013) , 1-6.

[7] H., Milsch, M., Priegnitz, G. Blöcher, Permeability of gypsum samples dehydrated in air, Geophysical Research Letters, 38, (2011).

[8] L. C. Yee, Water desorption characteristic of red gypsum, (2015), 1-24.

[9] N.I. Gamayunov, S.N. Gamayunov, Change in the structure of colloidal capillary-porous bodies in the process of heat and mass transfer, Journal of Engineering Physics and Thermophysics, 69, 721–725, (1996)

[10] E.E. Holt, Early age autogenous shrinkage of concrete, Technical Research Centre of Finland, VTT Publications 446, (2001).

[11] Handbook of Porous Media , Third Edition, Edited by Kambiz Vafai, CRC Press, Chapter 2, (2015), 47-62.

[12] S. Klin, Analysis of the variation of strength and deformability of gypsum in various states of stress and humidity, Institute Of Environmental Engineering, Zeszyty Rolnicze Akademii Naukowej we Wrocławiu, 510, (2005), 1-30.

[13] J.L. Amoros, E. Sanchez, V. Cantavella, J.C. Jarque, Evolution of the mechanical strength of industrially dried ceramic tiles during storage, Journal of the European Ceramic Society, 23, (2003), 1839–1845.

[14] A. Rybicki, Sterowanie procesami suszenia materiałów wrażliwych na uszkodzenia skurczowe. Wydawnictwo Politechniki Poznańskiej, 482, (2012), 116.

[15] G. Musielak, Modelowanie i symulacja numeryczna zjawisk transportu oraz naprężeń suszarniczych w materiałach kapilarno-porowatych, Wydawnictwo Politechniki Poznańskiej, 386, (2004), 147.

[16] S.J. Kowalski, A. Rybicki, K. Rajewska, Intensification of drying processes due to optimal operations, Chemical Engineering and Processing, 86, (2014), 22-29.

Anna W. Sobańska, Paulina Jakubczyk, Jarosław Pyzowski, Elżbieta Brzezińska
Department of Analytical Chemistry, Faculty of Pharmacy, Medical University of Lodz
ul. Muszyńskiego 1, 90-151 Lodz, Poland, anna.sobanska@umed.lodz.pl

QUANTIFICATION OF SYNTHETIC FOOD DYES IN BEVERAGES OR PHARMACEUTICAL TABLETS BY SOLID PHASE EXTRACTION (SPE) FOLLOWED BY UV/VIS SPECTROPHOTOMETRY

Abstract
Synthetic food dyes (E102, E104, E110, E122, E124, E132, E133) were concentrated by solid phase extraction on aminopropyl modified silica with aqueous sodium hydroxide or selected amines as eluents. Ponceau 4R (E124) was used as the model dye in the studies of the elution step. The recoveries of E124 differed depending on the eluent and ranged from 76% (AMP) to over 90% (TEA, imidazole, NaOH). Diluted aqueous triethanolamine (TEA) was found to be a suitable eluent for E124 but other dyes were eluted more effectively with NaOH. The solid extraction process was combined with UV/VIS spectroscopy to quantify synthetic dyes in drinks and OTC pharmaceutical tablets. The SPE-UV/VIS spectroscopic method was validated in terms of linearity, accuracy (recovery of dyes from spiked preparations), precision (repeatability, intermediate precision) and limits of detection/quantification. The method was found sufficiently fast, easy and reliable for the routine control of dyes in these types of products.

Keywords
Food dyes, quantification, SPE, VIS spectrophotometry.

Introduction

Color is an important feature of food, often associated with its quality, taste, and flavor. Because the majority of foods consumed nowadays are processed, much of what we eat would not look good if it was not colored. Synthetic food dyes are frequently used for this purpose because they can be mass-produced at a fraction of the cost of manufacturing natural food colorings, their shelf life is longer than that of natural dyes and the variety of colors that can be artificially produced in a lab is almost unlimited.

Despite increasing awareness of their potential harmfulness, synthetic food dyes are commonly used in foods, beverages, pharmaceutical preparations and dietary supplements [1]. Analytical techniques used for their quantification in various matrices include chromatography (thin layer chromatography [2-5], reversed-phase [2, 6-9] or ion-pair [2, 9-12] liquid chromatography), electrochromatographic techniques (capillary electrophoresis [12-18], micellar electrokinetic chromatography [19,20] or microemulsion electrokinetic chromatography [21]), UV/VIS spectroscopy [22-26] voltammetry [27-29] or polarography [30]. Prior to further analysis sample pretreatment is usually needed. Dyes are often isolated by separation techniques such as ion-pair extraction [24,31] or solid phase extraction (SPE) [3,4,6,7,11,26,32,33]. The sorbent most commonly used for SPE of synthetic dyes is RP-18 [3,7,11], but other supports such as cotton [6], Amberlite XAD-2 [7], polyurethane foam [26], polyamide [7], N-vinylpyrrolidone and divinylbenzene copolymer [32], neutral primary amine modified divinyl benzene polymer [33] or amino-modified silica [4] have also been used.

The purpose of this study was to develop a simple and cost-effective method of determination of synthetic food dyes in beverages or pharmaceuticals by solid phase extraction combined with VIS spectrophotometry.

Experimental part

Instrumentation

SPE extraction was performed with the 12 position SPE manifold system purchased from Bioanalytic, Poland, connected to a water vacuum pump and equipped with Cronus SPE aminopropyl columns (200 mg/3 ml). Lambda 25 UV/VIS spectrophotometer from Perkin-Elmer was equipped with 10.02 mm quartz cuvettes from Kuvette, Marco Roth Karlsruhe, Germany.

Solvents, chemicals, dye standards

Methanol and sodium hydroxide were from Chempur, Poland. Morpholine, triethanolamine (TEA), imidazole and 2-amine-2-methyl-1-propanol (AMP) were purchased from Sigma-Aldrich. All solvents and chemicals were of analytical grade. Dyes used as standards were from Food Colours, Poland. Their purity was determined by UV/VIS spectrophotometry according to Ref. [34]. The following synthetic dyes were investigated: quinoline yellow (E104), tartrazine (E102), indigocarmine (E132), brilliant blue (E133), ponceau 4R (E124), orange yellow S (E110), azorubine (E122).

Solutions

Solutions of bases (0.1 and 0.01 mol L^{-1} NaOH, 0.1 mol L^{-1} AMP, 0.1 and 1.0 mol L^{-1} imidazole, 0.1 and 0.01 mol L^{-1} trietanolamine, 0.1 and 1.0 mol L^{-1} morpholine) were prepared in distilled water. Dye standard solutions used to generate calibration curves were prepared at concentrations 4, 8, 12, 15, 20 and 25 µg mL^{-1} in distilled water or in solutions of appropriate bases as listed above.

Commercial preparations

Commercial preparations analyzed throughout this study included:

- Over-the-counter sore throat tablets containing 2,4-dichlorobenzyl alcohol, amylmetacresol, levomenthol, peppermint essential oil, star anise essential oil, sucrose, glucose syrup, tartaric acid and ponceau 4R (E124)
- Fizzy drink containing water, carbon dioxide, sucrose, aspartame, citric acid, modified starch, ester gum (E445), sodium benzoate, grapefruit flavor, azorubine (E122)
- Isotonic drink containing water, dextrose, maltodextrose, citric acid, sodium chloride, potassium citrate, magnesium chloride, calcium chloride, potassium phosphate, strawberry and tropical fruit flavor, acacia gum (E414), ester gum (E445), acesulfam-K, sucralose, brilliant blue (E133).

Lab-prepared preparation

Samples of an un-colored, commercially available fizzy drink containing water, carbon dioxide, sucrose, aspartame, citric acid, modified starch, ester gum (E445), sodium benzoate and flavor were spiked with the following dyes: E110, E104, E102, E132 at concentrations given in Table 5.

Preparation of samples for SPE extraction

Aqueous solutions of Ponceau 4R used for SPE optimization were prepared at 0.2 µg mL^{-1} concentrations. Fizzy drinks samples (5 mL) were transferred to 50 mL volumetric flasks, degassed with ultrasounds and diluted to volume. Pharmaceutical tablets (5 pcs) were dissolved in distilled water (250 mL) at room temperature and 50 mL samples of this solution (corresponding to one tablet) were subjected to SPE extraction.

SPE extraction

SPE aminopropyl columns were conditioned with 2x3 mL methanol and not allowed to dry. Samples prepared according to the section "Preparation of samples for SPE" were passed through columns at *ca.* 2 mL min^{-1} flow rate. Sorbents containing adsorbed dyes were washed with distilled water (*ca.* 10 mL) to remove impurities. Adsorbed dyes were eluted with aqueous solutions of NaOH, TEA, imidazole, AMP or morpholine prepared according to the section "Solutions". The resulting solutions of desorbed dyes were collected in pre-weighed vials (for aqueous solutions of dyes) or in volumetric flasks (in the case of drinks or tablet samples). Samples collected in vials were weighted immediately after the collection to calculate their weight and volume; samples in volumetric flasks were diluted to volume with an appropriate eluent.

UV/VIS spectroscopy

The absorption spectra of dye standards and dyes isolated from samples *via* SPE were recorded between 350 and 650 nm. The selected spectra of dyes (20 µg mL^{-1} in 0.01 M NaOH) are presented in Figure 1. The analytical wavelengths used in spectrophotometric determinations were: E102 – 399 nm; E104 – 383 nm; E110 – 449 nm; E122 – 506 nm; E124 – 506 nm; E133 – 630 nm; E132 – 610 nm.

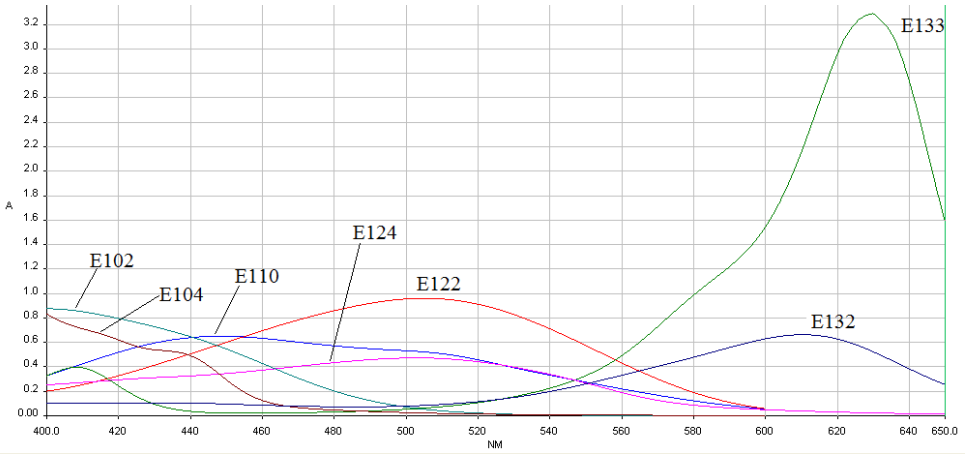

Fig. 1. Spectra of food dyes (20 µg mL^{-1} in 0.01 M NaOH)
Source: Author's

Results and discussion

SPE procedure optimization

Synthetic food dyes investigated throughout this study are commonly used in drinks, confectionery, dairy products, pharmaceuticals (e.g. tablets), oral care preparations (toothpastes and mouthwashes) and gelatin desserts. According to some studies their quantification does not require any sample pretreatment apart from dilution and filtration [22,23], but in the majority of cases dyes are isolated and purified by extraction prior to actual determination. From the chemical point of view many synthetic food dyes (including the compounds analyzed in this study) are strong organic acids (neutralized with suitable bases) and their acidic-basic properties make them suitable objects for procedures such as ion-pair solvent extraction or ion-pair chromatography. It seemed therefore reasonable to isolate them by solid phase extraction in the ion exchange mode. Such an approach has been seldom applied so far. In the majority of published studies synthetic dyes are subjected to SPE on C18, Amberlite XAD-2, polyamide or polyamide foam [3,6,7,11,26,32,33] - supports dedicated primarily to separation of neutral molecules of different polarity and size. Anions of carboxylic or sulfonic acids can be effectively separated on anion exchange sorbents [4,7,33,35]. Retention of an analyte, bearing a negative charge, requires a positively charged anion exchange sorbent to ensure suitable ionic interactions. This can be achieved on strong anion exchangers (SAX), where the sorbent (a silica bonded quaternary ammonium salt) bears a permanent positive charge or on weak anion exchangers (WAX) containing silica bonded neutral NH_2 groups that must be ionized during the retention step with the solution of the suitable pH (at least 2 pH units below the pKa of the sorbent). During the elution step the charge on either the sorbent or the analyte must be neutralized to break the ionic interactions that make the analyte bind to the sorbent. In the case of food dyes analyzed in the course of this study weak anion exchangers are more suitable since anions of very strong acids such as sulfonic acids may retain irreversibly on strong anion exchangers [35]. In previously published papers on isolation of synthetic food dyes on WAX type sorbents both strategies of elution were presented and the solutions used as eluents were either acidic (to neutralize the positive charge on the sorbent) or basic (to neutralize the negative charge on the analyte), respectively [4,33]. After the SPE extraction chromatographic (TLC [4] or UPLC [33]) determination of isolated dyes followed.

We have decided that prior to the spectrophotometric determination the synthetic dyes analyzed in this study should be isolated by solid phase extraction on the WAX type aminopropyl sorbent with basic rather than acidic elution. This step can be achieved with aqueous sodium hydroxide [35] or methanolic ammonia [33] but such conditions are not particularly mild. In the course of this study the solutions of selected organic bases (morpholine, imidazole, triethanolamine, aminopropylmethanol) were tested in search for mild yet effective conditions. The optimization of the elution step was carried out using ponceau 4R (E124, 40 µg in 200 ml water) as a model dye. The recoveries of this dye obtained by different basic eluents given in Table 1 were determined spectrophotometrically on the basis of calibration plots generated for E124 in the solutions of appropriate bases (Table 2). After the analysis of these recoveries the least effective of all organic bases (AMP, morpholine) were excluded from further studies. The effectiveness of imidazole solutions as eluents was also considered unsatisfactory since to achieve the reasonable rate of elution relatively high concentrations (compared to TEA) of this base were needed.

Table 1. Recoveries of E124 after SPE with different eluents. Volumes of solutions after the elution step were determined by weight. Standard solutions used to generate calibration plots were prepared in appropriate media as described above ("Solutions").

Eluent	**Volume after elution [ml]**	**Dye concentration [µg mL^{-1}]**	**Dye weight [µg]**	**Recovery [%]**
TEA 0.1 M	1.39	26.6	37.0	92.5
TEA 0.01 M	2.83	13.0	36.9	92.2
imidazole 1 M	1.36	27.5	37.4	93.6
imidazole 0.1 M	4.47	8.3	37.2	93.0
morpholine 1 M	1.25	24.2	30.3	75.8
morpholine 0.1 M	1.30	25.5	33.2	83.0
AMP 0.1 M	1.19	25.6	30.5	76.2
NaOH 0.01 M	2.27	16.4	37.3	93.3

Source: Author's

Table 2. Calibration plots for Ponceau 4R (E124) in different media

	Imidazole 0.1M	**Imidazole 1M**	**Morpholine 0.1M**	**Morpholine 1M**	**TEA 0.01M**	**TEA 0.1M**	**NaOH 0.01M**
a (slope)	0.043	0.043	0.042	0.040	0.043	0.042	0.025
b (intercept)	0.004	0.0065	0.0047	0.0053	0.0079	0.0037	-0.009
S_a	0.00025	0.00018	0.00027	0.00010	0.00022	0.00022	0.00050
S_b	0.0038	0.0027	0.0040	0.0015	0.0033	0.0033	0.0075
R^2	0.9999	0.9999	0.9999	0.9999	0.9999	0.9999	0.9985
S_{xy}	0.0041	0.0029	0.0043	0.0017	0.0036	0.0035	0.0081
LOD/LOQ [µg mL^{-1}]	0.29/0.87	0.21/0.63	0.31/0.93	0.12/0.36	0.25/0.75	0.26/0.78	0.99/2.97
Linearity range [µg mL^{-1}]	0-30	0-30	0-30	0-30	0-30	0-30	0-30

Source: Author's

Spectrophotometric calibration in selected media

Further SPE experiments involved elution with either NaOH or TEA. It was established that synthetic dyes differ significantly in terms of their affinity to the aminopropyl sorbent. Elution with diluted aqueous organic amines is possible in all cases, but the necessary amount of the eluent is different for different dyes so in most cases (E122, E133, E110, E104, E102, E132) aqueous NaOH was preferred to keep the eluent volume within reasonable limits. 0.01M NaOH was effective for all dyes but further reduction of the eluent volume was possible with NaOH at higher concentrations (e.g. 0.1M). Parameters of calibration plots generated for different synthetic dyes in 0.01M NaOH are presented in Table 3 and for E122 and E133 in 0.1M NaOH in Table 4.

Table 3. Parameters of calibration plots of different dyes in 0.01M NaOH

	E122	**E110**	**E104**	**E102**	**E124**	**E133**	**E132**
a (slope)	0.045	0.029	0.053	0.040	0.025	0.162	0.037
b (intercept)	0.016	0.011	0.017	0.014	-0.017	0.099	-0.012
S_a	0.00046	0.00036	0.00052	0.00042	0.0005	0.003	0.00042
S_b	0.0074	0.0060	0.0078	0.0071	0.0075	0.04	0.0060
R^2	0.9996	0.9994	0.9996	0.9996	0.9985	0.9989	0.9995
S_{xy}	0.0081	0.0065	0.0084	0.0076	0.0081	0.038	0.0065
LOD/LOQ [µg mL^{-1}]	0.54/1.62	0.68/2.04	0.49/1.47	0.59/1.77	0.99/2.97	0.81/2.43	0.53/1.59
Linearity range [µg mL^{-1}]	0-30	0-30	0-30	0-30	0-30	0-20	0-30

Source: Author's

Table 4. Parameters of calibration plots in 0.1M NaOH

	E122	**E133**
a (slope)	0.045	0.155
b (intercept)	0.0079	0.093
S_a	0.00023	0.0032
S_b	0.0036	0.042
R^2	0.9999	0.9987
S_{xy}	0.0039	0.040
LOD [µg mL^{-1}]	0.26	0.89
LOQ [µg mL^{-1}]	0.78	2.67
Linearity range [µg mL^{-1}]	0-30	0-20

Source: Author's

Table 5. Recoveries of dyes – pure[a] and spiked[b] products

Product	**Dye**	**Mean determined dye content [µg mL^{-1} of drink] [µg per tablet], n=3 *(SD [%])***	**Expected dye content [µg mL^{-1} of drink] [µg per tablet]**	**Recovery [%]**
Pink drink	Azorubine E122	13.9[a] *(5.9)*	-	-
		29.5[b] *(7.8)*	30.5	96.7
		47.3[b] *(6.5)*	47.1	100.4
Blue drink	Brilliant blue E133	3.4[a] *(5.6)*	-	-
		8.0[b] *(5.1)*	7.4	108.0
		11.8[b] *(7.0)*	11.4	103.5
Red tablet	Ponceau 4R E124	335.0[a] *(4.0)*	-	-
		416.6[b] *(4.6)*	412.0	101.1
		474.3[b] *(6.2)*	489.0	97.0
Lab-prepared fizzy drinks	Orange yellow E110	9.1 *(6.8)*	10.0	91.0
		27.3 *(8.1)*	30.0	91.0
		47.5 *(7.3)*	50.0	95.0
	Quinoline yellow E104	9.5 *(4.9)*	10.0	95.0
		29.1 *(5.3)*	30.0	97.0
		48.6 *(9.1)*	50.0	97.1
	Tartrazine E102	10.3 *(5.8)*	10.0	103.0
		31.0 *(3.7)*	30.0	103.3
		50.1 *(6.3)*	50.0	100.0
	Indygo Carmine E132	9.4 *(6.5)*	10.0	94.0
		28.8 *(4.9)*	30.0	96.0
		48.9 *(5.4)*	50.0	97.8

Source: Author's

Table 6. Repeatability and intermediate precision of dyes determinations

Product	**Dye**	**Determined dye content [µg mL^{-1} of drink], [µg per tablet]**		
		Day I, Analyst A	**Day I, Analyst B**	**Day II**
Pink drink	Azorubine E122	13.9	13.8	14.0
Blue drink	Brilliant blue E133	3.4	3.5	3.3
Red tablet	Ponceau 4R E124	335.0	338.0	335.0
Lab-prepared fizzy drinks	Orange yellow E110	9.1	8.9	9.1
	Quinoline yellow E104	9.5	9.4	9.4
	Tartrazine E102	10.3	10.2	9.8
	Indigo Carmine E132	9.4	9.3	9.5

Source: Author's

Determination of synthetic dyes in selected commercial preparations

Samples of beverages and tablets colored with food dyes under investigation were prepared according to the section "Preparation of samples for SPE". Elution of E122 and E133 was achieved according to the section "SPE extraction" with 0.1M NaOH, E110, E104, E102 and E132 with 0.01M NaOH and E124 with 0.01M TEA and the concentrations of dyes in the resulting solutions were determined spectrophotometrically according to the section "UV/VIS Spectroscopy" (Table 5).

Procedure validation

To estimate the accuracy of the proposed procedure samples of drinks and tablets analyzed during these investigations were spiked with appropriate dyes and subjected to SPE extraction followed by spectrophotometry. The expected dye contents, results of experimental determinations and recoveries are presented in Table 5. The method precision was also evaluated - the repeatability was tested according to [36] by replicating the entire method on the same day, using the same products, batches of solvents and SPE columns, by the same analyst (Day I, Analysis A and B). Intermediate precision was verified according to [36] by repeating the procedure on the same products but on a different day, by a different analyst, using other batches of solvents and SPE columns (Day II). The results of these experiments presented in Table 6 prove that the method accuracy and precision are sufficient for determination of selected food dyes in beverages and pharmaceutical tablets.

Limits of detection and quantification of the spectrophotometric determinations were estimated on the basis of the parameters of the calibration curves according to the formulas: $LOD=3.3*s_b/a$ and $LOQ=3*LOD$, where a is a slope and s_b – a standard deviation of the intercept, respectively (Ref. [36]).

Conclusions

Synthetic food dyes may be effectively quantified in beverages and pharmaceutical tablets by VIS spectroscopy after isolation by SPE extraction on the aminopropyl sorbent. The elution of the dyes from the sorbent can be achieved with aqueous NaOH or diluted amines. The calibration plots of Ponceau 4R (E124) used as the model dye differ significantly in terms of slope depending on the eluent – the sensitivity is better when TEA is used instead of NaOH. Other dyes, however, e.g. brilliant blue (E133) or azorubine (E122) are eluted faster with aqueous NaOH than with amines so for the elution of these colorants NaOH is the reagent of choice. Substances present in drinks and tablets (actives, sweeteners, flavors) do not interfere.

Acknowledgements

This research was supported by an internal grant of the Medical University of Lodz, Poland, no. 503/3-016-03/503-31-001.The authors declare that there is no conflict of interest regarding the publication of this manuscript.

References

[1] C. Sociaciu (Ed.), Food colorants. Chemical and Functional Properties, Tylor and Francis 2008, 533-547.

[2] M. Kucharska, J. Grabka, A review on chromatographic methods for determination of synthetic food dyes, Talanta 80 (2010) 1045-1051.

[3] T. Tuzimski T, Determination of Sulfonated Water-Soluble Azo Dyes in Foods by SPE Coupled with HPTLC-DAD, J. Planar Chromatogr. 24 (2010) 281-289.

[4] A.M. Anderton, C.D. Incarvito, J. Sherma, Determination of natural and synthetic colors in alcoholic and non-alcoholic beverages by quantitative HPTLC, J. Liq. Chromatogr. Rel. Techn. 20 (1996) 101-110.

[5] F. Soponar, A. Catalin Mot, C. Sarbu, Quantitative determination of some food dyes using digital processing of images obtained by thin-layer chromatography, J. Chromatogr. A 1188 (2008) 295-300.

[6] M. Gonzalez, M. Gallego, M. Valcarcel, Liquid Chromatographic Determination of Natural and Synthetic Colorants in Liophilized Foods Using an Automatic Solid-Phase Extraction System, J. Agric. Food Chem. 51 (2003) 2121-2129.

[7] J. Kirschbaum, C. Krause, H. Bruckner, Liquid chromatographic quantification of synthetic colorants in fish roe and caviar, Eur. Food. Res. Technol. 222 (2006) 572-579.

[8] J. Kirschbaum et al, Development and evaluation of an HPLC-DAD method for determination of synthetic food colorants, Chromatographia 57 (2003) S115-S119.

[9] M.G. Kiseleva, V.V. Pimenova, K.I. Eller, Optimization of conditions for the HPLC determination of synthetic dyes in food, J. Anal. Chem. 58 (2003) 766-772.

[10] M.C. Gennaro, E. Gioannini, S. Angelino, R. Aigotti, D. Giacosa, Identification and determination of red dyes in confectionery and determination by ion-interaction HPLC, J. Chromatogr. A 767 (1997) 87-92.

[11] M. Perez-Urquiza, M.D.Prat, J.L. Beltran, Determination of sulphonate dyesin water by ion-interaction high-performance liquid chromatography, J. Chromatogr. A 871 (2000) 227-234.

[12] A. DeVilliers, F. Alberts, F. Lynen, A. Crouch, P. Sandra, Evaluation of liquid chromatography and capillary electrophoresis for the elucidation of the artificial colorants brilliant blue and azorubine in red wines, Chromatographia 58 (2003) 393-397.

[13] M.C. Boyce, Determination of additives in food by capillary electrophoresis, Electrophoresis 22 (2001) 1447-1459.

[14] R.A. Frazier, E.L. Inns, N. Dossi, J.M. Ames, H.E. Nursten, Development of a capillary electrophoresis method for the simultaneous analysis of colours, preservatives and sweeteners in soft drinks, J. Chromatogr. A 876 (2000) 213-220.

[15] H.Y. Huang *et al*., Analysis of food colorants by capillary electrophoresis with large volume sample stacking, J. Chromatogr. A 995 (2003) 29-36.

[16] K.L. Kuo, H.Y. Huang, Y.Z. Hsieh. High-performance capillary electrophoretic analysis of synthetic food colorants, Chromatographia 47 (1998) 249-256.

[17] M. Masar, D. Kaniansky, V. Madajova, Separation of synthetic food colorants by capillary zone electrophoresis in a hydrodynamically closed separation compartment, J. Chromatogr. A 724 (1996) 327-336.

[18] J.J. Berzas Nevado, C. Guilberteau Cabanillas, A.M. Contento Salcedo, Anal. Chim. Acta378 (1999) 63-71.

[19] C.O Thompson, V.C. Trenerry, Determination of synthetic colours in confectionery by micellar electrokinetic capillary chromatography, J. Chromatogr. A 704 (1995) 195-201.

[20] S.S. Chou, Y.H. Lin, C.C. Cheng, D.F. Hwang, Determination of synthetic colors in soft drinks and confectioneries by micellar electrokinetic capillary chromatography, J. Food Sci, 67 (2002) 1314-1318.

[21] H.Y. Huang, Determination of food colorants by microemulsion electrokinetic chromatography, Electrophoresis 26 (2005) 867-877.

[22] S. Sayar, Y. Ozdemir, First-derivative spectrophotometric determination of Ponceau 4R, Sunset Yellow and Tartrazine in confectionery products, Food Chem. 61 (1998) 367-372.

[23] S. Sayar, Y. Ozdemir, Determination of Ponceau 4R and Tartrazine in Various Food Samples by Derivative Spectrophotometric Methods, Turk. J. Chem. 21 (1997) 182-187.

[24] O.W. Lau, M.M.K. Poon, S.C. Mok, F.M.Y. Wong, S.F. Luk, Spectrophotometric determination of single synthetic food colour in soft drinks using ion-pair formation and extraction, Int. J. Food Sci. Technol. 30 (1995) 793-798.

[25] E.C. Vidotti, M.C.E. Rollemberg, Derivative spectrophotometry: a simple strategy for simultaneous determination of food dyes, Quim. Nova 29 (2006) 230-233.

[26] E.C. Vidotti, J.C. Cancino, C.C. Oliveira, M.C.E. Rollemberg. Simultaneous Determination of Food Dyes By First Derivative Spectrophotometry with Sorption onto Polyuretane Foam, Anal. Sci. 21 (2005) 149-153.

[27] Y. Ni, J. Bai, L. Jin, Simultaneous adsorptive voltammetric analysis of mixed colorants by multivariative calibration approach, Anal Chim Acta 329 (1996) 65-72.

[28] Y. Ni, J. Bai, Simultaneous determination of Amaranth and Sunset Yellow by ratio derivative voltammetry, Talanta 44 (1997) 105-109.

[29] J.J.B. Nevado, J.R. Flores, Square wave adsorptive voltammetric determination of sunset yellow, Talanta 44 (1997) 467-474.

[30] S. Combeau, M. Chatelut, O. Vittori. Identification and simultaneous determination of Azorubin, Allura red and Ponceau 4R by differential pulse polarography: application to soft drinks, Talanta 56 (2002) 115-122.

[31] M. Puttemans, L. Dryon, D.L. Massart, Extraction of water-soluble acid dyes by ion-pair formation with tri-n-octylamine. Anal. Chim. Acta 113 (1980) 307-314.

[32] F. Feng, Y. Zhao, W. Yong, L. Sun, G. Jiang, X. Chu, Highly sensitive and accurate screening of 40 dyes in soft drinks by liquid chromatography–electrospray tandem mass spectrometry, J. Chromatogr. B 879 (2011) 1813-1818.

[33] X. Liu, J.L. Yang, J.H. Li, X.L. Li, J. Li, X.Y. Lu, J.Z. She, Y.W. Wang, Z.H. Zhang, Analysis of water-soluble azo dyes in soft drinks by high resolution UPLC–MS, Food Add. Cont. 28 (2011) 1315-1323.

[34] K.S. Minioti,, C.F. Sakellariou, N.S. Thomaidia, Determination of 13 synthetic food colorants in water – soluble foods by reversed – phase high – performance liquid chromatography coupled with diode – array detector, Anal. Chim. Acta 583 (2007) 103-110.

[35] Supelco: Guide to Solid Phase Extraction, Bulletin 910, Internet: http://www.sigmaaldrich.com/Graphics/Supelco/objects/4600/4538.pdf

[36] P. Konieczko, J. Namieśnik, Ocena i kontrola jakości wyników pomiarów analitycznych, Wydawnictwo Naukowo – Techniczne, Warszawa 2007, pp. 52-54, 225-298.

Ewa Szymanek
Institute of Thermal Machinery, Faculty of Mechanical Engineering and Computer Science,
Czestochowa University of Technology, Armii Krajowej 21, 42-201 Czestochowa, ewaszymanek@vp.pl

USE OF FRACTIONAL CALCULUS IN MODELING OF HEAT TRANSFER PROCESS THROUGH EXTERNAL BUILDING PARTITIONS

Abstract
This paper is devoted to experimental and numerical studies of heat distribution in an external building bulkhead. It analyzes the variation of temperature across the width of the bulkheads including the impact of changing external conditions. Mathematical model used in the research is formulated based on a fractional differential equation, which was proven to be a useful tool for describing this type of process in previous paper. Numerical results are compared with experiment data for different bulkhead configurations.

Key words
Fractional equations, building bulkhead, heat flow

Introduction

Reduction of the negative human impact on the climate is one of the challenges for European Union Member States, which is reflected in both its legislation and strategic priorities adopted in the next financial perspectives [1,2,3,4]. Currently, EU actions are aimed, among other things, at reducing the greenhouse gas emissions by 80% by 2050 year compared to the 1990 level with transition stages up to 2030 (40% reduction) and until 2040 (40% reduction). Undoubtedly, realization of such assumptions requires an active participation of all Member States. That is why in recent years a huge progress has been made in Poland in the field of energy efficiency. In the national legislation on energy, environmental protection and construction law, significant changes have been introduced to support energy efficiency [5,6,7]. Certainly, the leading roles in a low-emission economy will be played by sustainable construction. Due to the low standard of a large part of Polish buildings, the energy consumption is inefficient. In many cases the consumed energy is wasted as the heat "escapes" through poorly constructed and insulated walls and roofs. The most important challenge for achieving such results in 2050 will be thermo-modernization of existing buildings. It should be emphasized that currently as much as 70 percent of flats and houses in Poland are not insulated, and their thermo-modernization would allow at low cost to reduce the heat losses, which could cause significant a drop in energy demand. At present, at the investment stage, which requires a building permit, energy-saving documents are necessary. One of the actions that are taken to improve the energy parameters in existing buildings is the insulation of external walls, where the heat losses are in the range 24% - 35%. The most common is the insulation in the form of adding additional insulating material to the existing wall from outside. Partitions (walls) used in the construction industry consist of many layers of different materials firmly adjacent to each other. Styrofoam or mineral wool layer are the most popular, however, fillings in the form of rigid foam or various mixtures are also used [8]. Knowledge of physical processes and chemical phenomena occurring in building materials [9] facilitates their proper selection and allows designing buildings with regard to energy saving [10]. Heat transfer occurring in the interior of solid materials consists in the transfer of energy between adjacent particles. The intensity of this process depends on the structure and properties of the material. That is why the construction of external partitions is very important in construction industry. The basis of the heat exchange phenomenon is the temperature difference. Therefore, one should look for solutions that allow to correctly defining the temperature distribution in its interior. More accurate understanding of the heat transfer phenomenon between particular bulkhead layers (insulating walls) will allow better control of temperature changes. A big problem in the detailed description of the heat flow process is the multitude of dependencies and factors needed to describe the structure of insulating walls. Definition of general dependence allowing determining the thermal conductivity is complicated due to the thermal properties of individual components.

From the literature it can be stated that in the classic approach the heat flow is described by the Kirchhoff equation. The basic disadvantage of this model is the necessity of knowing all material parameters of the insulating layers and the numerous empirical correlations needed to describe their thermal properties. For this reason, in this work it was decided to move away from the classic approach and replace it with a new model

based on fractional calculus. Models using the fractional derivatives are considered to be an excellent tool for describing the memory and hereditary properties of various materials and processes. Fractional differential equations, both ordinary and partial, are used in the modelling of various phenomena in the fields of physics, mechanics, control theory, biochemistry, bioengineering and economics [11-17]. Their application is also found in mechanics, in the field of signal processing [18] and in modelling of phenomena occurring in construction industry [19]. As a result, the fractional differential equations gain more and more applications and importance. In [20] the classical thermal conductivity equation was replaced with an ordinary differential equation containing the composition of the left and right-sided fractional derivative. The equations of this type are obtained by modification the least action principle and the use of fractional method of integration by parts [21,22,23]. One of the basic problems which appears while modelling the heat flow in a complex system is the multiplicity of interrelations, factors and coefficients necessary to describe the structure of the examined system. This paper proposes a description which does not investigate the structure but assumes some degree of its heterogeneity. When used with a simple differential equation including left- and right-sided fractional derivatives we arrive at a model which has such a quality that it does not investigate the structure and does not include such a number of factors. The considered problems faced in the process of heat flow during the paper will be analysed from the practical and theoretical points of view. In this paper a fractional differential equation containing the left and right-sided Caputo derivative in the restricted area was applied. One of the basic problems that arise in the fractional equations is a lack or very complex form of analytical solutions. The fractional equation are discretized because the results obtained so far, including those based on the fixed-point theorem [24], do not give the possibility to apply them in practice. The solution in discretized form is presented as a series of left and right sides of fractional integrals. In the paper, the simulations of heat flow through one, two and three-layer barriers were performed and their inner temperature distributions were determined. The results obtained using the commercial Leca program are also presented. A description of the temperature distribution based on fractional calculus has been proposed and the obtained results were compared with the experimental data.

Experiment

Simulations of heat flow and temperature distributions in building partitions allow designing them in a way reducing the cost of building to minimum. Because external walls have a big influence on the energetic characteristics of the buildings the knowledge of temperature distributions inside them is so important. It allows correct evaluation of their insulation. The article presents the results of research on the heat flow through the external layers with three types of partitions: one-layer, two-layer and three-layer.

Fig.1. A partition prepared for testing
Source: *Author's*

The first of them was built of cellular concrete (48 cm). The two-layer partition (48 cm) consisted with cellular concrete layer (32 cm) and was additionally supplemented with a layer of styrofoam EPS 032 (16 cm). The three-layer partition (48 cm) consisted of a cellular concrete layer (32 cm), styrofoam EPS 032 (8 cm) and an elevation brick (8 cm). Each wall was covered on both sides with cement and lime plaster. The thermal parameters of the materials used were as follows: concrete (density 2100 kg/m^3, thermal conductivity coefficient 1,1 W/(m·K), specific heat 840 J/(kg·K)), styrofoam EPS 032 (density 40 kg/m^3, thermal conductivity coefficient 0,032 W/(m·K), specific heat 1460 J/(kg·K)), elevation brick (density 1900 kg/m^3, thermal conductivity coefficient 1,05 W/(m·K), specific heat 880 J/(kg·K)). Measurements of thermal conductivity were carried out using a plate apparatus with a a heat flux density sensor HFM P.A. Hilton B480. The specific heat was determined by the calorimetric method, while the density measurement was based on Archimedes' law. An example of the tested wall composed of two layers (cellular concrete and styrofoam) is presented in Figure 1.

Figure 2 presents a symbolic construction of the tested wall and temperature distribution in one, two and three-layer partitions determined using the commercial calculation program Leca. It can be seen that the temperature across particular layers changes linearly. As will be shown later such an approximation is inconsistent with the experiment and simulations performed by the fractional calculus method.

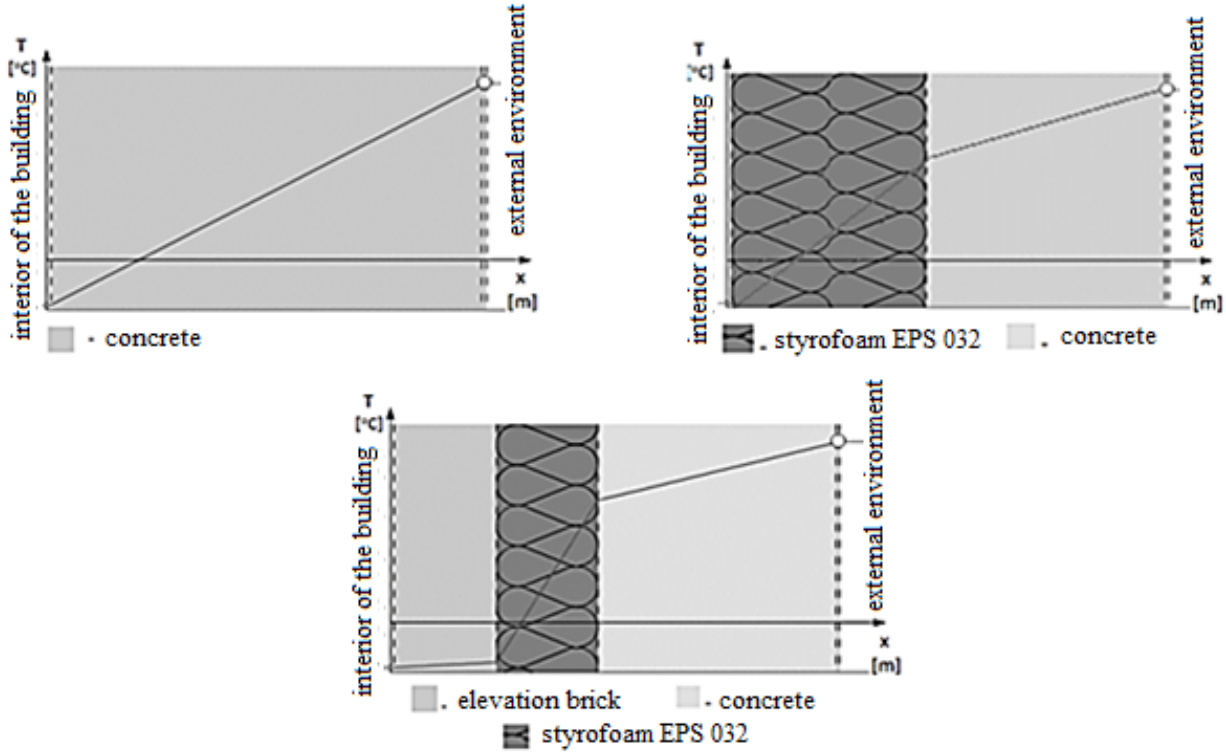

Fig.2. Construction and distribution of temperatures in one, two and three-layer partitions determined by Leca's commercial calculation program.
Source: Author's

Measurements of the temperature were performed by thermocouples placed in the holes drilled inside the layers. Empty spaces between the test center and the thermocouple were filled with drilling dust or pieces of styrofoam, so that the thermocouple adhered closely to the material tested. The tested partitions were 30x30x48 cm. Thermocouples in each partition were placed on 7 levels (level every 8 cm). Five thermocouples were installed in each of the following configurations (cm, cm): T1: (X, Y) = (7.5,7.5), T2: (X, Y) = (7,5,22.5), T3: (X, Y) = (15.15), T4: (X, Y) = (22.5,7.5), T5: (X, Y) = (22.5,22.5). This arrangement was intended to minimize measurement errors. As the data from the thermocouples on the individual levels were similar, they were averaged and added as one measuring point on the graph. The walls constructed in this way were placed in a climatic chamber (Fig. 3), which enabled setting of external temperatures and their precise control during the whole experiment. External temperature values were changed in a similar way to daily temperature fluctuations in Poland.

Fig.3. Climatic chamber
Source: Author's

Model

The complexity of the heat transfer process generates the need to create new models for its description. Numerical methods, such as the method based on fractional calculus, are increasingly being used for such purposes. As already mentioned, in the comparison to classical methods it requires much smaller number of coefficients. In this work we apply an ordinary differential equation containing the composition of left and right-sided derivatives of a non-integer order. To describe the considered phenomenon, a non-integer equation is proposed with the left and right-sided Caputo derivative in the form:

$$ {}^{C}D_{b-}^{\alpha}\,{}^{C}D_{a+}^{\alpha}T(x)+\lambda T(x)=0,\ x\in[a,b]. \qquad (1)$$

where T – temperature, λ - scale parameter, α - order of derivative. The fractional derivatives have the following form [25]:

$$ {}^{C}D_{a+}^{\alpha}T(x)=\frac{1}{\Gamma(1-\alpha)}\int_{a}^{x}\frac{T'(\tau)}{(x-\tau)^{\alpha}}d\tau \qquad (2)$$

$$ {}^{C}D_{b-}^{\alpha}T(x)=\frac{-1}{\Gamma(1-\alpha)}\int_{x}^{b}\frac{T'(\tau)}{(\tau-x)^{\alpha}}d\tau \qquad (3)$$

The formulas (2) and (3) are respectively the left-sided and the right-sided Caputo derivative. It is assumed that temperature varies only in the "x" direction perpendicular to the partition.

Equation (1) has been supplemented with the boundary conditions:

$$\begin{aligned} T(0) &= Ta \\ T(L) &= Tb \end{aligned} \qquad (4)$$

where the length of the layer is assumed L=1.

Numerical solution

Here, mathematical analysis is used increasingly often for designing granular material assemblies, such as, for example, fractional differential equation, which requires a significantly-smaller number of coefficients. The form of the analytical solution of equation (1) is complicated [26] and it is not possible to apply it for the analysed phenomenon. Therefore, equation (1) is discretized by means of a series of expansions with coefficients ν. Along with the boundary conditions (4) it can be written in the following form [20,27]:

$$\begin{gathered} \mathrm{T_a} = \mathrm{Ta} \\ \sum_{\mathrm{k=i}}^{\mathrm{n}}\left[\nu(\mathrm{n}-\mathrm{i},\mathrm{n}-\mathrm{k})\cdot\sum_{\mathrm{j=0}}^{\mathrm{k}}\nu(\mathrm{k},\mathrm{j})\mathrm{T_j}\right]+\lambda\mathrm{T_i}=0, \qquad \text{for} \quad \mathrm{i}=1,\dots,\mathrm{n}-1 \\ \mathrm{T_b} = \mathrm{Tb} \end{gathered} \qquad (5)$$

where n is number of nodes, T_i is the value of the function T at point x_i and coefficient ν is defined as

$$\nu(\mathrm{i},\mathrm{j}) = \frac{(\Delta \mathrm{x})^{\alpha}}{\Gamma(2-\alpha)}\begin{cases} -\mathrm{i}^{1-\alpha}+(\mathrm{i}-1)^{1-\alpha} & \text{for} \quad \mathrm{j}=0 \\ (\mathrm{i}-\mathrm{j}+1)^{1-\alpha}-2(\mathrm{i}-\mathrm{j})^{1-\alpha}+(\mathrm{i}-\mathrm{j}-1)^{1-\alpha} & \text{for} \quad \mathrm{j}=1,\dots,\mathrm{i}-1 \\ 1 & \text{for} \quad \mathrm{j}=\mathrm{i} \end{cases} \qquad (6)$$

where $\Delta x = L/(N-1)$ stands for a distance between the computational nodes, which number changes in the range $N = 20 \div 140$. The symbol Γ in Eq.(6) is the Gamma function.

The convergence rate (EOC) of series (5) for parameters $Ta = 1$, $Tb = 0$ and $\lambda = 0.02$ is determined according to the equation:

$$EOC = \frac{1}{9}\sum_{i=1}^{9} EOC_{i,\alpha}^{(\Delta x)} \qquad (7)$$

where

$$EOC_{i,\alpha}^{(\Delta x)} = \log_2\left(\frac{t_{i,\alpha}^{(\Delta x)} - t_{i,\alpha}^{(2\Delta x)}}{t_{i,\alpha}^{(\Delta x/2)} - t_{i,\alpha}^{(\Delta x)}}\right) \qquad (8)$$

is the order of the method determined on the basis of one of 9 selected points in the computation area. Analysis of convergence rate was determined for four computation grids with Δx = 1/20, 1/40, 1/80, 1/120. Note that $t_{i,\alpha}^{(\Delta x)}$ are numerical value in the points $x_{i/10\Delta x}$ for $i = 1,2,\dots,9$. Table 1 shows the EOC values for $\alpha \in \{0.1,0.3,0.5,0.7,0.9\}$ and $\lambda = 0.02$.

Tab. 1. Estimation of the discretization order of (5) for four computational grids

	EOC				
Δx	α =0.1	α =0.3	α =0.5	α =0.7	α =0.9
1/20	1.21	1.11	0.96	0.80	0.65
1/40	1.10	1.08	1.00	0.87	0.74
1/80	1.05	1.05	1.00	0.91	0.79
1/120	1.03	1.03	1.00	0.94	0.83

Source: *Author's*

Analysing the values in Table 1, it can be observed that the convergence rate of (5) slightly depends on the α parameter and its value is close to 1. Figure 4 presents the solutions of equation (1) for different values of the parameter α. It shows that the temperature profiles are strongly dependent on it. The deviation of α from integer value (equal to 1 in classical approach) causes that the obtained solutions behave as if they were obtained using the classical method with variable heat conductivity of the layer.

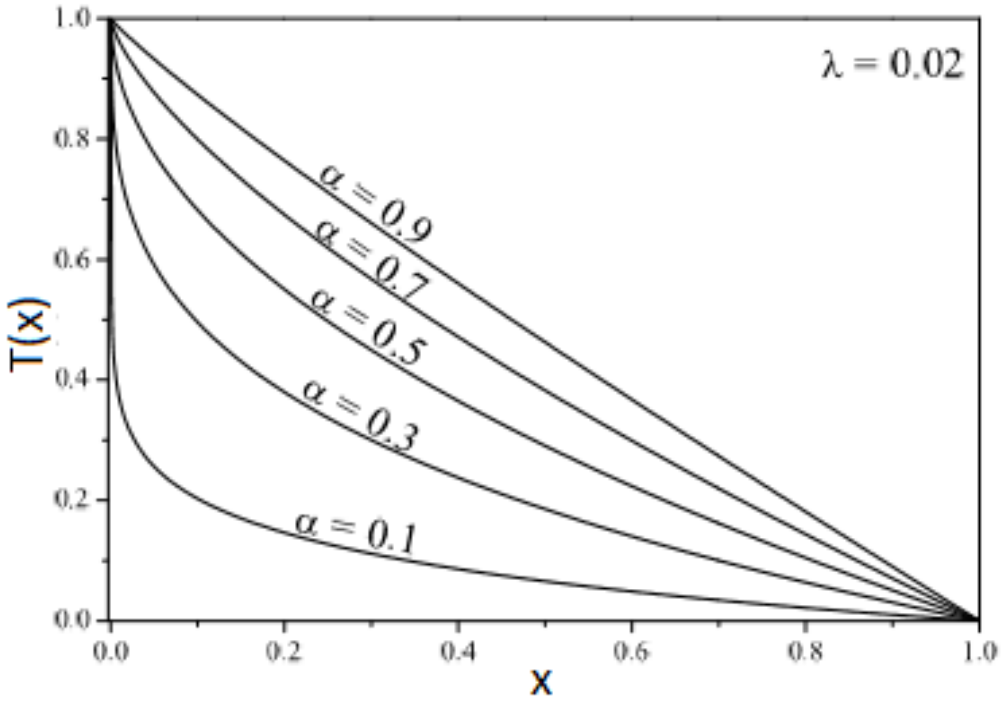

Fig. 4. Numerical solutions of the equation (1) for λ=0.02 I α∈ {0.1; 0.3; 0.5; 0.7; 0.9}
Source: *Author's*

Results

Figures 5-7 present the experimental and numerical temperature profiles inside the partitions. The temperature distributions were determined for the outside temperature T(L) changing from -20 ° C to 18 ° C at the outer layer. The steady states were selected for further analysis. In this case we considered the layers with L=48cm. The temperature on the inner side T(0) was computed assuming the Neumann boundary conditions. During the experiment, the thermocouples were placed in the same distance from each other and from the outer and inner layers. The graphs show experimental data for selected time moments. The results presented 14,200 second from the beginning of measurements when the outside temperature was 9°C. For comparison the results obtained using the classical approach are also presented in the figures. They are denoted as "mathematical integer order". It can be seen that the results obtained the fractional order are much more accurate.

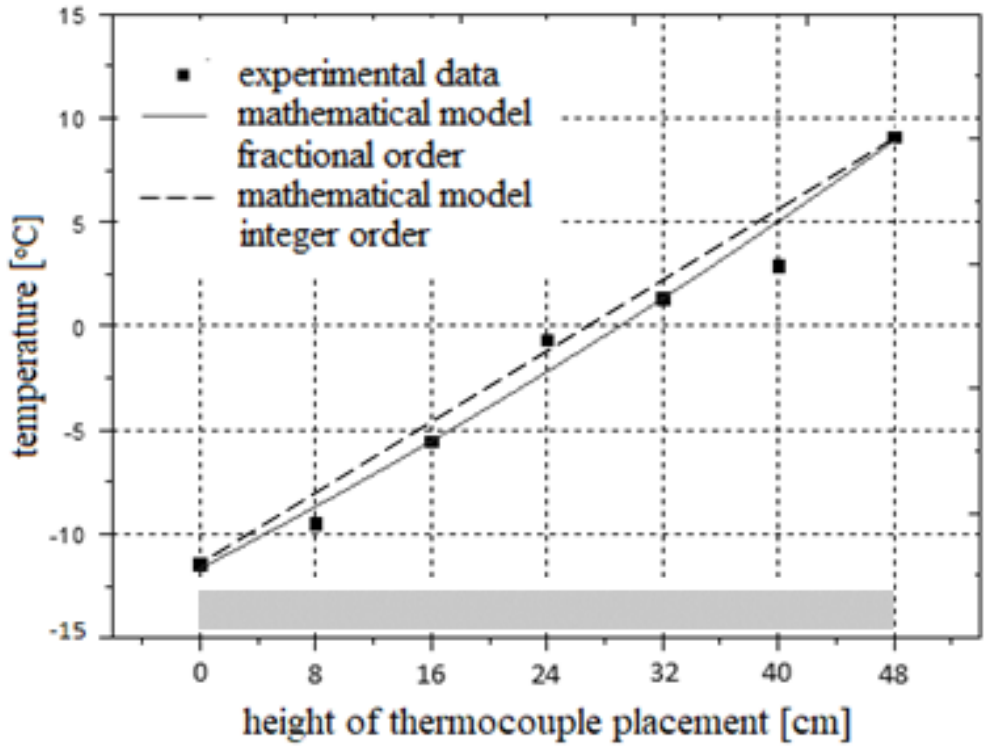

Fig. 5. Comparison of the numerical solution with experimental data for a single-layer partition for an external temperature of 9°C, α=0,85
Source: *Author's*

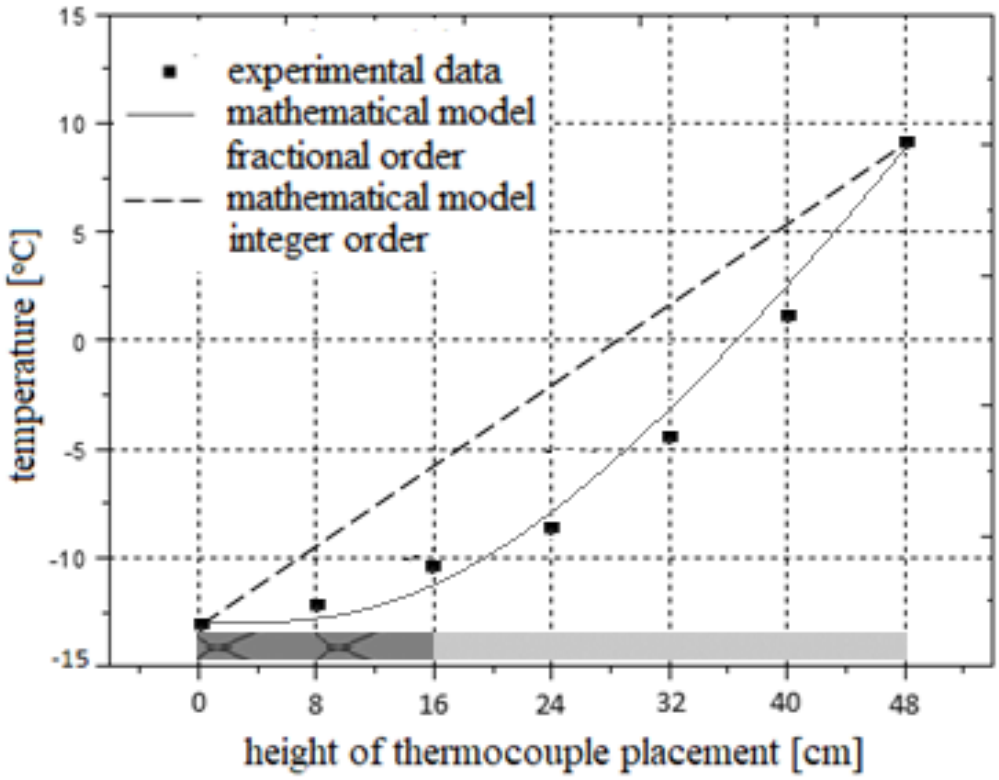

Fig.6. Comparison of the numerical solution with experimental data for a two-layer partition for an external temperature of 9°C, α=0,25
Source: *Author's*

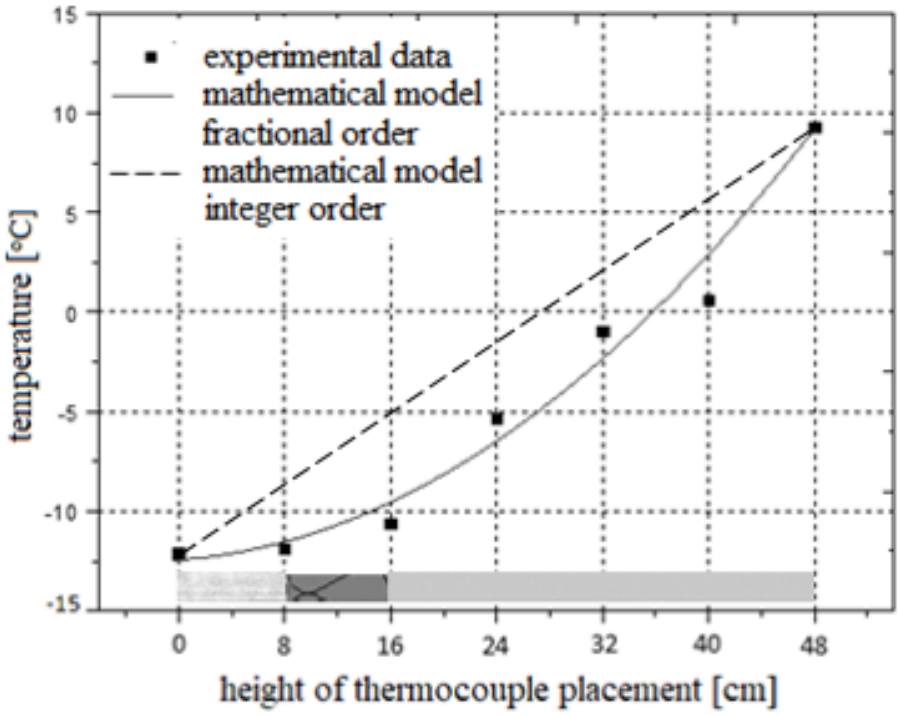

Fig.7 Comparison of a numerical solution with experimental data for a three-layer partition for an external temperature of 9°C, α=0,3
Source: *Author's*

As can be seen in Fig.5 for the monolayer partition consisting of cellular concrete the measured data only slightly differ from the simulation results. It is visible that at all measuring points the deviations were at a similar level. Accidental larger discrepancies could be due to a measurement error estimated at 2°C. Differences in temperature values for two-layer partition are also small, as can be seen in Fig.6. Depending on the measurement point, the results are over and underestimated in relation to the experimental data. These fluctuations did not occur regularly and therefore their origin could not be identified. The largest deviations from the curve obtained on the basis of simulations can be seen for three-layer partition (see Fig. 7). The differences occur here in the whole width of the partition and are the most pronounced among the tested partitions. Most likely, in this case the discrepancies between the simulation and measurements results from a complex structure of partitions. However, the trend of the temperature variations is well captured. In general, when comparing experimental data with the results of a fractional model, it can be noticed that the differences between experimental and numerical data are small. The method proposed in this paper allows modelling of real external temperature changes and allows for analysis of temperature distribution inside the partitions.

Summary

The article presented the results of research on heat transfer phenomenon in external building walls composed of one, two and three-layered partitions. The experimental tests and simulations were conducted under variable temperature conditions reflecting daily temperature fluctuations. Both the cellular concrete layer and the insulator were considered, which in the present case was a styrofoam and a material in the form of a elevation brick. The mathematical model presented in the paper was based on fractional differential calculus and it turned out to be an efficient and accurate tool, which characterized stable convergence rate. The proposed model allows to describe the theoretical problem of thermal conductivity and may be regarded as an alternative to others classical approaches known for problems with the multitude of different types of correlations and coefficients. Relatively small differences between the numerical and experimental results indicate high accuracy of the proposed model. It is believed that it can be used for optimization purposes during the construction of partitions, achieving measurable economic effects.

Acknowledgements
This work was supported by National Science Centre, Poland (Grant no. 2017/27/N/ST8/02318). The author is grateful to A. Tyliszczak for his fruitful comments on the initial version of this manuscript.

References

[1] COM, 885 final, Commission communication Energy Action Plan by 2050

[2] Report from the Commission to the European Parliament and the Council, Evaluation of Member States' progress towards national targets for energy efficiency 2020 and progress in implementing Directive 2012/27 / EU on energy efficiency as required by Art. 24 sec. 3 of Directive 2012/27 / EU on energy efficiency, Brussels, 13.1.2017, COM (2015) 574.

[3] Directive of the European Parliament and of the Council 2012/27 / EU of 25 October 2012 on energy efficiency

[4] The Energy Performance of Buildings Directive 2002/91/EC

[5] Energy policy of Poland until 2030, pp.7-8, http: //www.mg.gov.pl/ Bezpieczenstwo + gospodarcze/ Energetyka /Polityka + energetyczna

[6] Monitor Polski, Dziennik Urzędowy Rzeczpospolitej Polskiej, Warszawa, dnia 16 lipca 2015 r. Poz. 614 Uchwała nr 91 Rady Ministrów z dnia 22 czerwca 2015 r. w sprawie przyjęcia „Krajowego planu mającego na celu zwiększenie liczby budynków o niskim zużyciu energii"

[7] http: //www.mg.gov.pl/ bezpieczeństwo + gospodarcze/Energetyka/Efektywnosc + energetyczna

[8] J. Mikoś, Budownictwo ekologiczne, Wydawnictwo Politechniki Śląskiej, Gliwice, 2000

[9] E. Kotela, J. Leszczyński, T. Błaszczyk, M. Hall, Wykorzystanie rachunku różniczkowego niecałkowitego rzędu do opisu jednowymiarowego profilu temperatury w stanie ustalonym, II Kongres Mechaniki Polskiej, 29-31.08.2011, Poznań

[10] W. Dubas, Podstawy budownictwa energooszczędnego, Budownictwo energooszczędne, Przegląd budowlany 5/2006

[11] J. Sabatier, O. Agrawal, M. Tenreiro Machado, Advances in Fractional Calculus. Theoretical Developments and Applications in Physics and Engineering, Springer-Verlag, Berlin 2007

[12] R.L. Magin, Fractional Calculus in Bioengineering, Begell House Inc., Redding, 2006

[13] E. Scalas, R. Gorenflo, F. Mainardi, Fractional calculus and continuous time finance, Physica A, 284, (2000), 376–384.

[14] T.K. Nowak, K. Duzinkiewicz, Analiza modelu ułamkowego rzędu procesów szybkich reaktora jądrowego, 1, (2014), 44-47.

[15] M. Długosz, P. Piątek, J. Baranowski, P. Skruch, Algorytmy sterowania i zarzadzania budynkami mieszkalnymi, AGH Akademia Górniczo-Hutnicza,(skrypt), Wydział EAIiE, Katedra Automatyki.

[16] A. Loverro, Fractional Calculus: History, Definitions and Applications for the Engineer, Department of Aerospace and Mechanical Engineering University of Notre Dame Notre Dame, IN 46556, (2004).

[17] M. Dalir, Applications of Fractional Calculus, Applied Mathematical Sciences, 4 (21), (2010, 1021 – 1032

[18] B. Kuldeep, A. Kumar, G.K. Singh, Design of quadrature mirror filter bank using Lagrange multiplier method based on fractional derivative constraints, Engineering Science and Technology, (2015).

[19] E. Szymanek, The application of fractional order differential calculus for the description of temperature profiles in a granular layer, Advances in the Theory and Applications of Non-integer Order Systems, (257), (2013), 243–248.

[20] T. Błaszczyk, E. Kotela, M.R. Hall, J.S. Leszczyński, Analysis and applications of composed forms of caputo fractional derivatives, ActaMechanica et Automatica, (2011), 1-4.

[21] O.P. Agrawal, Formulation of Euler-Lagrange equations for fractional variational problems, J. Math. Anal. Appl., 272, (2002), 368-379.

[22] M. Klimek, Lagrangean and Hamiltonian fractional sequential mechanics, Czech. J. Phys., 52, (2002), 1247-1253.

[23] F. Riewe, Nonconservative Lagrangian and Hamiltonian mechanics, Phys. Rev. E, 53, (1996), 1890-1899.

[24] M. Klimek, Solutions of Euler-Lagrange equations in fractional mechanics, AIP FgrunConference Proceedings 956. XXVI Workshop on Geometrical Methods in Physics. Bialowieza, (2007), 73-78.

[25] A.A. Kilbas, H.M. Srivastava, J.J. Trujillo, Theory and Applications of Fractional Differential Equations, Elsevier, Amsterdam, (2006).

[26] M. Klimek, G -Meijer functions series as solutions for certain fractional variational problem on a finite time interval. Journal Europeen des Systemes Automatises (JESA) 42, 653-664 (2008)

[27] T. Blaszczyk, M. Ciesielski, M. Klimek, J. Leszczynski, Numerical solution of fractional oscillator equation. Appl. Math. Comput. 218, (2011),2480-2488.